COMILLAS
UNIVERSIDAD PONTIFICIA
ICAI

GRADO EN INGENIERÍAEN TECNOLOGÍAS INDUSTRIALES

TRABAJO FIN DE GRADO

DESIGN OF A SYRINGE-BASED EXTRUSION MECHANISM FOR 3D FOOD PRINTER

Autor: Marta Iribarren García

Director: Elsayed Aziz Ramadan

Madrid

Junio de 2019

AUTHORIZATION FOR DIGITALIZATION, STORAGE AND DISSEMINATION IN THE NETWORK OF END-OF-DEGREE PROJECTS, MASTER PROJECTS, DISSERTATIONS OR BACHILLERATO REPORTS

1. Declaration of authorship and accreditation thereof.

The author Mr. /Ms. Marta Iribarren García

HEREBY DECLARES that he/she owns the intellectual property rights regarding the piece of work: Design Syringe-Based Extrusion Mechanism for 3D Food Printer that this is an original piece of work, and that he/she holds the status of author, in the sense granted by the Intellectual Property Law.

2. Subject matter and purpose of this assignment.

With the aim of disseminating the aforementioned piece of work as widely as possible using the University's Institutional Repository the author hereby **GRANTS** Comillas Pontifical University, on a royalty-free and non-exclusive basis, for the maximum legal term and with universal scope, the digitization, archiving, reproduction, distribution and public communication rights, including the right to make it electronically available, as described in the Intellectual Property Law. Transformation rights are assigned solely for the purposes described in a) of the following section.

3. Transfer and access terms

Without prejudice to the ownership of the work, which remains with its author, the transfer of rights covered by this license enables:

a) Transform it in order to adapt it to any technology suitable for sharing it online, as well as including metadata to register the piece of work and include "watermarks" or any other security or protection system.

b) Reproduce it in any digital medium in order to be included on an electronic database, including the right to reproduce and store the work on servers for the purposes of guaranteeing its security, maintaining it and preserving its format.

c) Communicate it, by default, by means of an institutional open archive, which has open and cost-free online access.

d) Any other way of access (restricted, embargoed, closed) shall be explicitly requested and requires that good cause be demonstrated.

e) Assign these pieces of work a Creative Commons license by default.

f) Assign these pieces of work a HANDLE (*persistent* URL). by default.

4. Copyright.

The author, as the owner of a piece of work, has the right to:

a) Have his/her name clearly identified by the University as the author

b) Communicate and publish the work in the version assigned and in other subsequent versions using any medium.

c) Request that the work be withdrawn from the repository for just cause.

d) Receive reliable communication of any claims third parties may make in relation to the work and, in particular, any claims relating to its intellectual property rights.

5. Duties of the author.

The author agrees to:

a) Guarantee that the commitment undertaken by means of this official document does not infringe any third party rights, regardless of whether they relate to industrial or intellectual property or any other type.

b) Guarantee that the content of the work does not infringe any third party honor, privacy or image rights.
c) Take responsibility for all claims and liability, including compensation for any damages, which may be brought against the University by third parties who believe that their rights and interests have been infringed by the assignment.
d) Take responsibility in the event that the institutions are found guilty of a rights infringement regarding the work subject to assignment.

6. Institutional Repository purposes and functioning.

The work shall be made available to the users so that they may use it in a fair and respectful way with regards to the copyright, according to the allowances given in the relevant legislation, and for study or research purposes, or any other legal use. With this aim in mind, the University undertakes the following duties and reserves the following powers:

a) The University shall inform the archive users of the permitted uses; however, it shall not guarantee or take any responsibility for any other subsequent ways the work may be used by users, which are non-compliant with the legislation in force. Any subsequent use, beyond private copying, shall require the source to be cited and authorship to be recognized, as well as the guarantee not to use it to gain commercial profit or carry out any derivative works.
b) The University shall not review the content of the works, which shall at all times fall under the exclusive responsibility of the author and it shall not be obligated to take part in lawsuits on behalf of the author in the event of any infringement of intellectual property rights deriving from storing and archiving the works. The author hereby waives any claim against the University due to any way the users may use the works that is not in keeping with the legislation in force.
c) The University shall adopt the necessary measures to safeguard the work in the future.
d) The University reserves the right to withdraw the work, after notifying the author, in sufficiently justified cases, or in the event of third party claims.

Madrid, on 3 of June, 2019.

HEREBY ACCEPTS

Signed.....

Reasons for requesting the restricted, closed or embargoed access to the work in the Institution's Repository

Declaro, bajo mi responsabilidad, que el Proyecto presentado con el título

Design of Syringe-based Extrusion Mechanism for 3D Food Printer

en la ETS de Ingeniería - ICAI de la Universidad Pontificia Comillas en el curso académico Spring.2019. es de mi autoría, original e inédito y no ha sido presentado con anterioridad a otros efectos. El Proyecto no es plagio de otro, ni total ni parcialmente y la información que ha sido tomada de otros documentos está debidamente referenciada.

Fdo.: (Nombre del alumno) Fecha: 5.../20.../2019

Autorizada la entrega del proyecto

EL DIRECTOR DEL PROYECTO

Fdo.: (Nombre del Director) Fecha: 5.../20.../2019

Sayed S. Aziz

GRADO EN INGENIERÍAEN TECNOLOGÍAS INDUSTRIALES

TRABAJO FIN DE GRADO

DESIGN OF A SYRINGE-BASED EXTRUSION MECHANISM FOR 3D FOOD PRINTER

Autor: Marta Iribarren García

Director: Elsayed Aziz Ramadan

Madrid

Junio de 2019

DISEÑO DE UN MODELO 3D DE LA JERINGUILLA PARA UNA IMPRESORA DE COMIDA 3D

Autor: Iribarren García, Marta

Directores: Aziz Ramadan, Elsayez

Entidad Colaboradora: Stevens Institute of Technology

1. Introducción

El presente trabajo tiene por objeto el análisis de las viabilidad de la impresión 3D aplicada a los alimentos humana. Para conseguir esta posibilidad es preciso, en primer lugar, que el producto elaborado sea una comida al menos de la misma calidad y, en segundo lugar, que su preparación con las impresoras 3D ofrezca ventajas respecto al método de cocina convencional.

La impresoras 3D capaces de elaborar productos alimenticios no están en la actualidad desarrolladas íntegramente pues existe un conflicto entre el tiempo y la precisión de la impresión. Además no presentan una ejecución de la comida más simple o rápida de la actual. Sin embargo, ofrecen los medios para obtener comidas completamente personalizadas dando la posibilidad al consumidor de controlar las propiedades nutritivas de la comida. Por otra parte, las impresoras 3D para comida permiten la introducción de alimentos con propiedades proteicas muy favorables, con resultados similares a las comidas convencionales, sin apenas detectar diferencias de sabor o tacto. Esto supone una gran ventaja en el ámbito medioambiental pues la utilización de nuevas fuentes alimenticias sostenibles que pueden sustituir a las actuales significando la reducción del uso de estas. Además, según los expertos, se estima que la población mundial en 2050 rodeará las 9000 millones y consecuentemente habrá escasez de recursos naturales.

Las impresoras 3D para comida no presentan muchas diferencias con una impresora 3D habitual en lo que al mecanismo de funcionamiento se refiere. Las impresoras para comida introducen como mecanismo la extrusión del material, que en este caso será un puré de comida, a través de una jeringuilla. Este mecanismo es muy habitual en las impresoras 3D para imprimir filamentos de materiales termoplásticos, dicho proceso se aplica a tecnologías de Modelado por Deposición Fundida (MDF). La principal diferencia entre la aplicación de este mecanismo a una impresora de 3D para comida y a una impresora 3D normal es que el material termoplástico es derretido a la vez que es extruido mientras que para imprimir la comida, la impresión se realiza a temperatura ambiente o a la temperatura de gelificación. La temperatura de gelificación para los materiales utilizados en una impresión de una comida es mucho menor que la temperatura para derretir un termoplástico, por ello en la impresión de un termoplástico hay que utilizar una fuente térmica aplicada a la jeringuilla. La ausencia de dicha fuente hace que el comportamiento

del material alimenticio sea más fácil de describir pues el material no sufre un cambio de estado lo que supone que las propiedades del material no cambian radicalmente.

Después de hacer un diseño en 3D de lo que se quiere imprimir y convertirlo en un archivo STL, la impresión de comida de realiza a través de un mecanismo que controla la extrusión del material. Existen tres configuraciones principales para ello, la primera es controlada mediante un pistón y un motor paso a paso; la siguiente consiste en producir la extrusión mediante aire comprimido; y, en la tercera configuración, la extrusión se lleva a cabo a través de un tornillo rotativo. Para que el material tenga las propiedades deseadas para que la impresión sea lo más óptima posible y tenga las propiedades deseadas nutricionalmente, son añadidos hidrocoloides a las materiales alimenticios.

En este proyecto, se analiza el funcionamiento de la extrusión controlada por un motor paso a paso y un pistón. En el análisis se diseña una jeringuilla y se simula el flujo de chocolate por ella.

2. Metodología

Para el diseño de la jeringuilla se formuló un problema de optimización cuyo objetivo fue maximizar la velocidad de extrusión para así reducir el tiempo de impresión. Con el fin de obtener un problema sencillo de optimización y situarnos en el peor escenario, se supuso que el chocolate se comporta como un fluido newtoniano. En realidad, el chocolate se comporta como un fluido no newtoniano pseudoplástico, cuya viscosidad aparente se reduce con el gradiente del esfuerzo cortante, por lo tanto la viscosidad de un fluido newtoniano siempre será mayor y por la tanto la velocidad menor y, consecuentemente, el esfuerzo cortante en las paredes internas de la jeringuilla será mayor. Para ello, se obtuvieron una serie de restricciones y condiciones que el material, en este caso el chocolate, debía cumplir. Estas condiciones fueron principalmente derivadas de la Ecuación de Bernoulli y de aplicación de la ley de Poiseuille a las ecuaciones de Navier Stokes. Las demás condiciones se centran en limitaciones geométricas y estructurales para no sobrepasar ningún límite de rigidez con el fin de evitar grietas en la jeringuilla.

Le ecuación de Bernoulli fue aplicada a lo largo de la jeringuilla teniendo en cuenta las perdidas primarias en los dos tramos diferentes de la estructura de la jeringuilla y las perdidas secundarias correspondientes a la vena contacta. Estableciendo la presión de salida a la ambiente se pudo obtener la presión ejercida por el pistón al comienzo de la extrusión en función de la velocidad en dicho punto, la velocidad de salida y las dimensiones de la jeringuilla.

Por otra parte, la Ley de Poiseuille, se aplicó en los dos tramos diferenciados por la geometría de la jeringuilla. Tras aplicar dicha ley utilizando condiciones de contorno se obtuvo el esfuerzo cortante y la velocidad en función del radio de la jeringuilla pudiendo así obtener los valores máximos de ambas.

Para evitar grietas en la superficie de la jeringuilla se estudió el espesor mínimo de esta y el tipo de grieta creado por la tensión normal a la que esta sometida la jeringuilla debido a la presión que ejerce el fluido. Para evitar que el fluido provocase tensiones en la jeringuilla superiores al límite elástico se obtuvo la tensión principal máxima, teniendo en cuenta el esfuerzo normal creado por la presión y el esfuerzo cortante debido al fluido en movimiento, y estableciendo que fuesen menores que el límite elástico.

Una vez obtenido el diseño de la jeringuilla se realizó una simulación utilizando SolidWorks. Esta simulación se realizo con las propiedades correspondientes al chocolate, es decir, su comportamiento pseudoplástico. En dicha simulación se utilizó el diseño obtenido en el problema de optimización y se analizó la distribución de presión, velocidad, viscosidad aparente y esfuerzo cortante. Además el chocolate es un material viscoelástico, es decir, tiene comportamiento elástico lo que significa que no es incomprensible. Por lo tanto, se analizó el comportamiento teórico del fluido ignorando su carácter viscoelástico y se comparó con los resultados obtenidos por la simulación para entender la influencia de la viscoelasticidad.

3. Resultados

Para el programa de optimización la presión de salida se fijó a la de ambiente y el flujo a laminar. Teniendo esto en cuenta y utilizando MATLAB se obtuvo los siguientes resultados:

$$D_1: 0.0755\ m$$

$$L_1: 0.1510\ m$$

$$D_2: 0.0151\ m$$

$$L_2: 0.0050\ m$$

$$v_1: 0.0627\ \frac{m}{s}$$

$$v_2: 0.2292\ \frac{m}{s}$$

$$P_1: 100000\ Pa$$

$$P_1': 1000 Pa$$

$$h_T: 7.5655\ m$$

$$t: 0.01\ m$$

Con estos resultados se pudo obtener la siguiente jeringuilla:

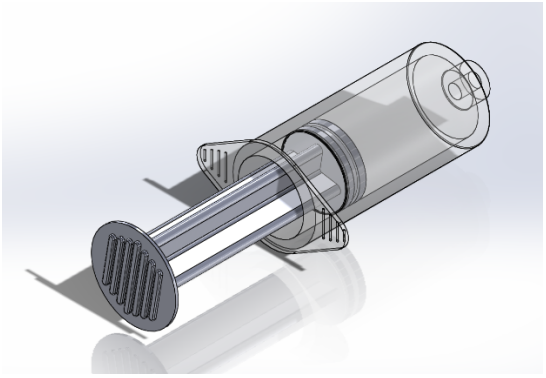

Una vez obtenida la jeringuilla se diseño una serie de estructuras para que el flujo a través de ella estuviese controlado por un motor paso a paso

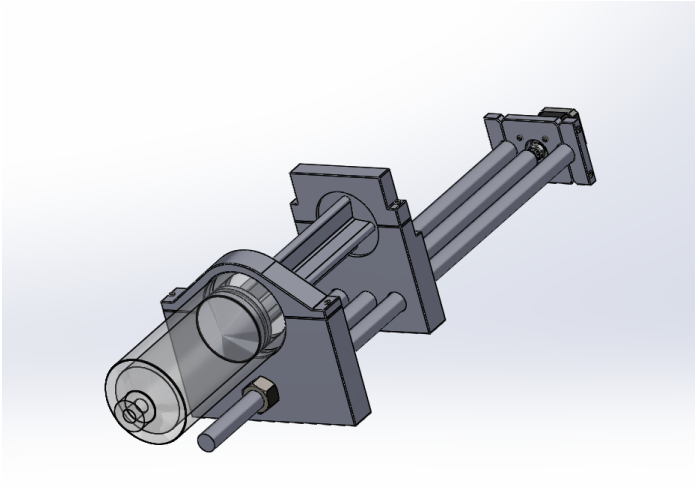

A continuación se realizó la simulación introduciendo las propiedades del chocolate en SolidWorks y fijando la presión de salida a la ambiente y la velocidad de pistón a la obtenido por el problema de optimización. Los resultados de la distribución y variación de los parámetros estudiados fueron:

- Viscosidad aparente:

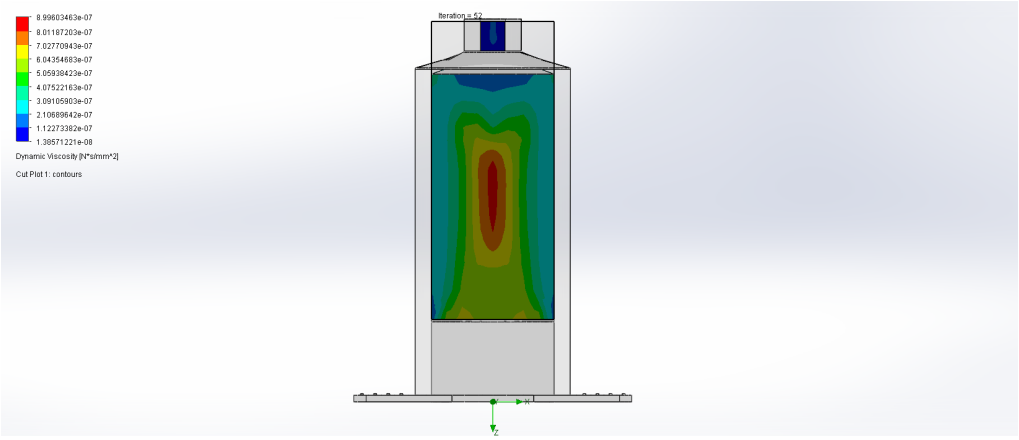

- Presión:

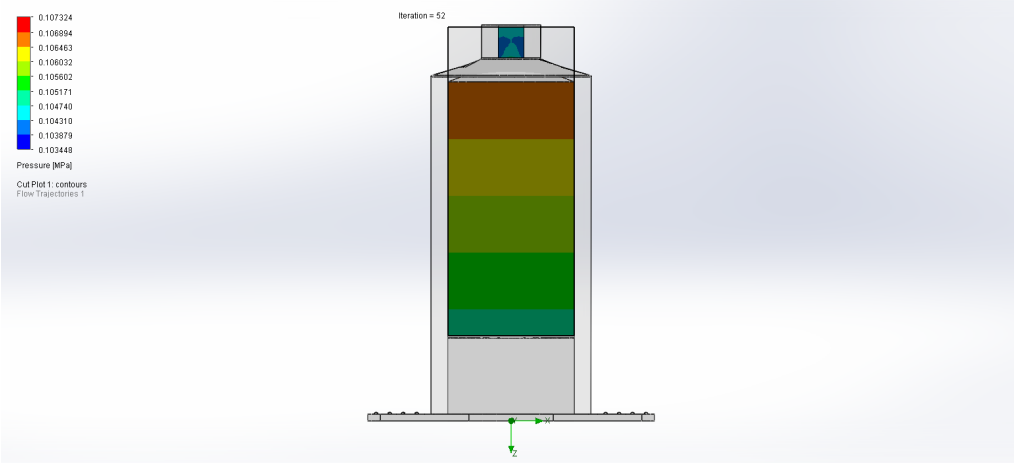

- Esfuerzo cortante:

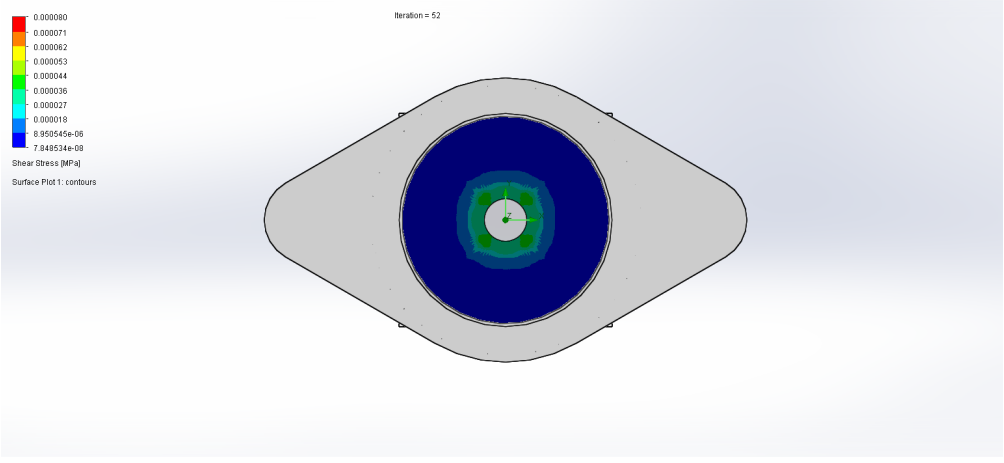

- Velocidad:

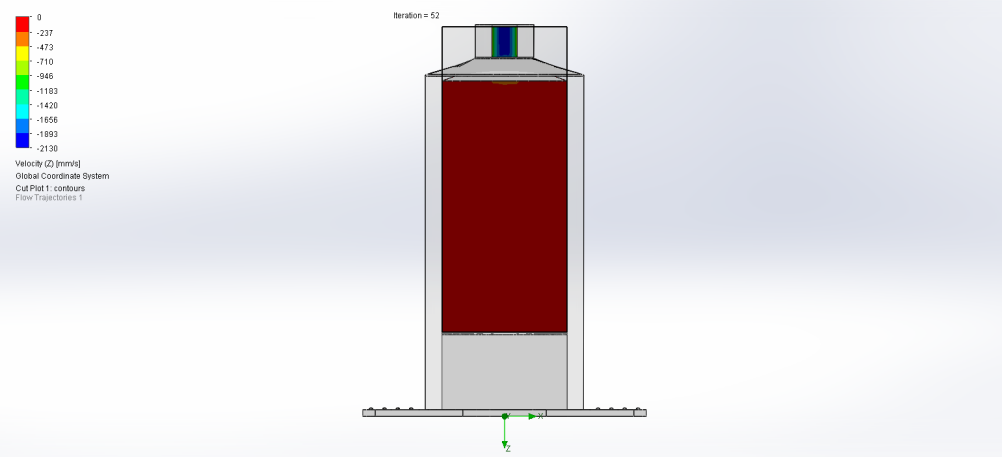

Para finalizar, se llevó a cabo un análisis teórico del fluido teniendo en cuenta que se comporta como un fluido no newtoniano y se obtuvieron los siguientes resultados:

$$v_2 = 1.5675 \frac{m}{s}$$

$$rpm = 25.08\, rpm$$

$$p_1 = 12313.8068\, Pa$$

$$P_1 = 113613.8068\, Pa$$

$$F_1 = 501.9304\, N$$

4. Conclusiones

Como todo proyecto innovador, para la completa introducción en la sociedad de las impresoras 3D para comida, es necesario seguir un gran desarrollo del producto para que satisfaga todas las necesidades del consumidor. El hecho de que en la actualidad no sea un producto viable para el uso domestico no implica que en un futuro no lo sea. Uno de los objetivos de este proyecto ha sido buscar formas de mejorar el producto con el fin de adaptarlo a las cocinas de hoy en día centrándose así en reducir el tiempo de impresión.

Respecto a los resultados obtenidos en SolidWorks y en el análisis teórico se puede

observar las diferencias entre un fluido newtoniano y uno pseudoplástico pues estos últimos permiten que el fluido alcance velocidades mayores con menor esfuerzo cortante. Además, describir el comportamiento de un fluido viscoelastico es una tarea de gran complejidad pues dicho análisis es integral o diferencial con expresiones de alta dificultad. Gracias a ambos resultados se pudo comprobar como todos los parámetros calculados dependen de esta propiedad.

DESIGN SYRINGE-BASED EXTRUSION MECHANISM FOR 3D FOOD PRINTER

Author: Iribarren García, Marta

Directors: Aziz Ramadan, Elsayed

Collaborating Entity: Stevens Institute of Technology

1. Introduction

This document presents the introduction of 3D printing applied to food in society. In order to achieve the implantation of 3D food printers to be viable nowadays, they need to offer advantages among conventional cooking at the same that they solve a problem.

Nowadays, food printers are not completely developed since there is a trade-off between time and accuracy of printing. In addition, they do not present an easier of faster execution of the food than the actual way of cooking. However, food printers offer the opportunity of obtaining food which is completely personalized giving the possibility to the consumer to control the nutritional properties of the food. Food printers also allow the introduction of aliments with great protein properties that are not common without hardly having influence in the taste or feeling. This ability means a great advantage in the environmental field since the use of these new sustainable food sources can substitute the common sources reducing the use of them. Furthermore, experts expect the population to grow to 9000 million in 2025 and consequently there will be a shortage of resources.

Regarding the operation, 3D food printers do not present a lot of differences with a regular 3D printer. Food printers introduce as mechanism material extrusion, which in this case the material will be food puree, along a syringe. This mechanism is very common in 3D printers that use filaments of thermoplastic, this process is applied to Fused Deposited Modeling (FDM). The principal difference between the application of this mechanism to a food 3D printer and a regular 3D printer is that the thermoplastic material needs to be melted at the same time it is extruded while in the food printing process, the printing is usually done at environmental temperature or at gelation temperature. Gelation temperature of the food inks used in food printing is much lower than the temperature needed to melt a thermoplastic. Therefore, in the printing of a thermoplastic, a thermal source is required at the nozzle. The lack of this thermal source makes the food ink behavior much easier to describe since the food material does not suffer a change of state, and therefore, its properties do not change drastically.

After designing a 3D prototype of the food to be printed and converting it in a STL file, the printing of food is done thanks to a mechanism that controls the material extrusion.

There are three main configurations to do so. The first one is controlled by a piston and a stepper motor, the second uses compressed air to extrude the material and in the third configuration, the extrusion is done by a rotating screw. In order to achieve the best material properties so that the printing is the most optimized possible and the food material has the desired nutritional properties, hydrocolloids are added to the food inks.

In this project, the performance of the extrusion was controlled by a stepper motor and a piston. In this analysis, a syringe was designed and simulation of the flow of chocolate along the syringe was run.

2. Methodology

For the syringe design, an optimization problem was formulated. The objective of this optimization problem was to maximize the velocity of extrusion so the time of printing was reduced. In order to get a simple optimization problem and study the worst scenario, it was supposed that the chocolate has a Newtonian behavior. In reality, chocolate behaves as a non-Newtonian with shear thinning characteristics, these are that the apparent viscosity decreases when shear stress is increased. Therefore, the viscosity of a Newtonian fluid will be always greater and, therefore, velocity will be lower and, consequently, the shear stress on the inside walls of the syringe will be greater. For the problem formulation, some constraints, which the flow of chocolate needed to meet, were obtained. These constraints were mainly obtained from Bernoulli's Equation and the application of Poiseuille's Law to Navier Stokes Equations. The rest of the constraints focus on geometric and structural limitations so that any elastic limit was exceeded to avoids cracks on the surface of the syringe.

Bernoulli's Equation was applied along the syringe having into account that there are different primary losses in the two different parts of the syringe and the secondary losses due to the vena contacta. Once the pressure at the exit of the nozzle was set to the environmental, the pressure of the piston on the material at the beginning of the extrusion could be obtained in function of the piston velocity at that point, the exit velocity and the syringe dimensions.

Then, Poiseulle's Law was applied in the two geometric different parts. After applying Poiseulle's Law and the boundary conditions, the shear stress and the velocity in function of the radius of the syringe were obtained, which allowed to also obtain the maximum values of both parameters.

In order to avoid cracks in the surface of the syringe, the minimum thickness of the syringe was studied as well as the type of crack induce by the normal stress created by the pressure of the fluid on the syringe. To avoid the fluid to provoke stresses greater than the elastic limit the maximum principal stress was calculated. To calculate the principal stresses, the normal stress due to pressure and the shear stress created by the movement of the fluid.

Once the design of the syringe was obtained, a simulation using SolidWorks was run. This simulation was done using the chocolate properties corresponding to its shear thinning behavior. In this simulation, the design obtained by the optimization problem was used and the pressure, velocity, viscosity and shear stress distribution was analyzed. Chocolate is also a viscoelastic material, which means that has elastic behavior, this is to say that it is not incompressible. Therefore, ignoring the viscoelastic property of chocolate, the theoretical behavior of the shear thinning was studied and compared with the results obtained by the simulation. This comparison allows understanding the influence of the viscoelasticity on a material flow.

3. Results

For the optimization problem, the exit pressure was set to the environmental pressure and the flow was supposed laminar. Having all this into account and using MATLAB, the next results could be obtained:

$$D_1: 0.0755\ m$$

$$L_1: 0.1510\ m$$

$$D_2: 0.0151\ m$$

$$L_2: 0.0050\ m$$

$$v_1: 0.0627\ \frac{m}{s}$$

$$v_2: 0.2292\ \frac{m}{s}$$

$$P_1: 100000\ Pa$$

$$P_1': 1000 Pa$$

$$h_T: 7.5655\ m$$

$$t: 0.01\ m$$

With these results the next syringe was obtained:

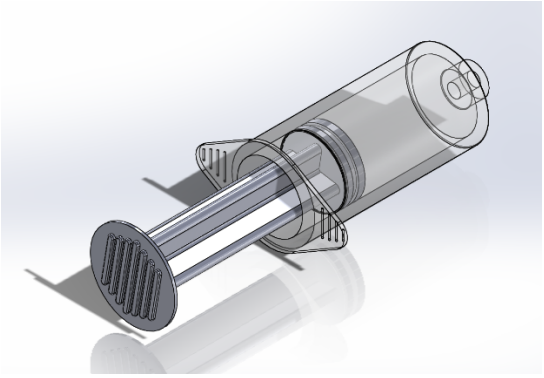

Once the syringe was designed, some structures needed to be also designed so the extrusion of the food material was controlled by a stepper motor

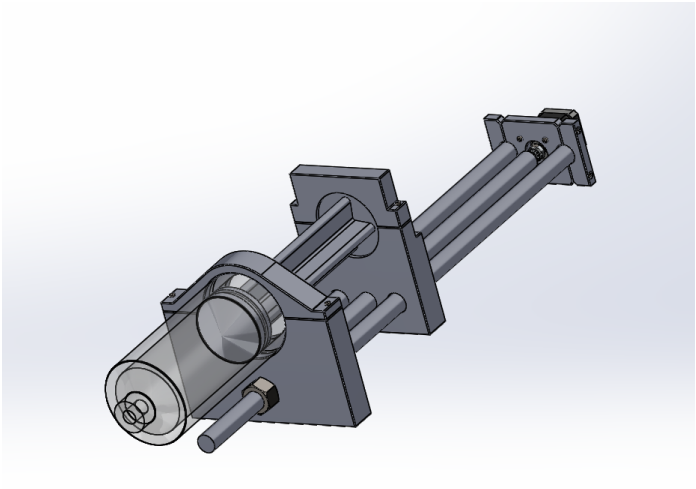

Then, a simulation was run. For the simulation, the chocolate properties in SolidWorks were introduced and the exit pressure was set to the environmental pressure and the piston velocity was set to the velocity obtained by the optimization problem. The results of the distribution and variation of the parameters studied were:

- Apparent viscosity:

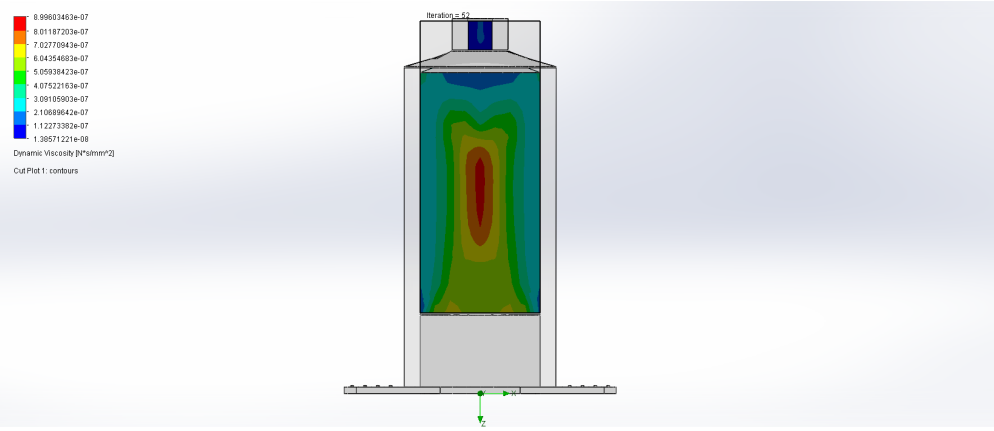

- Pressure:

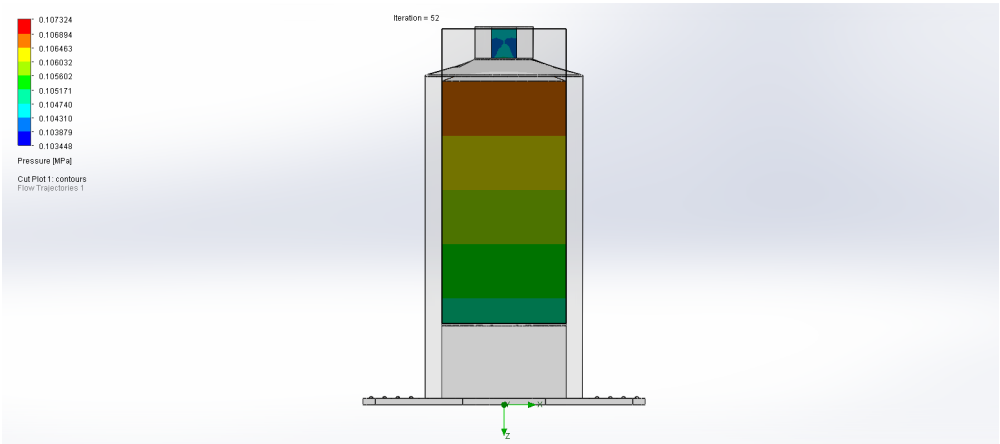

- Shear Stress

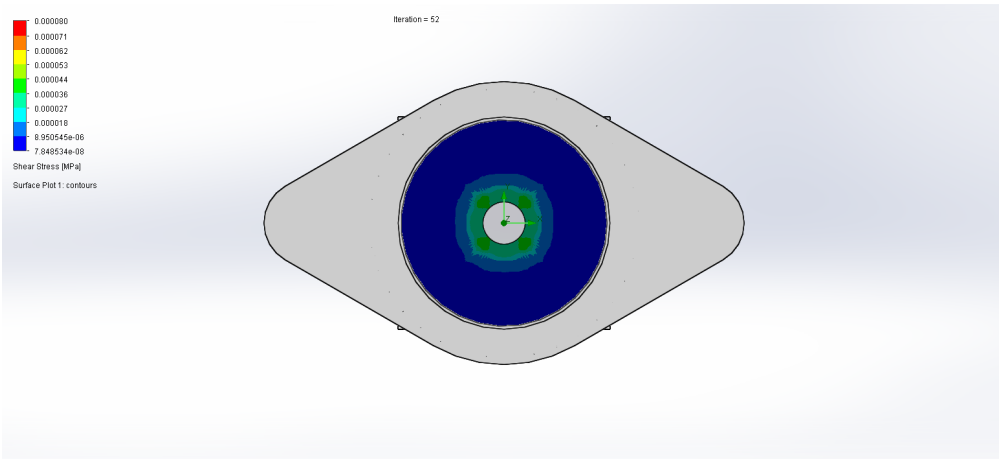

- Velocity:

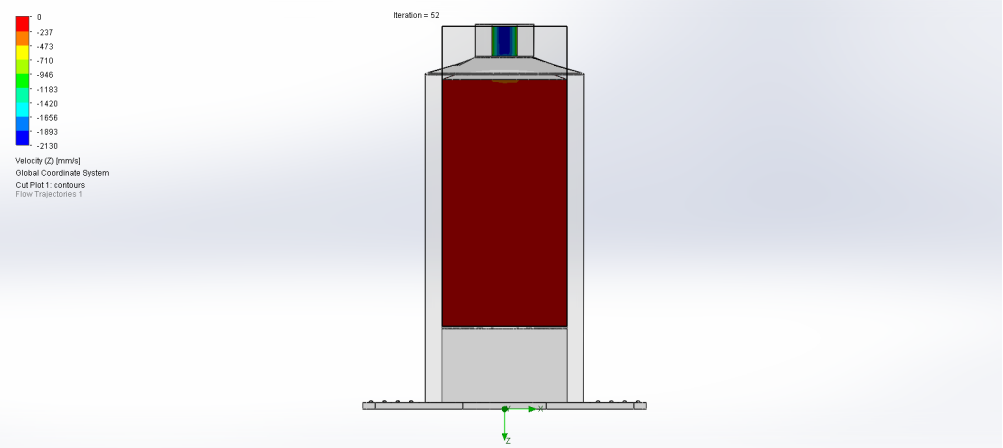

To finish with the analysis, a theoretical analysis having into account that it has a non-Newtonian behavior and the next results were obtained:

$$v_2 = 1.5675 \frac{m}{s}$$

$$rpm = 25.08\ rpm$$

$$p_1 = 12313.8068\ Pa$$

$$P_1 = 113613.8068\ Pa$$

$$F_1 = 501.9304\ N$$

4. Conclusions

Like every innovative project, to achieve a complete introduction in society of 3D food printers a great development of the product needs to be done so it satisfies all the consumer's necessities. The fact that nowadays 3D food printers is not a viable product does not mean that in the future it won't. One of the objectives of this project was to find ways to improve the product with the finality to adapt it the current kitchens and way of cooking focusing on reducing the time of printing.

Regarding the results obtained in SolidWorks and the theoretical analysis, differences between the Newtonian fluids and shear thinning fluids could be observed. Shear thinning fluids allow the material to move at greater velocities with lower shear stress.

Index

Index of figures

Chapter 1:

Descriptive Memory

1.1. Introduction

3D printers are a new generation of machines considered remarkable. 3D printers have the ability to produce, using different materials, different kinds of objects and all coming from the same machine [1]. 3D printing, also known as additive manufacturing and rapid prototyping, meant a new way to manufacture since it gives the opportunity of not using a mold [2]. The first 3D printing attempt started with Dr. Kodama and his development of a rapid prototype technique in 1980. This technique describes a layer by layer approach for manufacturing. Over less than ten years later, 3D printing was born [3]. Since then the development of 3D printing has grown significantly having a great number of different applications in various fields. 3D printers are mainly used for product development, manufacturing aids, end-use parts, architecture concepts or medical procedures [4]. But that is not it, due to its great development and to new necessities, 3D printers have new and innovative applications leading to the creating of 3D food printers.

Broadly speaking, a food printer is a machine that can turn digital recipes into edible and even delicious morsels. The need for 3D food printers is to design and produce personalized food in an affordable way. They would also aim to make food more testable in order to achieve a better eating experience. At first, 3D food printing may seem a way to get unhealthy and more processed food. But what is needed to keep in mind is that the ingredients used to produce the food can be chosen when sometimes we don't know what it's in some of the foods bought in the supermarket. Some types of ingredients are fruits and vegetables, doughs and batters, wheat and grains, proteins, sauces, dairy products, candy, chocolates, sugars or algae [5]. Also, unusual ingredients that are high in nutrition can be converted into 3D printing ingredients such as algae, insects and beet leaves creating new tastes. Therefore, 3D printing means a new way to produce innovative food quickly and with less waste while making food more attractive and more nutritious by adding special ingredients to recipes [6].

The most important application for 3D food printers is in the medical field. First of all, the meal can be perfectly adaptable to the patient's nutritional needs and lead to a better recovery. There is even the possibility to introduce the medicine in the food without the patient noticing any difference in taste or shape of the food. One major example is the case of dysphagia. Dysphagia is a condition where a patient is incapable to swallow food in a safe manner. The use of 3D printing will allow transforming shapeless purees into 3D structures that patients will recognize as conventional food. 3D printers also give the opportunity to obtain specific nutritional content by carefully selecting the food ink formulation [7].

The basic concept of 3D printing is similar to a regular printer. While in regular printing the printer only needs to print one layer of ink on a flat 2D printing paper, in 3D printing there is one extra dimension [8]. The way to achieve this third dimension is, first, obtaining a digital design using a CAD program of the desired product. The next step is to dismantle the 3D model into individual print layers and the required printing parameters are defined. In order to make this design printable, the 'G-code' file containing all relevant information, such as movement coordinates and movement speed, is transferred to the printer [9].

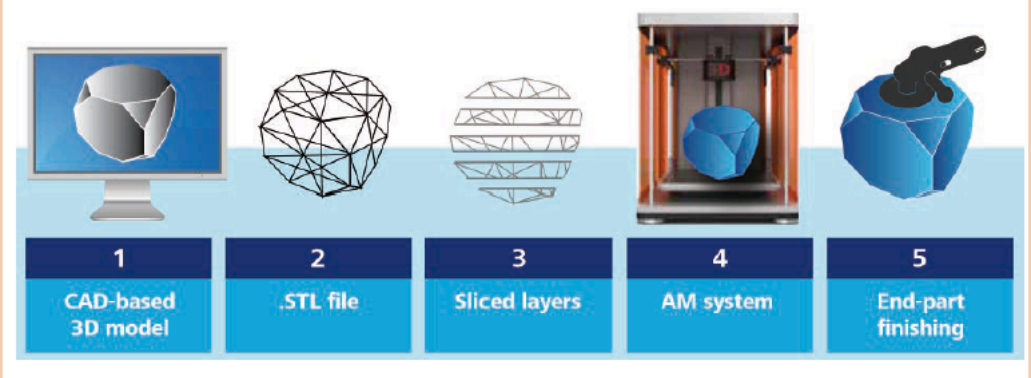

Figure 1: General production process in 3D printing [10]

Depending on the material used and the type of product we want to get there are different technologies and printers [8][11]:

1. Material Extrusion: A filament of thermoplastic material is extruded through a heated nozzle while it gets melted. The material is then deposited on a build platform along a predetermined path controlled by a computer. Once the material is on the build platform the filaments cool down and solidify to form a solid object. This process is applied to Fused Deposition Modeling (FDM) technology which is the most common and cheapest.
2. Vat Polymerization: a vat of liquid photopolymer resin is used and cured by ultraviolet light. There are two technologies that use this process:
    - Stereolithograohy (SLA): SLA printers use two mirrors with one located on the X axis and the other one in the Y axis. The mirrors aim a laser beam across a vat resin selectively curing and solidifying a cross-section of the object.
    - Digital Light Processing (DLP): A digital light projector flashes one image of each layer at once. Using LED screens and UV light sources, light is projected onto the resin.
3. Powder Bed Fusion: A thermal energy source will selectively induce fusion between powder particles in order to create a solid object. The scanned powder due to melting will bind together while the un-scanned powder will still be loose and remains in position. This process is used in Selective Laser Sintering (SLS) technology. In SLS, polymer powder is first heated to a temperature below the melting point. Then, a very thin layer of the powdered material is deposited by a recoating blade or wiper on the built platform. The laser will sinter the following cross-sections onto the previously solidified.
4. Material Jetting: Photopolymers or wax droplets are selectively deposited and cure. The print head jets hundreds of tiny droplets of material and then solidifies them with the help of ultraviolet light. One technology that uses this process is Drop on Demand (DOD) that uses a pair of inkjets. One deposits the build material while the other one is used for dissolvable support material.
5. Binder Jetting: a liquid bonding agent selectively links regions of a powder bed. Materials usually need another process after printing in order to improve material properties. There are two different ways to apply this process:

- Sand Binder Jetting: In order to obtain full-color models, the printer head first needs to jet the binding agent while a secondary print head jets in color. Once the parts are fully cured, they are removed from the loose unbounded powder and cleaned.
- Material Binder Jetting: First a binding agent is used to bound the metal powder particles to form a ‘’green state’’ object. Once the objects are cured, they will be removed from the loose powder and placed in a furnace where the binder will be burnt out. Next, bronze is used to infiltrate the voids via capillary action.

6. Powder Bed Fusion: This process uses a thermal source that induces fusion between metal powder particles one layer at a time with the objective of producing solid objects. The two technologies that use this process are:
   - Direct Metal Laser Sintering (DMLS)/ Selective Laser Melting (SLM): They are both similar to SLS. DMLS heats the powder to a point so that can fuse together on a muscular level. SLM will use laser technology to obtain a full melt of a metal powder forming a homogeneous part.
   - Electron Beam Melting (EBM): Uses a high energy beam, or electrons, to induce fusion between the particles of metal powder. A focused electron beam scans across a thin layer of powder causing localized melting and solidification of a specific cross-sectional area.

1.2. Problem Statement

The essential difference for 3D food printing is the use of food materials instead of plastics or metals for the 3D printing process. Therefore, the working principle of 3D printing is applied to 3D food printers. However, there are different methods depending on the nature of the source material [8]:

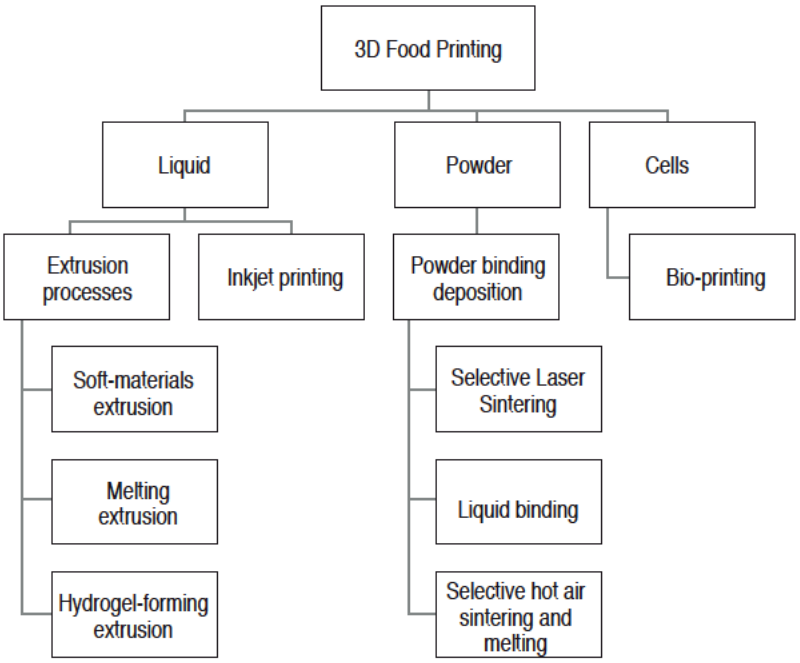

Figure 2: Classification of the different mechanisms of 3D food printing[10]

1. Extrusion-based methods and methods on pulverized foods: Liquid or soft foods such as melted chocolate, fondant, pasta, dough, as well as fruit and vegetable purees are used. The mass is first filled into a cartridge and then squeezed under pressure through an extrusion nozzle. The selection and nature of the foodstuffs determine the dimensional and form stability. Accordingly, the printed object can maintain their form due to their rheological properties, the subsequent cooling phase or the additional use of hydrogel.
2. Powder-based: Some materials such as sugar, cocoa powder or seasoning are used in order to create more complex forms. The material is first spread over a level surface which can be lowered. A heat source is used to heat the particle of each layer along the coordinates and thus melt together at the appropriate places. The building platform is then lowered by one layer thickness and a new set of powder material will be spread over. This process will be repeated until the object is completely printed.

The most common technology for 3D food printing is extrusion-based since they seem to be the easiest option to implant a huge scale and the range of food options is greater. Among the extrusion-based printers, there are different types. The first classification is according to the multi-axis stage [11]:

1. Cartesian: Due to its simplicity and intuitive control, this system is the most common. In this configuration, there are X, Y and Z axes to control the movement of the syringe: left to right, front to back and up and down motion respectively.

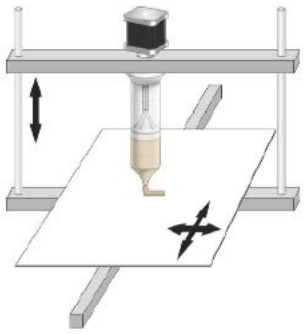

Figure 3: Cartesian configuration [13]

2. Delta: The print head of the nozzle is mounted on a base at the intersection of three carriages relative to each other. This configuration carries very little weight on the base which allows the print head to move faster.

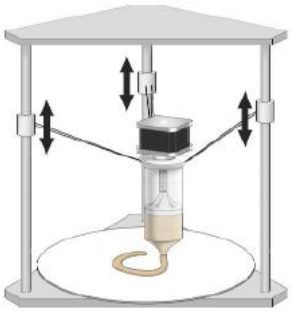

Figure 4: Delta configuration [13]

3. Polar: This configuration uses polar coordinates to describe on a circular grid. Polar food printers usually have a print head that moves up-down along Z axis and left-to left along X and Y tangentially in addition to a spinning stage. It is easy to calibrate and can build greater volume objects at a greater speed.

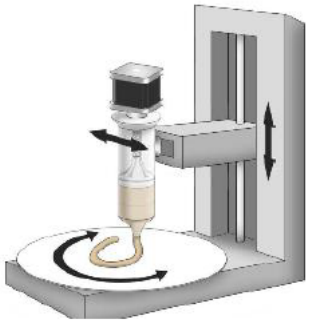

Figure 5: Polar configuration [13]

4. Selective Compliant Assembly Robot Arm (SCARA): This design consists of a robot arm moving along X-Y plane. They also have an actuator to move along Z axis.

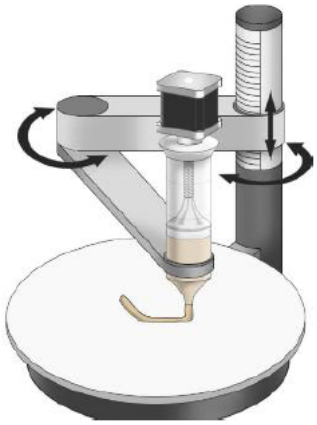

Figure 6: SCARA configuration [13]

For extrusion-based 3D printers, there are two major components. The first one would be the printer which has the objective of controlling the movement and position of the nozzle and the second component is the extruder which controls the material flow. The three most common types of extrusion systems are:

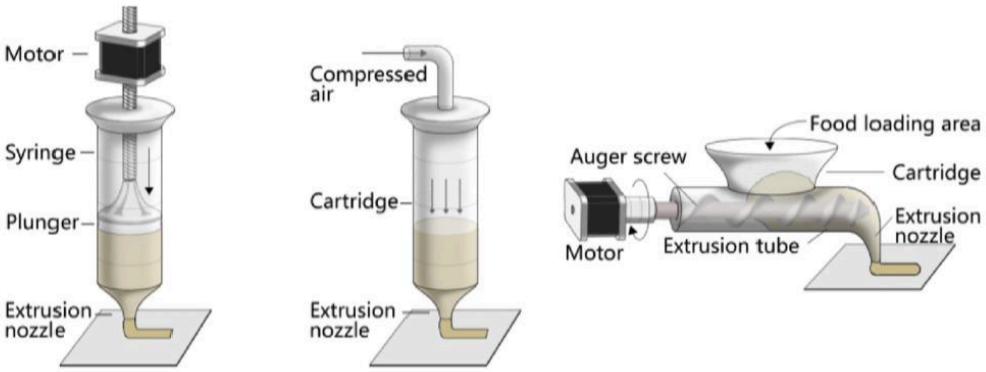

Figure 7: Types of extrusion mechanism [13]

1. Stepper motor driven piston: The stepper motor will make the gear turn controlling the movement of the piston. The piston will, then, push the material down. Since there is physical contact between the material and the piston, the control of the extrusion rate will be better. The material will be extruded through the nozzle into the build platform. However, there is a time delay when starting and stopping the extrusion process which affect on the accuracy of the object printed. [11].
2. Pneumatic extrusion: In this system, the driving force for extrusion is compressed gas. Since the cartridge can be pressurized and despressurized very fast, this system can extrude a wide range of viscoelastic inks with a fast response [11].
3. Extrusion by means of rotating screw: A single screw extruder to deliver material from the hopper to the nozzle is used. The screw rotates and conveys the material into a chamber that is heated from the outer side by heating elements. Then the material will be extruded through the nozzle onto the build platform. This system of extrusion allows continuous printing since the material can be loaded as required. In addition, the rotating screw also helps mix the material as it is being printed ensuring the homogeneity and preventing phase separation. One disadvantage of

this design is that since the material is not stored in separate cartridges, there is a possibility of cross-contamination [12].

1.3. Motivation

Foods are starting to be more customized and consumers seek food that tastes great, looks even greater while being healthy. Technologies which were developed for general manufacturing have been adapted for a specific use in food manufacturing. Some of this technologies are steam power, mechanical mixing, electrical heating, computer and robotic manipulation. Every of these technologies has meant a change in food manufacturing as we knew it. Therefore, the introduction of 3D food printing is expected to have at some point the same effect [13].

3D food printing is an emerging technology which has the ability of manufacturing food with a desired shape, taste and structure. Nowadays, consumers' attitude for food decision is based on nutrition, taste, cost and convenience. However, due to costumer's growing attention to personal health, products that focus on personal care and healthy concepts are considered to be a new trend. It is known that food and its effect on the metabolism changes among all the different individuals. Therefore, the market to produce personalized healthy food is growing very fast [14].

3D Food printing is also an introduction to use another type of aliments with great nutritional properties that we are not used to, such as insects or algae. In 2050, the population is expected to be around 9 billion people. Therefore, by then some changes in the food chains as well as in the resources used need to change since most of them are not renewables and will be almost gone. The use of 3D printing has the potential to fix this situation in an easy and non-socking way by producing recognized conventional food [2].

However, in the present 3D food printing is not relevant for mass production. There is a gap between consumers' needs and current functionalities of the food printer. Furthermore, there is a trade-off between production time and quality [8]. In addition, an accurate selection of materials with appropriate properties is essential.

The aim of this project will be to design an extrusion-based syringe by means of a stepper motor driven by a piston. In the design of the extruder, one of the most important aspects is to determinate the dimensions of the extruder, as well as the extrusion velocity. All values will depend on the material used. The two most important properties of the material will be the viscosity and the viscoelasticity.

The overall perception of food design covers visual appearance, sense of touch, first bite, chewing, swallowing and residual effect on the mouth. However, since the purpose of a 3D food printer is to make food and the material will be the ingredients of the food obtained, the choice of material will be one of the most important things to decide.

1.4. Project objectives

The main objective of this project is to design the extruder of the printer. To do so, we need to determinate:

1. The most generic material to use for the design so that we don't have to try with every material.
2. The dimensions of the extruder, especially the dimensions of the syringe since it will determinate the amount of material and the force needed.
3. Obtain an approximate optimum design so a simulation can be done.

1.5. Methodology of work

In order to design the syringe, first different materials and their properties from the literature will be analyzed to find one that can be considered as a model for the rest of the materials. Then, applying mechanical of fluids and thermodynamics the stresses on the piston and the syringe will be calculated. With this data, the material flow through the nozzle can be calculated as well as its behavior.

Once the parameters of the design are known, a 3D model will be obtained using SolidWorks and some test will be run to test and analyze how the syringe works.

The work plan can be:

1. Week1: (05/25-05/31): Analysis of materials
2. Week2: (04/1-04/7): Parameters of syringe
3. Week3: (04/8-04/14): Model in solid works and simulation
4. Week4: (04/15-04/21): Conclusions

1.6. Resources

The resources used will be basically the literature available on this topic that would be helpful to get experimental data such as the type of motor, the limits on the syringe size, flow speed, as well as material properties. Then, SolidWorks will be used to get a 3D design and to simulate.

Chapter 2:

Materials Review

2.1. Introduction

3D food printing can be considered a new technology that was born from the development of 3D printing. There are different mechanisms and techniques from 3D printing that can be applied to 3D food printers. Since most 3D food printers adopt the FDM mechanism, we would be centered in this mechanism designing the syringe for the extrusion process. In more detail, the extrusion system studied and, for which the syringe will be designed for, is by a stepper motor driven piston. With the design of the syringe, we are seeking to obtain the right dimensions and functioning parameters to obtain the most accurate and precise results possible.

The functioning of a 3D printer depends basically on the material used. In fact, the main difference between a 3D food printer and a 3D regular printer is the material used. Since the material used in 3D food printing is food, which is very different from the materials used in regular 3D printers that are mostly plastics, some adaptations need to be done.

2.2. Types of mechanisms

The material extruded in 3D food printing has more importance because it represents the ingredients of the recipes. Depending on the nature of the material, food ink, and the extrusion technique applied, materials can be divided into three groups [11]:

1. Cold extrusion: This technique is also known as room temperature extrusion. As its name indicates, the extrusion is done at room temperature, therefore, there is no temperature manipulation. Food inks used in cold extrusion have good rheology properties so there is no need to change the nature of it by heating the materials. However, the properties can be improved by adding thickeners or changing the composition.

2. Hot-melt extrusion: Hot-melt extrusion needs an initial heating phase so the material can flow through the syringe. The food material will be then heated to a few degrees above the gelation point which for the material used is around 30-40ºC which is much lower than the melting point for plastics such as ABS used in 3D regular printers. Those food inks that have a gelation temperature around or below room temperature need a cooling step so the ink solidifies once it's on the platform.
3. Gel-forming extrusion: The chemical or physical cross-linking of the material is needed for this extrusion technique. Unlike hot-melt extrusion, ionic species or ultra-violet lights are to achieve the gelation of the material.

2.3. Types of hydrocolloids

In addition to these techniques, to obtain better properties of the materials used to the food materials are printable and to obtain the results desired, hydrocolloids are added to food inks. Hydrocolloids are food additives that have the ability to interact and aim with water which allows them to act as a gelling agent, thickener or stabilizer. By controlling the amount of hydrocolloid, it's possible to achieve the shear thinning behavior desired, which has a high dependency on particle size [7]. There a lot of different types but the most common ones used in 3D printing are starch, xanthan gum, pectin, alginate, carrageenan and gelatin.

1. Starch: This hydrocolloid is composed by glucose monomers bonded by α-(1,4) linkages in amylose and α-(1,4) linkages and about 5% α-(1-6) branches linkages in amylopectin. Starch represents the primary source of energy and it can be found in green plants, seeds, fruits, stems, roots and tubers. Depending on the chain length, the ratio between amylopectin and amylose or the branching pattern and ratio, starch can be presented in different structures [16][17]. Starch has a high viscosity which slows down the digestion process as well as decreases blood glucose level. One example is potato starch in lemon juice.

2. Xanthan gum: Xanthan gum is an anionic polysaccharide due to the carboxylic acid groups found on its chains. It is formed by linear β-(1-4) linked glucose backbone with trisaccharide side chains. It has the ability to increase the viscosity of solutions with low concentrations which also slows down digestion and controls blood glucose level [11]. Xanthan gum solutions behave like a pseudoplastic fluid.
3. Pectin: It forms part of the polysaccharides and its composition is linear polymers of D-galactopyranosyluronic acid units joined in α-D(1-4) glycosidic linkages. The polymer chains are also esterified to different degrees with methanol. As most polysaccharides, pectin solutions present a pseudoplastic behavior [18]. Pectin has been used mixed with purees made from bananas, white canned beans, dried non-fat milk, lemon juice or dried mushrooms.
4. Alginate: Alginates are also polysaccharides obtained from brown seaweeds and are composed of β-D-mannuronic acid and α-L-guluronic acid [19]. It has a great number of applications due to its favorable properties, including biocompatibility and ease of gelation. It is very common in a solution mixed with sodium and calcium [20].
5. Carrageenan: This other hydrocolloid is composed of alternate units of D-galactose and anhydro-galactose linked by α-(1-3) and β-(1-4) glycosidic links. Viscosity increases exponentially with a higher molecular weight and higher solution concentration [21]. Carrageenan is usually used with alginate mixed with calcium.
6. Gelatin: It is a protein derived from collagen by controlled hydrolysis. The temperature has a lot of effect in gelatin solutions' viscosity showing different behaviors and forms such as viscoelastic liquid or gels [22]. Gelatin is the perfect hydrocolloid to use with meat.

Chapter 3:

Rheology Properties

3.1. Introduction

The importance of the properties of the materials is related to how they flow during the extrusion. The properties to study and analyze are the rheology properties that are the ones who describe how materials deform and flow. The two main properties are viscosity and viscoelasticity.

3.2. Viscosity

Viscosity is a specific property of fluids and describes the resistance to be deformed, which is related to tensile stress. It also provides information about the maximum source and tensile strength. Fluids can be classified according to which variables are the viscosity dependent [23]:

1. Newtonian fluids: The viscosity value of these fluids just depends on the temperature. Fluids with a small molecule size such as water, air, alcohol, or mineral oil are considered Newtonian fluid. For these fluids, the viscosity is described by Newton's Law:

$$\tau = \mu \frac{du}{dy} = \mu \frac{d\gamma}{dt}$$

Equation 1: Newton's Law

   The viscosity of Newtonian fluids can be considered constant since the relation between the shear stress and the shear rate varies linearly.

2. Non-Newtonian Fluids: Viscosity is dependent on many variables such as temperature, time or shear stress. These type of fluids are more difficult to describe their behavior since they have different behavior depending on the material. There are a few approximate models, one of them is the Power Law:

$$\tau = \eta \frac{d\gamma}{dt} \quad , \quad \eta = K \left(\frac{d\gamma}{dt}\right)^{n-1}$$

Equation 2: Power Law

In this case, the viscosity is represented by η, K is the consistency coefficient and n is the flow behavior index.

At the same time, depending on the behavior of these fluids with the shear rate are divided in:

- Shear thickening: This behavior is characteristic of those fluids that increase their viscosity when the shear stress rate is also increased. The number of fluids that are part of this group is not very high, some of them are some starch solutions or PVC solutions. The value of the flow behavior index is greater than one.
- Plastic behavior: This behavior is typical of those materials that act like elastic solid subjected to stresses lower than the yield stress. Once the stress is greater than the yield stress, the material is deformed as a fluid. Some examples of this type of materials are toothpaste, cream, jam or mayo.
- Shear thinning: Viscosity of these type of fluids is reduced when the shear stress rate is increased. The values of the flow index are between zero and one. There are a lot of materials that follow this behavior and the grade of viscosity has a great dependency on molecular mass and structure.

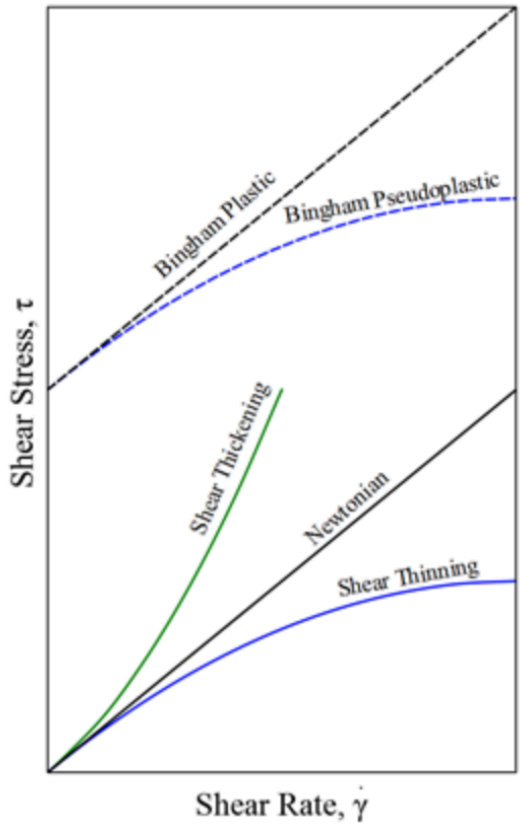

Plot 1: Graph showing the shear rate dependency in shear stress for different behaviors [24]

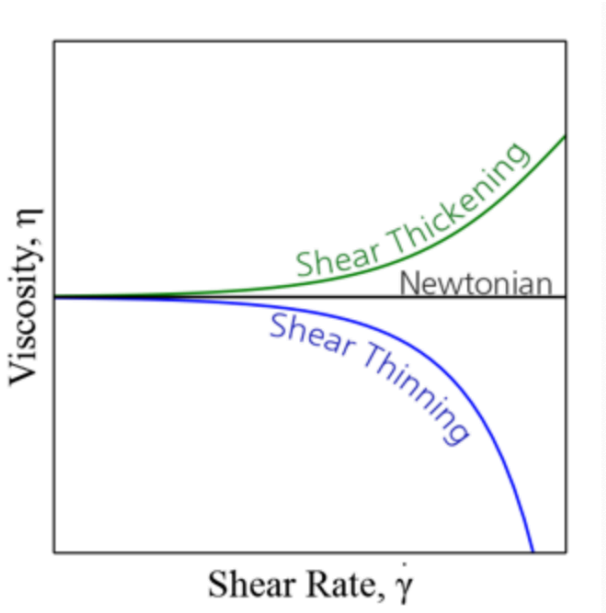

Plot 2: Graph showing the shear rate dependency in the viscosity for different behaviors [24]

3.3. Viscoelasticity

Viscoelasticity is the property that present materials that under deformation they have viscous and elastic characteristics. Since the viscoelasticity depends on the viscosity, there two types of behavior depending on if the fluid is Newtonian or non-Newtonian, in other words, if the viscosity is constant or not.

1. Linear behavior [25]: For the elastic behavior, mechanic properties are described by Hooke's Law stating that deformation is proportional to the stress. On the other hand, viscosity behavior will be described by Newton's Law:

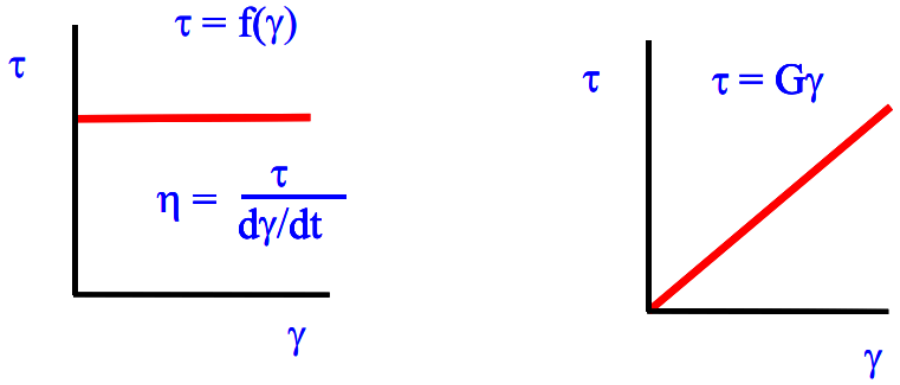

Plot 3: Representation of Newton's and Hooke's Laws [25]

To classify the different materials a parameter called Debora's number is used:

$$De = \frac{\tau}{t}$$

Equation 3: Debora's number Equation

According to Debora's number, all fluids can flow after waiting for the needed time. Depending on its value, materials are divided in:

- De<1: Viscous behavior
- De=1: Viscoelastic behavior
- De>1: Elastic behavior

The development of the linear viscoelasticity behavior is based on the principle that the deformation at any time is proportional to the stress. Therefore, if deformation and its velocity are infinitesimals and the relationship between stress and deformation depends on the time, it can be described by differential equations with constant coefficients.

$$\tau(t) = \int_{-\infty}^{t} G(t-t')\frac{d\gamma(t')}{dt'}dt' = \int_{-\infty}^{t} M(t-t')\gamma(t,t')dt'$$

Equation 4: Shear stress for linear viscoelasticity

Where t is the actual time and t' is the previous instant before every process, G(t) is the complex modulus and M(t-t') is known as memory function.

2. Nonlinear behavior [26]: Since most non-Newtonian fluids follow a shear thinning behavior, the analysis of the nonlinear viscoelasticity will be centered on pseudoplastics. The models to describe this behavior can be differential or integral:
    - Differential model: Jeffreys' Equation for linear viscoelasticity behavior can be adapted for nonlinear:

$$\tau + \lambda_1\tau_{(1)} = -\eta_0(\gamma_{(1)} + \lambda_2\gamma_{(2)})$$

Equation 5: Jeffreys' Equation

Where η_0 is the value for lower shears, λ_1 is the time for relaxation and λ_2 is the retard time

    - Integral model: Lodge model

$$\tau(t) = M(t-t')\gamma_{(0)}(t,t')dt' \quad , \quad M(t-t') = \frac{\partial G(t-t')}{\partial t'}$$

Equation 6: Lodge Model

Chapter 4:

Analysis Design

4.1. Introduction

Viscous flows in a pipeline are very hard to describe because they depend on a lot of factors. This process can be simplified and described by differential equations and theorems from the mechanics of fluids.

4.2. Differential Analysis

In order to start with a differential analysis, first, we will define the velocity and, consequently, the acceleration in the coordinates chosen [27].

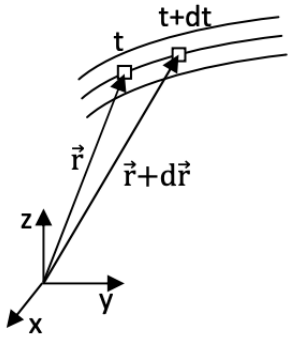

Figure 8: Vector representation in cartesian coordinates [27]

$$\boldsymbol{V}(\boldsymbol{r},t) = u(x,y,z,t)\boldsymbol{i} + v(x,y,z,t)\boldsymbol{j} + w(x,y,z,t)\boldsymbol{k}$$

Equation 7: Velocity vector expression

$$\boldsymbol{a} = \frac{d\boldsymbol{V}}{dt} = \frac{du}{dt}\boldsymbol{i} + \frac{dv}{dt}\boldsymbol{j} + \frac{dw}{dt}\boldsymbol{k}$$

Equa ntion 8: Acceleration expression

$$\frac{du}{dt} = \frac{\partial u}{\partial t} + (\boldsymbol{V}.\nabla)u \quad , \quad \frac{dv}{dt} = \frac{\partial v}{\partial t} + (\boldsymbol{V}.\nabla)v \quad , \quad \frac{dw}{dt} = \frac{\partial w}{\partial t} + (\boldsymbol{V}.\nabla)w$$

Equation 9: Derivatives of the three components of velocity

$$\boldsymbol{a} = \left[\frac{\partial u}{\partial t}\boldsymbol{i} + \frac{\partial v}{\partial t}\boldsymbol{j} + \frac{\partial w}{\partial t}\boldsymbol{k}\right] + [(\boldsymbol{V}.\nabla)u\boldsymbol{i} + (V.\nabla)v\boldsymbol{j} + (V.\nabla)w\boldsymbol{k}]$$

Equation 10: Expasion of acceleration expression

$$\boldsymbol{a} = \frac{\partial \boldsymbol{V}}{\partial t} + (\boldsymbol{V}.\nabla)\boldsymbol{V}$$

Equation 11: Compressed acceleration expression

Once, we have defined the acceleration, we will obtain the different differential equations applying the behavior equations to infinitesimal regions:

1. Differential mass equation:

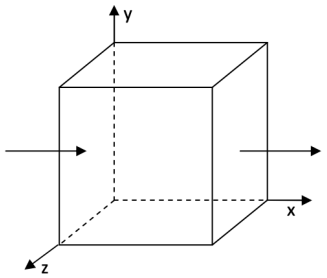

Figure 9: Infinitesimal region applied to mass balance [27]

Mass is conservative, in order words, the mass that enters the infinitesimal region is the same found at the exit. Therefore, the variation of mass in the infinitesimal region must be zero.

$$\frac{\partial \rho}{\partial t} + \nabla(\rho \boldsymbol{V}) = 0$$

Equation 12: Differential mass equation

This relation can be represented in:

- Cartesian coordinates:

$$\frac{\partial \rho}{\partial t} + \frac{\partial(\rho u)}{\partial x} + \frac{\partial(\rho v)}{\partial y} + \frac{\partial(\rho w)}{\partial z} = 0$$

Equation 13: Differential mass equation in cartesian coordinates

- Cylindrical coordinates:

$$\frac{\partial \rho}{\partial t} + \frac{1}{r}\frac{\partial (r\rho u_r)}{\partial r} + \frac{1}{r}\frac{\partial (\rho u_\theta)}{\partial \theta} + \frac{\partial (\rho u_z)}{\partial z} = 0$$

Equation 14: Differential mass equation in cylindrical coordinates

2. Differential movement equation:

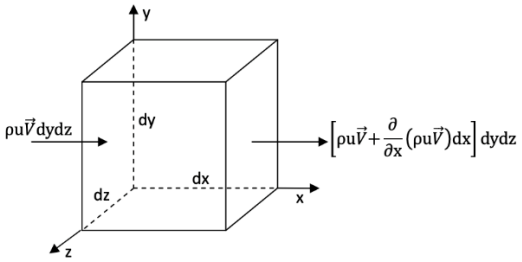

Figure 10: Infinitesimal region used for the dynamic analysis [27]

Newton's Law for dynamics states that the sum of external forces is equal to the mass times the acceleration. If we apply this law to an infinitesimal region we obtain:

$$\frac{\Sigma d\boldsymbol{F}}{dV} = \rho \frac{d\boldsymbol{V}}{dt} = \boldsymbol{f_m} + \boldsymbol{f_p} + \boldsymbol{f_v}$$

Equation 15: Differential movement equation

The external forces acting the fluid are:

- Volumetric forces due to the mass of the fluid

$$\boldsymbol{f_m} = \frac{d\boldsymbol{F_{grav}}}{dV} = \rho \boldsymbol{g}$$

Equation 16: Volumetric forces expression

- Superficial pressure forces due to pressure gradients

$$\boldsymbol{f_p} = \frac{\boldsymbol{dF_{pressure}}}{dV} = -\nabla p$$

Equation 17: superficial pressure forces expression

- Viscous superficial forces due to the resistivity of the fluid to flow

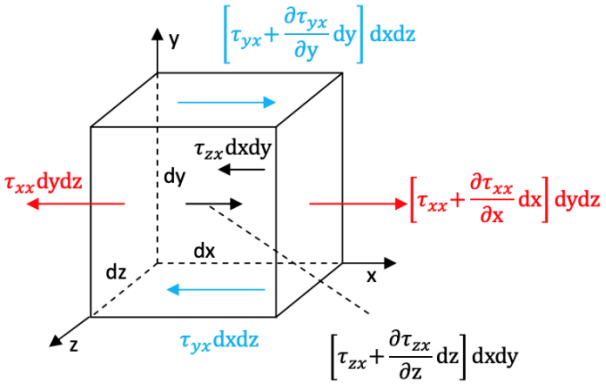

Figure 11: Infinitesimal region representing the shear stresses due to viscosity [27]

$$\boldsymbol{f_v} = \frac{\Sigma \boldsymbol{F_{VIS}}}{dV} = \nabla.\tau_{ij} \quad \rightarrow \quad \tau_{ij} = \begin{bmatrix} \tau_{xx} & \tau_{yx} & \tau_{zx} \\ \tau_{xy} & \tau_{yy} & \tau_{zy} \\ \tau_{xz} & \tau_{yz} & \tau_{zz} \end{bmatrix}$$

Equation 18: Viscous superficial forces expression

Introducing the expressions obtained for the different forces in the differential movement equation we obtain:

$$\rho \boldsymbol{g} - \nabla p + \nabla.\tau_{ij} = \rho \frac{d\boldsymbol{V}}{dt} = \rho \left[\frac{\partial \boldsymbol{V}}{\partial t} + (\boldsymbol{V}.\nabla)\boldsymbol{V}\right]$$

Equation 19: Expansion of differential movement expression

4.3. Bernoulli's Equation

Bernoulli's equation is used for incompressible fluids when they flow along a pipeline with a variable transverse area. Due to the non-continuity of the area, the velocity along the conduct changes creating an acceleration and consequently force. This force is created with the difference in pressure. This equation relates de difference on the pressure between two points relating it with the variations on velocity and height and the losses present in the pipeline. It is defined as:

$$\frac{p_1}{\rho g} + z_1 + \alpha_1 \frac{v_1^2}{2g} - h_T = \frac{p_2}{\rho g} + z_2 + \alpha_2 \frac{v_2^2}{2g}$$

Equation 20: Bernoulli's Equation

$$h_T = h_f + h_m$$

Equation 21: Losses expression

Due to the shear stress, there are losses along the pipeline which are represented by h. This factor is composed of:

- Primary losses: They are described by Darcy-Weisbach equation

$$h_f = f \frac{L}{D} \frac{v^2}{2g}$$

Equation 22: Darcy-Weisbach Equation for primary losses

The value of f depends if the fluid is laminar or turbulent. The nature of the fluid is determined by the Reynolds number:

$$Re = \frac{\rho v D}{\mu} \quad Re > 2300 \rightarrow Turbulent \;\; Re < 2300 \rightarrow Laminar$$

Equation 23: Reynolds' Nummer

If the fluid is laminar factor f is obtained by:

$$f = \frac{64}{Re}$$

Equation 24: Factor f expression

On the other hand, if the fluid is turbulent, to obtain the factor f Coolebrok's equation is applied:

$$f^{-\frac{1}{2}} = -2.0\, log_{10}\left(\frac{\varepsilon/D}{3.7} + \frac{2.51}{Ref^{1/2}}\right)$$

Equation 25: Coolebrok's Equation

Depending on the type of conduct this equation can be simplified. If the conduct is completely smooth, we obtain:

$$if\ \frac{\varepsilon u \rho}{\mu} < 5\ \ f^{-\frac{1}{2}} = -2.0\ log_{10}\left(\frac{2.51}{Ref^{1/2}}\right)$$

Equation 26: Coolebrok's Equation for smooth surfaces

However, if the conduct has roughness:

$$if < 5\frac{\varepsilon u \rho}{\mu} < 70\ f^{-\frac{1}{2}} = -2.0\ log_{10}\left(\frac{\varepsilon/D}{3.7} + \frac{2.51}{Ref^{1/2}}\right)$$

Equation 27: Coolebrok's equation for rough surfaces

Last, for conducts which are really wrinkled:

$$if\ \frac{\varepsilon u \rho}{\mu} > 70\ f^{-\frac{1}{2}} = -2.0\ log_{10}\left(\frac{\varepsilon/D}{3.7}\right)$$

Equation 28: Coolebrok's Equation for wrinkled surfaces

- Secondary losses: They are characteristic for those points where there is an abrupt change on velocity. In our geometry, we can see that change in the sudden contraction (vena contracta). This type of losses is defined by [28]:

$$h_m = k\frac{v^2}{2g}$$

Equation 29: Secondary losses expression

$$k = 0.5\left(1 - \left(\frac{D_1}{D_2}\right)^2\right)^2$$

Equation 30: Factor k expression

Chapter 5:

Problem Optimization

5.1. Introduction

Once we understand how the fluid works along with the syringe we would define an optimization problem to obtain the optimum dimensions of the conduct. The objective of the optimization will be maximizing the extrusion velocity since one of the main disadvantages of 3D food printers is the time printing.

First of all, some approximations will be made so the optimization is more simple. Even though, the type of behavior of the fluid that we are seeking to obtain is shear thinning we would assume the fluid behaves as a Newtonian fluid. This is not such as a bad approximation because Newtonian fluids have bigger shear stress values and for the design, the worst scenario will be studied to obtain a syringe that can be applied to fluids with worst properties.

5.2. Optimization problem

5.2.1. Equation Simplification

First of all, a system of coordinates needs to be defined. Since the syringe will have a circular section, the set of coordinates will be cylindrical. The origin of the coordinates will be established in the center of the top of the syringe in the contact between the piston and the fluid (point 1). Therefore, the axis z will be located along with the syringe having positive values in the nozzle direction.

To describe how the fluid flows through the syringe we will use Bernoulli's Equation and applying Poiseuille's Law to the differential analysis using Navier-Stokes' Equations:

1. Bernoulli's Equation:

$$\frac{p_1}{\rho g} + z_1 + \frac{v_1^2}{2g} - h_T = \frac{p_2}{\rho g} + z_2 + \frac{v_2^2}{2g}$$

Equation 31: Bernoulli's Equation applied to the problem

Point 2 represents the exit of the nozzle, in other words, the point where the material is being extruded to the platform of the 3D printer.

$$h_T = h_f + h_m = f\frac{L}{D}\frac{v^2}{2g} + 0.5\left(1 - \left(\frac{D_1}{D_2}\right)^2\right)^2\frac{v^2}{2g}$$

Equation 32: Losses expressions

hf needs to be calculated for the two different lengths and diameters.

We would consider that the flow is laminar and, therefore, Re needs to be lower than 2300, which would be one constraint. For Bernoulli's Equation, relative pressure values will be used. Therefore, the relative pressure of p_2 is zero since the fluid ends up in the atmosphere the equation result to be:

$$p_1 = \rho g\left(h_T + z_2 - z_1 + \frac{v_2^2 - v_1^2}{2g}\right)$$

Equation 33: Pressure expression after applying Bernoulli's Equation

The origin of the system of reference is located in point 1. Therefore:

$$z_2 = L_2 + L_1; \quad z_1 = 0$$

Equation 34: z_1 and z_2 expressions

$$p_1 = \rho g\left(f_1\frac{L_1}{D_1}\frac{{v_1}^2}{2g} + f_2\frac{L_2}{D_2}\frac{{v_2}^2}{2g} + 0.5\left(1 - \left(\frac{D_1}{D_2}\right)^2\right)^2\frac{{v_2}^2}{2g} + L_1 + L_2 + \frac{v_2^2 - v_1^2}{2g}\right)$$

Equation 35: Development of pressure expression after applying Bernoulli's Equation

$$f_1 = \frac{64}{Re_1} \;;\; Re_1 = \frac{\rho v_1 D_1}{\mu} \;;\; f_1 = \frac{64\mu}{\rho v_1 D_1}$$

$$f_2 = \frac{64}{Re_2} \;;\; Re_2 = \frac{\rho v_2 D_2}{\mu} \;;\; f_2 = \frac{64\mu}{\rho v_2 D_2}$$

Equation 36: Factor f expressions for the body (1) and the nozzle (2)

$$p_1 = \rho g \left(\frac{32 L_1}{D_1^2} \frac{v_1}{\rho g} + \frac{32 L_2}{D_2^2} \frac{v_2}{\rho g} + 0.5 \left(1 - \left(\frac{D_1}{D_2} \right)^2 \right) \frac{{v_2}^2}{2g} + L_1 + L_2 + \frac{v_2^2 - v_1^2}{2g} \right)$$

Equation 37: Expanded pressure expression after applying Bernoulli's Equation

2. Poiseuille's Law

Since the fluid is considered Newtonian its density and viscosity are constant, therefore applying Newton's Law for viscosity we obtain:

$$\tau_{xx} = 2\mu \frac{\partial u}{\partial x} \quad \tau_{yy} = 2\mu \frac{\partial v}{\partial y} \quad \tau_{zz} = 2\mu \frac{\partial w}{\partial z}$$

Equation 38: Newton's Law applied to the three coordinates

$$\tau_{xy} = \tau_{yx} = \mu \left(\frac{\partial u}{\partial x} + \frac{\partial v}{\partial y} \right) \quad \tau_{xz} = \tau_{zx=} \mu \left(\frac{\partial u}{\partial x} \frac{\partial w}{\partial z} \right) \quad \tau_{yz} = \tau_{zy} = \mu \left(\frac{\partial v}{\partial y} + \frac{\partial w}{\partial z} \right)$$

Equation 39: Newton's Law applied to shear stresses

Applying the differential equation for the movement we can obtain Navier-Stokes equations:

$$\rho \boldsymbol{g} - \nabla p + \nabla . \tau_{ij} = \rho \frac{d\boldsymbol{V}}{dt} = \rho \left[\frac{\partial \boldsymbol{V}}{\partial t} + (\boldsymbol{V} . \nabla) \boldsymbol{V} \right]$$

Equation 40: Navier Stokes Equation

$$\rho \left(\frac{\partial u}{\partial t} + u \frac{\partial u}{\partial x} + v \frac{\partial u}{\partial y} + w \frac{\partial u}{\partial z} \right) = - \frac{\partial p}{\partial x} + \mu \left(\frac{\partial^2 u}{\partial x^2} + \frac{\partial^2 u}{\partial y^2} + \frac{\partial^2 u}{\partial z^2} \right) + \rho g_x$$

$$\rho \left(\frac{\partial v}{\partial t} + u \frac{\partial v}{\partial x} + v \frac{\partial v}{\partial y} + w \frac{\partial v}{\partial z} \right) = - \frac{\partial p}{\partial y} + \mu \left(\frac{\partial^2 v}{\partial x^2} + \frac{\partial^2 v}{\partial y^2} + \frac{\partial^2 v}{\partial z^2} \right) + \rho g_y$$

$$\rho \left(\frac{\partial w}{\partial t} + u \frac{\partial w}{\partial x} + v \frac{\partial w}{\partial y} + w \frac{\partial w}{\partial z} \right) = - \frac{\partial p}{\partial z} + \mu \left(\frac{\partial^2 w}{\partial x^2} + \frac{\partial^2 w}{\partial y^2} + \frac{\partial^2 w}{\partial z^2} \right) + \rho g_z$$

Equation 41: Navier Stokes Equations in cartesian coordinates

Navier- Stokes Equations can also be referred to cylindrical coordinates:

$$\rho\left(\frac{\partial u_r}{\partial t}+\frac{u_r\partial u_r}{\partial r}+\frac{u_\theta}{r}\frac{\partial u_\theta}{\partial \theta}-\frac{u_\theta^2}{r}+\frac{u_z\partial u_r}{\partial z}\right)$$
$$=-\frac{\partial p}{\partial r}+\mu\left[\frac{\partial}{\partial r}\left(\frac{1}{r}\frac{\partial}{\partial r}(ru_r)\right)+\frac{1}{r^2}\frac{\partial^2 u_r}{\partial \theta^2}-\frac{2}{r^2}\frac{\partial u_\theta}{\partial \theta}+\frac{\partial^2 u_r}{\partial z^2}\right]+\rho g_r$$

$$\rho\left(\frac{\partial u_\theta}{\partial t}+\frac{u_r\partial u_\theta}{\partial r}+\frac{u_\theta}{r}\frac{\partial u_\theta}{\partial \theta}+\frac{u_r u_\theta}{r}+\frac{u_z\partial u_\theta}{\partial z}\right)$$
$$=-\frac{1}{r}\frac{\partial p}{\partial \theta}+\mu\left[\frac{\partial}{\partial r}\left(\frac{1}{r}\frac{\partial}{\partial r}(ru_\theta)\right)+\frac{1}{r^2}\frac{\partial^2 u_\theta}{\partial \theta^2}+\frac{2}{r^2}\frac{\partial u_r}{\partial \theta}+\frac{\partial^2 u_\theta}{\partial z^2}\right]$$
$$+\rho g_\theta$$

$$\rho\left(\frac{\partial u_z}{\partial t}+\frac{u_r\partial u_z}{\partial r}+\frac{u_\theta}{r}\frac{\partial u_z}{\partial \theta}+\frac{u_z\partial u_z}{\partial z}\right)$$
$$=-\frac{\partial p}{\partial z}+\mu\left[\frac{1}{r}\frac{\partial}{\partial r}\left(r\frac{\partial u_z}{\partial r}\right)+\frac{1}{r^2}\frac{\partial^2 u_z}{\partial \theta^2}+\frac{\partial^2 u_z}{\partial z^2}\right]+\rho g_z$$

Equation 42: Navier Stokes Equations in cylindrical coordinates

The fluid is stationary so all the derivatives respect to time are equal to zero. Also, since gravity and the difference in pressure are parallel to z the velocities in the θ and r axis are equal to zero. Applying this to the differential equation for continuity:

$$\frac{\partial \rho}{\partial t}+\frac{1}{r}\frac{\partial(r\rho u_r)}{\partial r}+\frac{1}{r}\frac{\partial(\rho u_\theta)}{\partial \theta}+\frac{\partial(\rho u_z)}{\partial z}=0\rightarrow\ \frac{\partial(u_z)}{\partial z}=0\ u_z=u_z(r)$$

Equation 43: Differential Equation for continuity

$$0=-\frac{\partial p}{\partial z}+\mu\left[\frac{1}{r}\frac{\partial}{\partial r}\left(r\frac{\partial u_z}{\partial r}\right)\right]+\rho g_z\rightarrow\frac{\partial p}{\partial z}=\mu\left[\frac{1}{r}\frac{\partial}{\partial r}\left(r\frac{\partial u_z}{\partial r}\right)\right]+\rho g_z$$

Equation 44: Pressure gradient respect to z expression

Integrating:

$$u_z(r)=\frac{1}{2\mu}\frac{r^2}{2}\frac{dp}{dz}+Alnr+B$$

Equation 45: Velocity function along z axis

To obtain the values of the constants A and B we apply boundary conditions. Since the shear stress and the velocity are related to Newton's Law.

$$\tau = \mu \frac{du}{dy}$$

Equation 46: Newton's Law

Also, applying the derivatives to obtain the maximum velocity, the maximum velocity will be where the derivative of the velocity is zero and, therefore, the shear stress is also equal to zero. The maximum velocity is known to be located in the center of the pipeline. Therefore, the first boundary condition is that the shear stress in the center of the syringe is equal to zero.

$$\frac{\partial u_z}{\partial r} = 0 \; when \; r = 0 \; \rightarrow A = 0$$

Equation 47: Application of first boundary condition

The other boundary condition is that the velocity of the fluid in contact with the surface of the syringe is equal to zero.

$$u_z = 0 \; when \; r = R \; \rightarrow B = -\frac{1}{2\mu}\frac{D^2}{8}\frac{dp}{dz}$$

Equation 48: Application of second boundary condition

$$\frac{dp}{dz} = \frac{\Delta p}{\Delta z}$$

Equation 49: Pressure gradient expression

Since there are two diameters we would have two different velocity profiles. This difference on the velocity distribution will happen in the vena contacta, which is located at the beginning of the nozzle. (point 1')

$$u_{z1}(r) = -\frac{1}{2\mu}\frac{r^2}{2}\frac{P_1 - P_1'}{L_1} + \frac{1}{2\mu}\frac{{D_1}^2}{8}\frac{P_1 - P_1'}{L_1}$$

Equation 50: Velocity distribution along the z axis in the base of the syringe

$$u_{z2}(r) = -\frac{1}{2\mu}\frac{r^2}{2}\frac{P_1{}'}{L_2} + \frac{1}{2\mu}\frac{D_2{}^2}{8}\frac{P_1{}'}{L_2}$$

Equation 51: Velocity distribution along the z axis in the nozzle of the syringe

Both velocity profiles are parabolic, therefore, the relation between the maximum velocity and the average velocity is:

$$v = 0.5u_{max}$$

Equation 52: Relation between the average velocity and máximum velocity

$$u_{max-1} = u_{z1}(r = 0) = \frac{1}{2\mu}\frac{D_1{}^2}{8}\frac{P_1 - P_1'}{L_1} \quad v_1 = \frac{1}{4\mu}\frac{D_1{}^2}{8}\frac{P_1 - P_1'}{L_1}$$

Equation 53: Maximum velocity in the base of the syringe

$$u_{max-2} = u_{z2}(r = 0) = \frac{1}{2\mu}\frac{D_2{}^2}{8}\frac{P_1{}'}{L_2} \quad v_2 = \frac{1}{4\mu}\frac{D_2{}^2}{8}\frac{P_1{}'}{L_2}$$

Equation 54: Maximum velocity in the nozzle of the syringe

Also, the fluid is considered to have constant properties, so it can be treated as an incompressible fluid. Since the fluid is incompressible the volume flow rate must remain constant:

$$Q = A_1 v_1 = A_2 v_2 \quad \rightarrow \quad v_2 = \left(\frac{D_1}{D_2}\right)^2 v_1$$

Equation 55: Conservative Equation

From the velocity distribution we can also obtain the shear stress distribution applying Newton's Law:

$$\tau = \mu\frac{du}{dr}$$

Equation 56: Newton's Law

$$\frac{du_{z1}}{dr} = -\frac{1}{\mu}\frac{r}{2}\frac{P_1 - P_1'}{L_1} \quad \rightarrow \quad \tau_1(r) = -\frac{r}{2}\frac{P_1 - P_1'}{L_1}$$

Equation 57: Shear stress in the base of the syringe

$$\tau_{max-1} = \tau_1\left(r = \frac{D_1}{2}\right) = -\frac{D_1}{4}\frac{P_1 - P_1'}{L_1}$$

Equation 58: Maximum shear stress in the base of the syringe

$$\frac{du_{z2}}{dr} = -\frac{1}{\mu}\frac{r}{2}\frac{P_1{}'}{L_2} \quad \rightarrow \quad \tau_1(r) = -\frac{r}{2}\frac{P_1{}'}{L_2}$$

Equation 59: Shear stress in the nozzle of the syringe

$$\tau_{max-2} = \tau_2\left(r = \frac{D_2}{2}\right) = -\frac{D_2}{4}\frac{P_1{}'}{L_2}$$

Equation 60: Maximum shear stress in the nozzle of the syringe

The average velocities can be written in function of the absolute value of the maximum shear stress:

$$v_1 = \frac{\tau_{max-1}}{8\mu}D_1 \quad v_2 = \frac{\tau_{max-2}}{8\mu}D_2$$

Equation 61: Average velocity in function of the máximum shear stress

If these values are substituted in the next relation, we obtain:

$$v_2 = \left(\frac{D_1}{D_2}\right)^2 v_1 \quad \rightarrow \quad \tau_{max-2} = \left(\frac{D_1}{D_2}\right)^3 \tau_{max-1}$$

Equation 62: Relation between both velocities ans shear stresses

Applying this relation, we can obtain:

$$\tau_{max-2} = \left(\frac{D_1}{D_2}\right)^3 \tau_{max-1} \quad \rightarrow \frac{D_2}{4}\frac{P_1{}'}{L_2} = \left(\frac{D_1}{D_2}\right)^3 \frac{D_1}{4}\frac{P_1 - P_1'}{L_1}$$

$$P_1' = P_1 \left(\frac{D_1^4 L_2}{D_2^4 L_1 + D_1^4 L_2} \right)$$

Equation 63: Relation between the pressure at the beginning of the extrusión and the beginning of the nozzle

5.2.2. Problem Formulation

In order to formulate the optimization problem, some constraints and the objective function need to be formulated:

1. We want the syringe to have a minimum volume capacity. This volume will be 100 ml. The volume capacity of the syringe is:

$$V = \frac{\pi}{4}(D_1^2 L_1 + D_2^2 L_2)$$

Equation 64: Volume expression

$$g_1(D_1, L_1, D_2, L_2) = 0.0001 - \frac{\pi}{4}(D_1^2 L_1 + D_2^2 L_2) \leq 0$$

Equation 65: First constraint

2. Because we want the syringe to have a structure where D_1 and L_1 are greater than D_2 and L_2 respectively, we also seek for the ratio on diameters and in length to be at least 5.

$$g_2(D_1, D_2) = 5D_2 - D_1 \leq 0$$

Equation 66: Second constraint

$$g_3(L_1, L_2) = 5L_2 - L_1 \leq 0$$

Equation 67: Third constraint

So the problem is well bounded we need a limit for the length of the syringe:

$$g_4(L_1) = L_1 - 1 \leq 0$$

Equation 68: Forth constraint

3. To apply the relations obtained we need the flow to be laminar, which means that Reynolds' number needs to be less than 2300 for both parts of the syringe:

$$Re = \frac{\rho v D}{\mu} < 2300$$

Equation 69: Laminar condition

$$g_5(D_1, v_1, \rho, \mu) = \frac{\rho v_1 D_1}{\mu} - 2300 \leq 0$$

Equation 70: Constraint for laminar flow in the base of syringe

$$g_6(D_2, v_2, \rho, \mu) = \frac{\rho v_2 D_2}{\mu} - 2300 \leq 0$$

Equation 71: Constraint for laminar flow in the nozzle of the syringe

Using the relation between the velocities we can determine which Reynolds number will be always greater. Just limiting the higher Reynolds number we can drop one of the constraints

$$Re_1 = \frac{\rho v_1 D_1}{\mu}$$

Equation 72: Reynolds' number

$$Re_2 \frac{\rho v_2 D_2}{\mu} = \frac{\rho v_1 D_1}{\mu} \left(\frac{D_1}{D_2}\right) = Re_1 \left(\frac{D_1}{D_2}\right)$$

Equation 73: Relation between Reynols' Numbers

Therefore, since the Reynolds number is greater for the nozzle we can just use a constraint for this value.

$$g_5(D_2, v_2, \rho, \mu) = \frac{\rho v_2 D_2}{\mu} - 2300 \leq 0$$

Equation 74: Fifth constraint

4. Due to the type of stress that the syringe is exposed to there is a risk of having cracks. Irwin established that the field of stress around the crack can be described by a factor called intensity of stress, K. The fracture occurs when the value K is greater than K_c. There are three ways to apply a force to enable a crack to propagate:

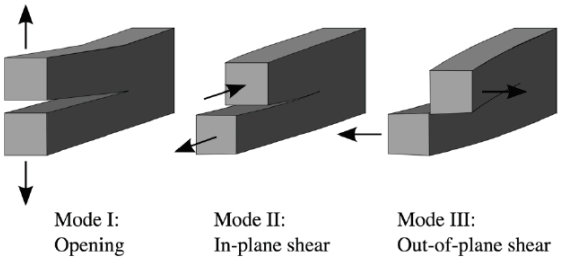

Figure 12: Types of cracks depending on the force applied [29]

- Mode I fracture (Opening mode): A tensile stress normal to the plane of the crack.
- Mode II fracture (Sliding mode): A shear stress acting parallel to the plane of the crack and perpendicular to the crack front.
- Mode III fracture (Tearing mode): A shear stress acting parallel to the plane of the crack and parallel to the crack front.

In this case, we are in risk of having a fracture type I, also known as opening mode. The variable K_I is described by:

$$K_I = Y\sigma\ (\pi a)^{\frac{1}{2}}$$

Equation 75: Intensity of stress expression

Y is a factor that depends on the type of crack and geometry of the object and a is the critic length of the crack.

The pressure in all the different points of the syringe creates normal stress that can be approximated by:

$$\sigma = \frac{pD}{2t}$$

Equation 76: Normal stress expression

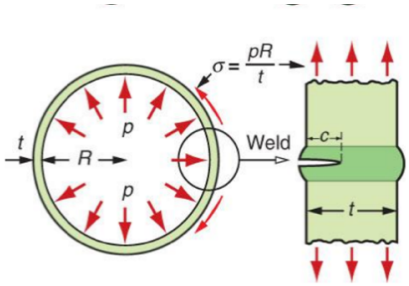

Figure 13: Force distribution due to the pressure [30]

The value of the principal stress needs to be always less than the yield stress. Since there is also shear stress we need to take it into consideration to calculate the maximum principal stress.

As it was obtained from Poiseuille's Law, there are two values for the maximum shear stress. Since both values can be related as:

$$\tau_{max-2} = \left(\frac{D_1}{D_2}\right)^3 \tau_{max-1}$$

Equation 77: Relation between máximum shear stress

Since D_1 has a greater value than D_2, it can be concluded that the shear stress in the nozzle (τ_{max-2}) is higher. Therefore, τ_{max-2} will be the shear stress to minimize.

$$\tau_{max-2} = \frac{D_2}{4}\frac{P_1'}{L_2}$$

Equation 78: Maximum shear stress in the nozzle

There are two critical points:

- Point 1: which represents the top of the syringe and has the following stresses:

$$\sigma = \frac{D_1 P_1}{2t} \quad \tau_{max-1} = \frac{D_1}{4}\frac{P_1 - P_1'}{L_1}$$

Equation 79: Stresses in the surface of the body of the syringe

$$\sigma_1 = \frac{\sigma_{rr}}{2} + \left(\left(\frac{\sigma_{rr}}{2}\right)^2 + \tau_{z\theta}^2\right)^{\frac{1}{2}} = \frac{D_1 P_1}{4t} + \left(\left(\frac{D_1 P_1}{4t}\right)^2 + \left(\frac{D_1}{4}\frac{P_1 - P_1'}{L_1}\right)^2\right)^{\frac{1}{2}}$$

Equation 80: Maximum principal stress in the surface of the body of the syringe

- Point 1': which represents the beginning of the nozzle and has the following stresses:

$$\sigma = \frac{D_2 P_1{}'}{2t} \quad \tau_{max-2} = \frac{D_2}{4}\frac{P_1'}{L_2}$$

Equation 81: Stresses in the surface of the nozzle of the syringe

$$\sigma_1 = \frac{\sigma_{rr}}{2} + \left(\left(\frac{\sigma_{rr}}{2}\right)^2 + \tau_{z\theta}^2\right)^{\frac{1}{2}} = \frac{D_2 P_1{}'}{4t} + \left(\left(\frac{D_2 P_1{}'}{4t}\right)^2 + \left(\frac{D_2}{4}\frac{P_1'}{L_2}\right)^2\right)^{\frac{1}{2}}$$

Equation 82: Maximum principal stress in the surface of the nozzle of the syringe

The normal stresses are usually much bigger than shear stresses, therefore, we will assume that point 1 is under worst conditions. After, the optimization we will make sure this is true.

To make sure a factor of safety equal to 1.5:

$$g_6(D_1, L_1, D_2, L_2, P_1, P_1', t) = 1.5 * \frac{D_1 P_1}{4t} + \left(\left(\frac{D_1 P_1}{4t}\right)^2 + \left(\frac{D_1}{4}\frac{P_1 - P_1'}{L_1}\right)^2\right)^{\frac{1}{2}} - \sigma_y \leq 0$$

Equation 83: Sixth constraint

We have to make sure that the shear stress value is not greater than the maximum value allowed. The maximum shear stress allowed will be calculated using the maximum shear stress theory known as Tresca's theory [31]. This theory states that the failure will occur when the maximum shear stress from a combination of principal stresses equals or exceeds the value obtained for the shear yielding in the uniaxial tensile test:

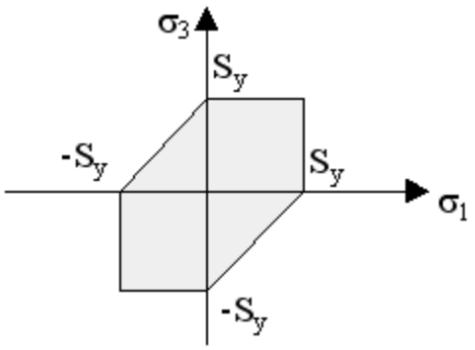

Plot 4: Representation of Tresca's theory [31]

$$g_7(D_1, L_1, D_2, L_2, P_1, P_1', t) = \frac{D_1}{4}\frac{P_1 - P_1'}{L_1} - \frac{D_1 P_1}{8t} - \frac{\left(\left(\frac{D_1 P_1}{4t}\right)^2 + \left(\frac{D_1}{4}\frac{P_1 - P_1'}{L_1}\right)^2\right)^{\frac{1}{2}}}{2} \leq 0$$

Equation 84: Seventh constraint

Once we know the type of stress, we can determine factor Y using the next tables:

Geometry	Stress Intensity Factor
1. Crack in an infinite body 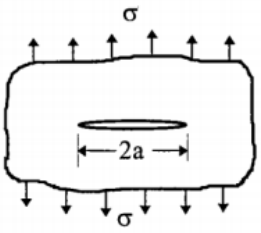	$K_I = \sigma\sqrt{\pi a}$
2. Centre crack in a strip of finite width 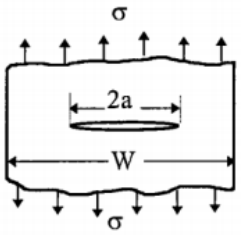	$K_I = \sqrt{\sec\frac{\pi a}{W}}\sigma\sqrt{\pi a}$
3. Edge crack in a semi-infinite body 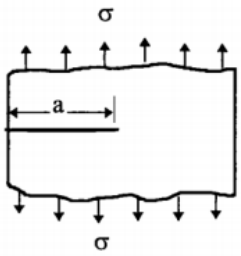	$K_I = 1.12\sigma\sqrt{\pi a}$
4. Centre crack in a finite width strip 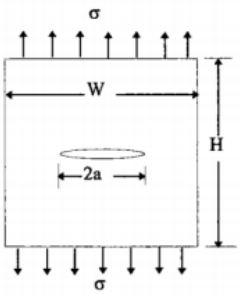	$K_I = f\left(\frac{a}{W}\right)\sigma\sqrt{\pi a}$

a/W	f(a/W)	
	$h/W=1.0$	$h/W=\infty$
0	1.12	1.12
0.2	1.37	1.21
0.4	2.11	1.35
0.5	2.83	1.46

Table 1: Values for the geometry factors depending on the type of crack [30]

5. Edge crack in a beam of width B subjected to bending

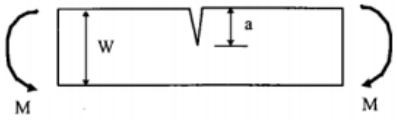

$$K_I = f\left(\frac{a}{W}\right)\sigma\sqrt{\pi a} \quad \text{where } \sigma = \frac{6M}{BW^2}$$

a/W	$f(a/W)$
0.1	1.044
0.2	1.055
0.3	1.125
0.4	1.257
0.5	1.500
0.6	1.915

6. Thin-section (plane stress) double split beam

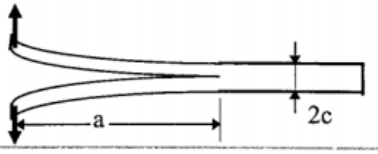

$$K_I = 2\sqrt{3}\frac{Pa}{c^{3/2}}$$

7. Circumferentially notched rod

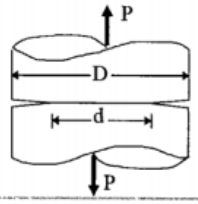

$$K_I = \frac{0.932P\sqrt{D}}{\sqrt{\pi d^2}} \quad \text{for } 1.2 \le \frac{D}{d} < 2.1$$

8. Compact tension specimen (CST)

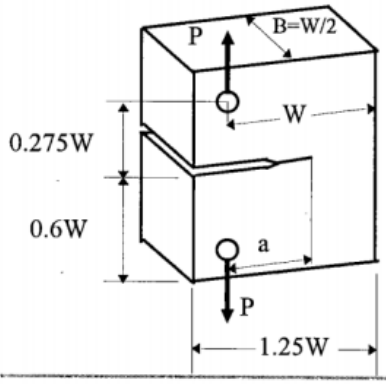

$$K_I = Y\frac{P\sqrt{\pi}}{B\sqrt{W}}$$

$$Y = 16.7\left(\frac{a}{W}\right)^{1/2} - 104.7\left(\frac{a}{W}\right)^{3/2} +$$

$$+ 369.9\left(\frac{a}{W}\right)^{5/2} - 573.8\left(\frac{a}{W}\right)^{7/2} +$$

$$+ 360.5\left(\frac{a}{W}\right)^{9/2}$$

Table 2: Values for the geometry factor depending on the type of crack [30]

The Y factor chosen is equation 3: edge crack in a semi-infinite body. Therefore:

$$K_I = 1.2\sigma\,(\pi a)^{\frac{1}{2}}$$

Equation 85: Intensity of stress expression

To make sure that the syringe doesn't break catastrophically, the thickness of the syringe needs to be lower than the value of the critic crack. The critic crack represents the length of the crack when the fracture happens. To make sure the thickness is never greater than a, we will apply a factor of safety of 1.5. Also, to study the worst scenario we use the stress in point 1(where the maximum stress happens).

$$K_I = 1.2\frac{D_1 P_1}{2t}\,(\pi a)^{\frac{1}{2}} \;\rightarrow\; a = \frac{\left(\frac{2tK_I}{1.2D_1P_1}\right)^2}{\pi}$$

Equation 86: Limit crack expression

$$g_8(D_1, t, P_1, K_I) = 1.5t - \frac{\left(\frac{2tK_I}{1.2D_1P_1}\right)^2}{\pi} \leq 0$$

Equation 87: Eighth constraint

To make the problem well bounded and to obtain reasonable values for the thickness of the syringe we need to set boundaries for it:

$$g_9(t) = -0.01 + t \leq 0$$

Equation 88: Ninth constraint

$$g_{10}(t) = 0.001 - t \leq 0$$

Equation 89: Tenth constraint

5. We need to add some equality constraints representing all the relations obtained using Bernoulli's Equation and Poiseuille' Law:

$$v_2 = \left(\frac{D_1}{D_2}\right)^2 v_1$$

Equation 90: Relation between velocities

$$h_1(D_1, D_2, v_1, v_2) = v_2 - v_1 \left(\frac{D_1}{D_2}\right)^2 = 0$$

Equation 91: First equality constraint

$$P_1' = P_1 \left(\frac{D_1^4 L_2}{D_2^4 L_1 + D_1^4 L_2}\right)$$

Equation 92: Relation between the pressure at the beginning of the extrusión and the beginning of the nozzle

$$h_2(D_1, L_1, D_2, L_2, P_1, P_1') = P_1' - P_1 \left(\frac{D_1^4 L_2}{D_2^4 L_1 + D_1^4 L_2}\right) = 0$$

Equation 93: Second equality constraint

$$p_1 = \rho g \left(h_T + L_2 + L_1 + \frac{v_2^2 - v_1^2}{2g}\right)$$

Equation 94: Pressure expression after applying Bernoulli's Equation

$$h_3(L_1, L_2, v_1, v_2, h_T, \rho, g) = p_1 - \rho g \left(h_T + L_2 + L_1 + \frac{v_2^2 - v_1^2}{2g}\right) = 0$$

Equation 95: Third equality constraint

$$h_T = \frac{32 L_1}{D_1^2} \frac{v_1}{\rho g} + \frac{32 L_2}{D_2^2} \frac{v_2}{\rho g} + 0.5 \left(1 - \left(\frac{D_1}{D_2}\right)^2\right)^2 \frac{{v_2}^2}{2g}$$

Equation 96: Total losses expression

$$h_4(D_1, L_1, D_2, L_2, v_1, v_2, \rho, g) = h_T - \frac{32 L_1}{D_1^2} \frac{v_1}{\rho g} + \frac{32 L_2}{D_2^2} \frac{v_2}{\rho g} + 0.5 \left(1 - \left(\frac{D_1}{D_2}\right)^2\right)^2 \frac{{v_2}^2}{2g} = 0$$

Equation 97: Forth equality constraint

Applying all these constraints we obtain the complete optimization formulation

$$\min_{\mathbf{x}} \quad \{-v_2\}$$

where $\mathbf{x} = (D_1, L_1, D_2, L_2, v_1, v_2, P_1, P_1', h_T, t)$

$\mathbf{p} = (\sigma_y, \rho, \mu, g, V_{max}, K_I)$

$$V = \frac{\pi}{4}(D_1^2 L_1 + D_2^2 L_2)$$

subject to

$$g_1(D_1, L_1, D_2, L_2) = 0.0001 - \frac{\pi}{4}(D_1^2 L_1 + D_2^2 L_2) \leq 0$$

$$g_2(D_1, D_2) = 5D_2 - D_1 \leq 0$$

$$g_3(L_1, L_2) = 5L_2 - L_1 \leq 0$$

$$g_4(L_1) = L_1 - 1 \leq 0$$

$$g_5(D_2, v_2, \rho, \mu) = \frac{\rho v_2 D_2}{\mu} - 2300 \leq 0$$

$$g_6(D_1, L_1, D_2, L_2, P_1, P_1', t) = 1.5 * \frac{D_1 P_1}{4t} + \left(\left(\frac{D_1 P_1}{4t} \right)^2 + \left(\frac{D_1}{4} \frac{P_1 - P_1'}{L_1} \right)^2 \right)^{\frac{1}{2}} - \sigma_y \leq 0$$

$$g_7(D_1, L_1, D_2, L_2, P_1, P_1', t) = \frac{D_1}{4} \frac{P_1 - P_1'}{L_1} - \frac{D_1 P_1}{8t} - \frac{\left(\left(\frac{D_1 P_1}{4t} \right)^2 + \left(\frac{D_1}{4} \frac{P_1 - P_1'}{L_1} \right)^2 \right)^{\frac{1}{2}}}{2} \leq 0$$

$$g_8(D_1, t, P_1, K_I) = 1.5t - \frac{\left(\frac{2tK_I}{1.2 D_1 P_1} \right)^2}{\pi} \leq 0$$

$$g_9(t) = -0.01 + t \leq 0$$

$$g_{10}(t) = 0.001 - t \leq 0$$

$$h_1(D_1, D_2, v_1, v_2) = v_2 - v_1 \left(\frac{D_1}{D_2}\right)^2 = 0$$

$$h_2(D_1, L_1, D_2, L_2, P_1, P_1') = P_1' - P_1 \left(\frac{D_1^4 L_2}{D_2^4 L_1 + D_1^4 L_2}\right) = 0$$

$$h_3(L_1, L_2, v_1, v_2, h_T, \rho, g) = p_1 - \rho g \left(h_T + L_2 + L_1 + \frac{v_2^2 - v_1^2}{2g}\right)$$

$$h_4(D_1, L_1, D_2, L_2, v_1, v_2, h_T, \rho, g)$$
$$= h_T - \frac{32 L_1}{D_1^2} \frac{v_1}{\rho g} + \frac{32 L_2}{D_2^2} \frac{v_2}{\rho g} + 0.5 \left(1 - \left(\frac{D_1}{D_2}\right)^2\right)^2 \frac{{v_2}^2}{2g} = 0$$

$where$

D_1: $diameter\ of\ wide\ part$

L_1: $length\ of\ wide\ part$

D_2: $diameter\ of\ the\ nozzle$

L_2: $length\ of\ the\ nozzle$

v_1: $average\ fluid\ velocity\ in\ the\ wide\ part$

v_2: $average\ fluid\ velocity\ in\ the\ nozzle$

P_1: $pressure\ at\ the\ piston$

P_1': $pressure\ at\ the\ contraction$

h_T: $total\ losses$

σ_y: $syringe\ maximum\ yield\ stress$

ρ: $fluid\ density$

μ: $fluid\ viscosity$

g: $gravity$

τ: $shear\ stress\ at\ the\ nozzle$

t: $syringe\ thickness$

K_I: $fracture\ toughness$

The parameters of the formulation are mainly the properties of the material used for the syringe and the fluid properties. The material chosen for the syringe is polypropylene since it's the most common material for syringes. Polypropylene (PP) is a hydrocarbon polymer with a great number of applications due to its rigidity and hardness while having a low density. Other properties are that it is semi-rigid, translucent, tough and has excellent electrical, chemical and fatigue resistance. The mechanical properties for the problem are [32]:

$$K_I = 2.5 \frac{MPa}{m^{\frac{1}{2}}} \quad \sigma_y = 33\ MPa$$

Then, a material for the optimization needs to be chosen. There are numerous food materials that can be studied for this optimization will choose melted chocolate. Since chocolate is a Non-Newtonian fluid with shear thinning properties we would use an average of the properties at 80 C retrieved from [33] :

$$\rho = 1320 \frac{kg}{m^3} \quad \mu = 2.3\ Pas$$

5.2.3. Results

The results obtained using MATLAB were:

$$D_1 : 0.0755\ m$$
$$L_1 : 0.1510\ m$$
$$D_2 : 0.0151\ m$$
$$L_2 : 0.0050\ m$$

$$v_1 : 0.0627 \frac{m}{s}$$

$$v_2 : 0.2292 \frac{m}{s}$$

$$P_1 : 100000\ Pa$$

$$P_1' : 1000Pa$$

$$h_T : 7.5655\ m$$

$$t : 0.01\ m$$

Also, since

$$\sigma_1 > \sigma_1{}'$$

we can conclude that point 1 is the critical point.

Chapter 6:

Simulation

6.1. Introduction

This part will present the design of the mechanism of the syringe as well as a simulation of the liquid chocolate flow through the syringe. The mechanism of the syringe is based on a pump run by a stepper motor. The simulation was run in SolidWorks. Since the material used for the simulation was fluid chocolate, this material had to be added into the list of materials of the software. The properties added were the thermal conductivity [34], the specific heat [35], the density, the consistency coefficient and the flow behavior [36]:

$$k = 0.75 \frac{W}{mK}$$

$$\rho = 1320 \frac{kg}{m^3}$$

$$K = 0.574 \ Pas$$

$$n = 0.57$$

Also, the model used for the simulation was the Power Law model. The chocolate needs to melt, therefore, the extrusion will be done at a temperature of 40C.

6.2. Design Description

The pump is based on different parts. First, the stepper motor who is the one that produces the movement of the plunger of the syringe and therefore the movement of the chocolate producing the flow of it along the syringe.

The different stepper motors used for this kind of mechanism are motor close to NEMA 17 size. Some examples are [7]:

1. Kysan 1124090/42BYGH4803
2. Rattm 17HS8401
3. Wantai 23BYGHW609

For our design done in SolidWorks the next stepper motor was designed:

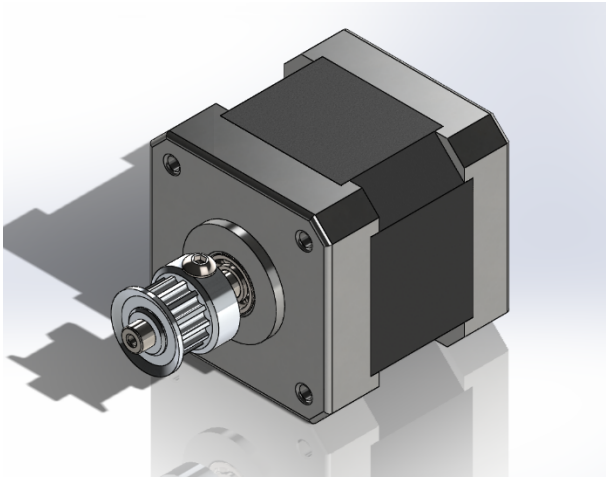

Figure 14: Stepper Motor model

Then, three structures were designed to maintain the syringe in the correct position and making the syringe still while the food material is extruded through the nozzle. These structures are:

1. Structure 1: This part goes screwed to the stepper motor. At the same time, it is composed of three parts. The middle part is the one who is screwed to the stepper motor. It has a hole in the middle where the pulley of the stepper motor is located. To the sides, it has screwed two other structures. The main objective of these two structures is to fix two rods that will give stability to the structure and allows the syringe body to be still.

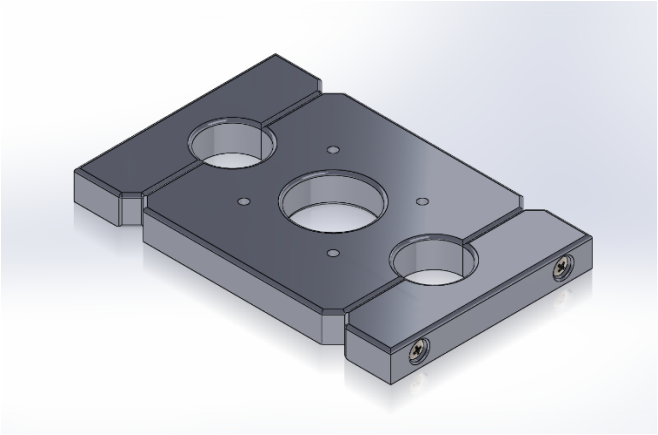

Figure 15: Structure 1 model

2. Structure 2: This part has three holes in the bottom of the structure. The hole in the middle will be threaded making the structure to move when the stepper motor is activated. At the top of the structure, there is a big hole where the base of the plunger of the syringe will be located. With the movement of this structure, the plunger will move inside the syringe producing the extrusion of the material ink.

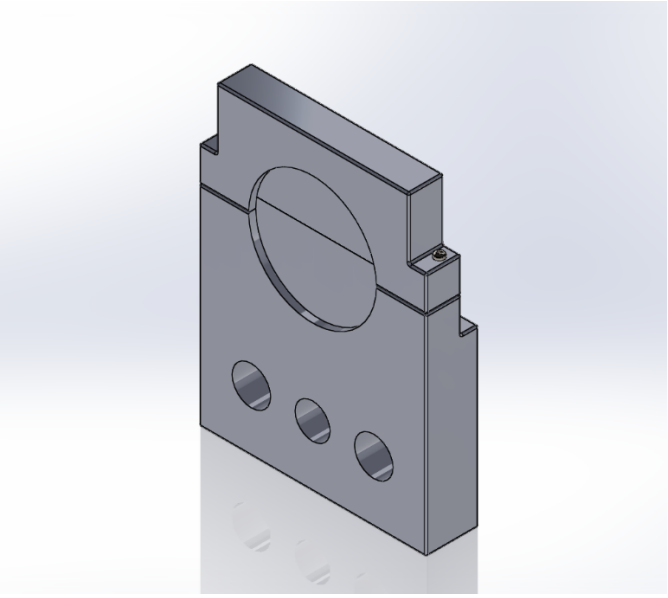

Figure 16: Structure 2 model

3. Structure 3: This last structure is where the syringe will be located and fixed. This structure will also be fixed. It is fixed because in the back side there are two holes for the stability rods. There is also a threaded hole for the threaded rod.

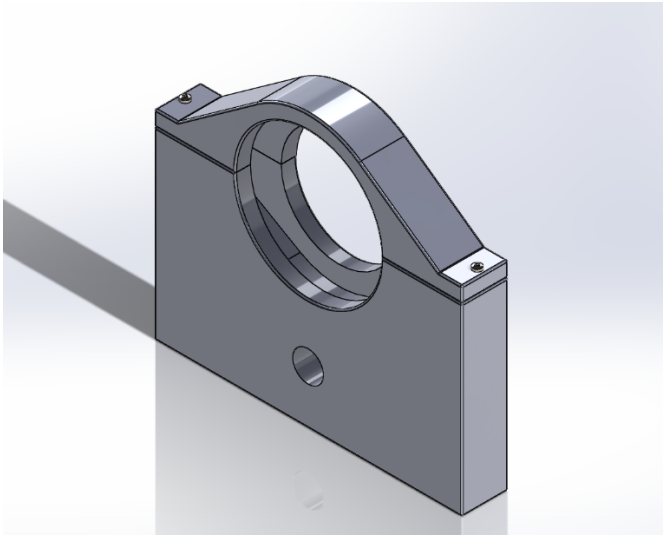

Figure 17: Structure 3 model

In order to achieve the movement desired and to provide movement to the plunger of the syringe, three rods were designed. One of the rods will be introduced to the pulley of the stepper motor and it will rotate with it. This rod will be threaded and will move the plunger while the other ones will ensure the perfect displacement of the structures. The smooth rods will also make the structure stable.

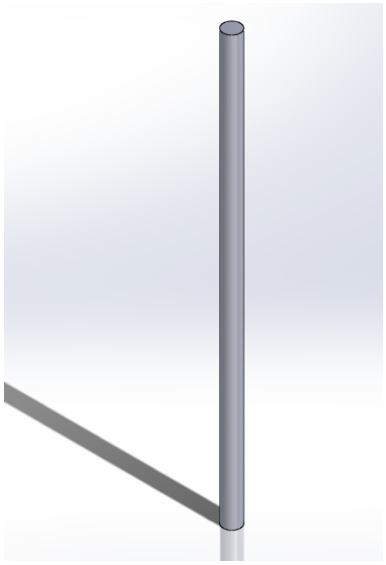

Figure 18: Smooth rod model

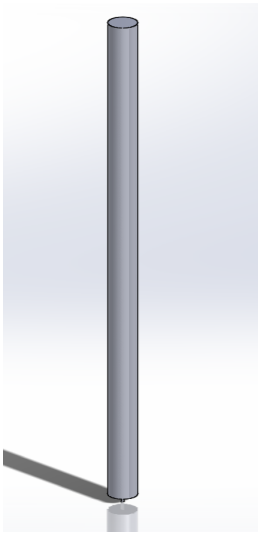

Figure 19: Threaded rod model

The last main component of the mechanism is the syringe. The design of the syringe will be the one obtained by the optimization problem. To make the dimensions more standardized some approximations were made.

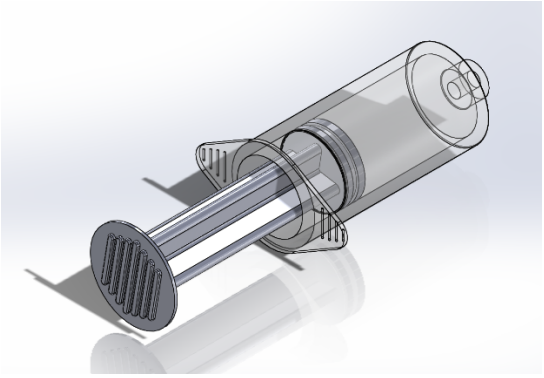

Figure 20: Syringe model

With all these components the next model could be created:

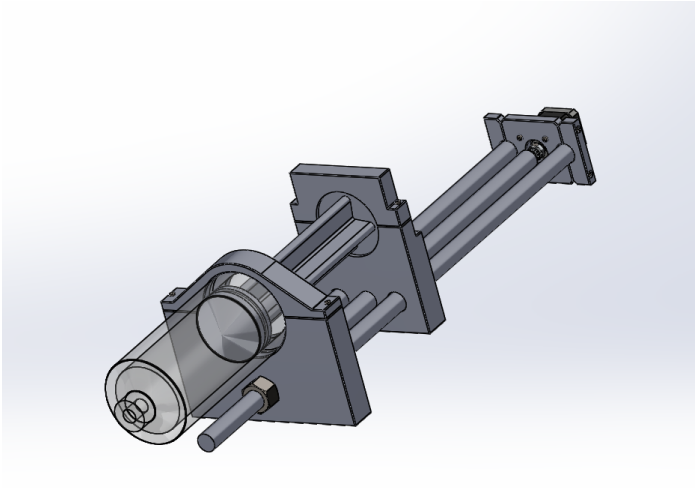

Figure 21: Pump model

This design will allow the desired extrusion using a simple mechanism. First, the stepper motor will rotate making the threaded rod introduce inside the axial rod of the stepper motor rotate as well. When the threaded rod starts rotating the pump will work as a normal screw. The rod starts becoming shorter making the structure situated in the middle to move. When the second structure moves it induces movement to the plunger, this movement will extrude the food material.

6.3. Simulation

For our simulation, we are only interested in the behavior of the food material in the syringe while it flows. Therefore, the simulation is only done on the syringe. The food material used for the simulation is melted chocolate at 40 C. The simulation was run introducing boundary conditions and the entry and exit. At the entry, we set the velocity we want the plunger to move which was determined by the optimization problem (v_1=0.0627 m/s). Then as an exit boundary, we set that the pressure needs to be the environmental pressure.

The simulation will be centered in the viscosity variation, the shear stress distribution, the pressure distribution and the velocity distribution.

1. Viscosity

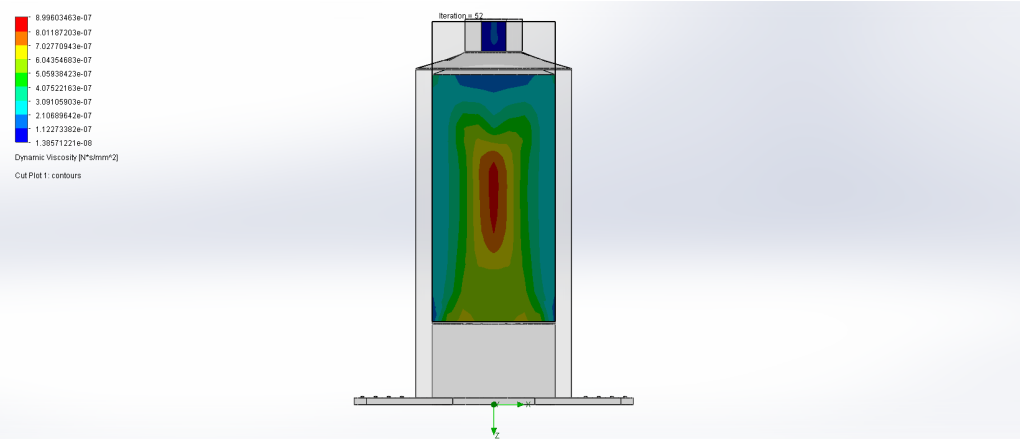

Figure 22: Viscosity distribution on the flow simulation

First of all, the results show a great variation of the values of the viscosity which was expected since the fluid is non-Newtonian. The value for n is lower than one, therefore the chocolate flow should behave as a shear thinning material. As appreciated, the dynamic viscosity is greater in the center of the syringe. This result could be expected since the shear stress in the center of the syringe is supposed to be near zero. We can also see how the values for the nozzle are much lower than the values for the viscosity in the part of the syringe with a greater diameter.

2. Shear stress

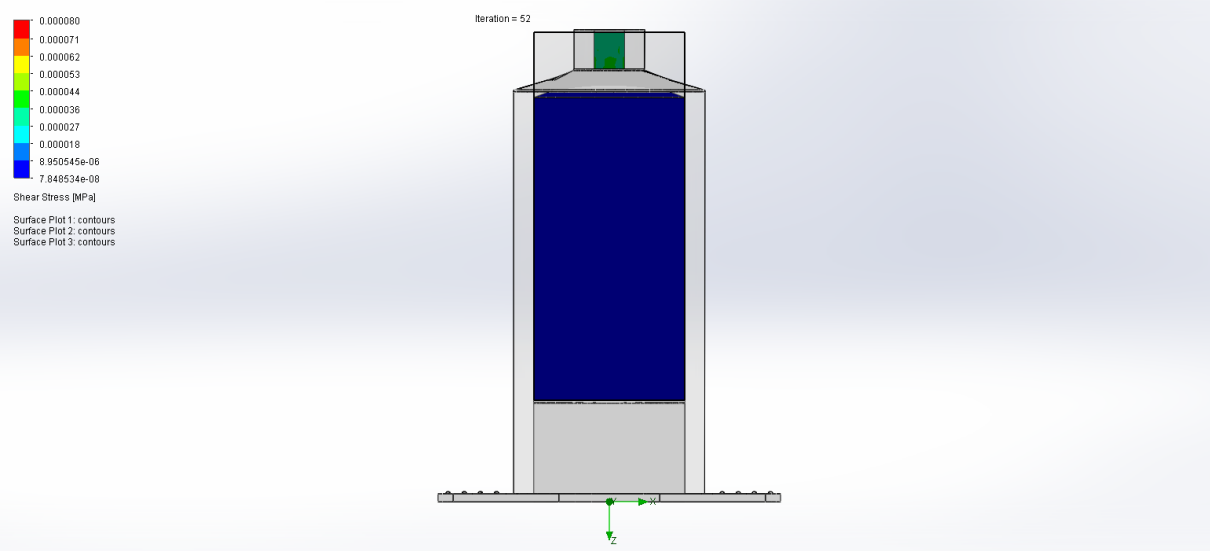

Figure 23: Shear stress distribution on the flow simulation

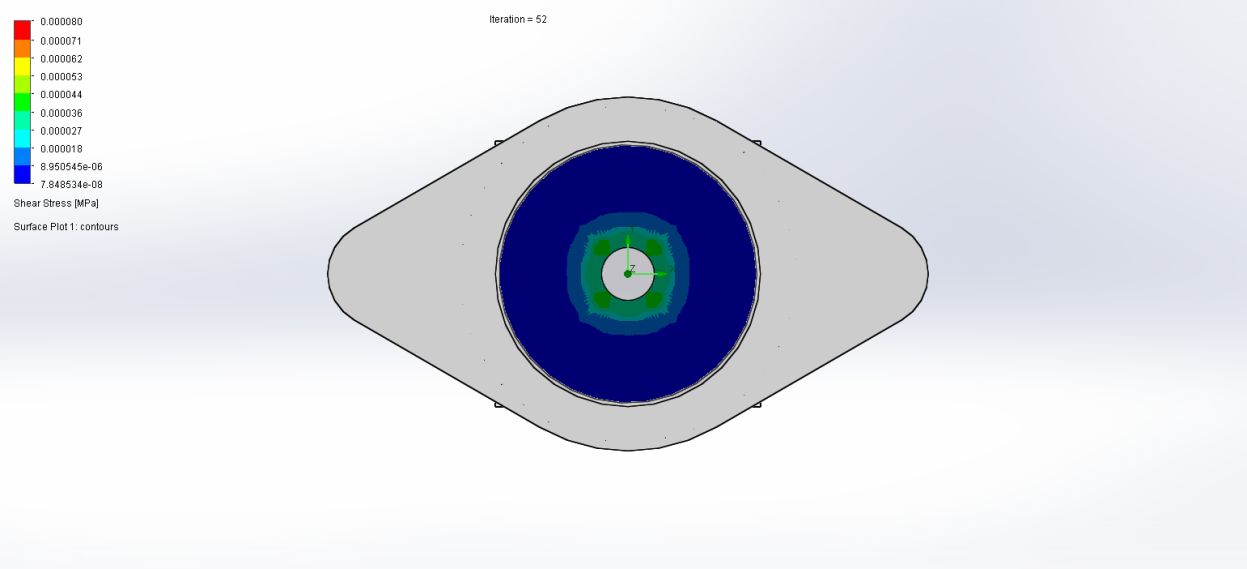

Figure 24: Shear stress distribution on the vena contacta on the flow simulation

With these results, we can confirm that the chocolate flow behaves as a shear thinning fluid. As we can see, the corresponding shear stress around the nozzle cavity is higher than the shear stress on the wider part of the syringe. However, we saw the opposite behavior in the viscosity variation, that is to say, the viscosity was

greater in the wider part than in the nozzle. As a conclusion, we can guess looking at the viscosity that in a constant area section the shear stress increases when the radio is increasing.

3. Pressure distribution

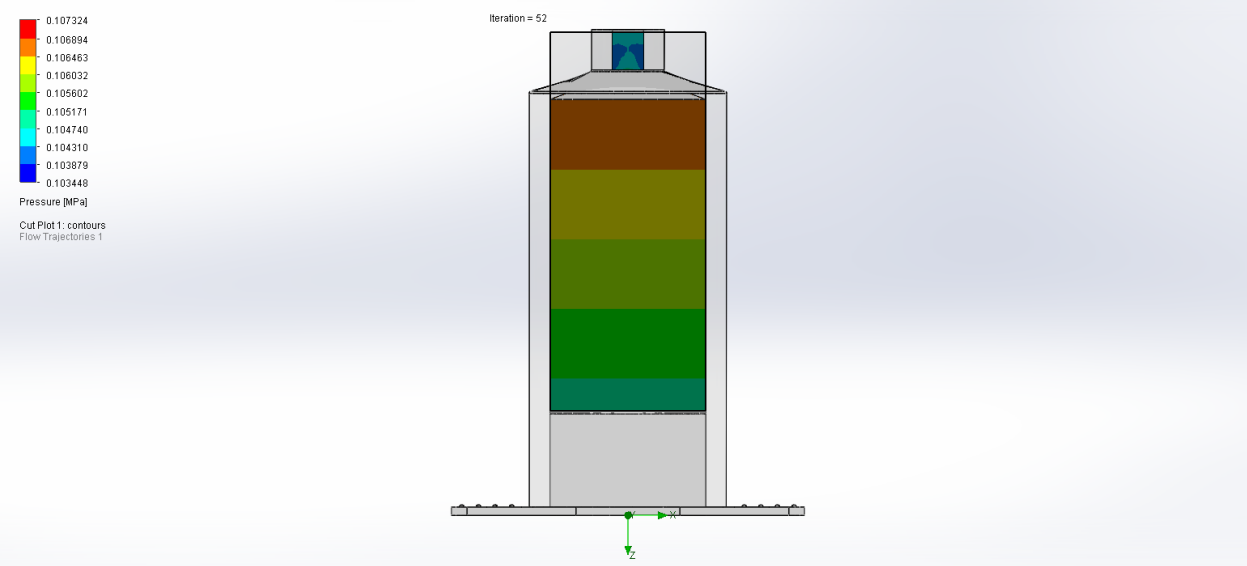

Figure 25: Pressure distribution on the flow simulation

The pressure has a very different behavior than the other two parameters. As it is expressed in the results, along the wide part of the syringe the pressure increases. In this part of the syringe, we can appreciate a pattern in the pressure behavior. It increases along the z axis starting with a value of 104740 Pa but there is no variation along the area section. In order words, pressure does not depend on the radius of the syringe which makes sense. However, the behavior in the nozzle is different since the pressure changes along the area section. This may be as an influence of the vena contacta. Either way, the pressure in the nozzle decreases respect to the pressure in the body of the syringe.

4. Velocity

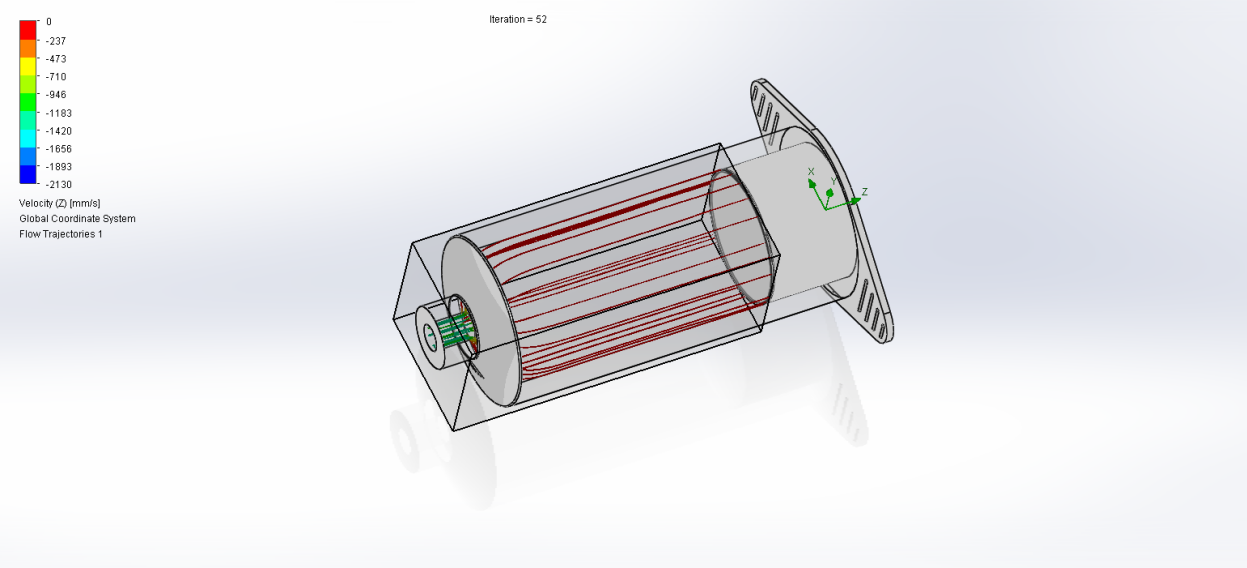

Figure 26: Flow trajectory of the velocity along the z axis on the flow simulation

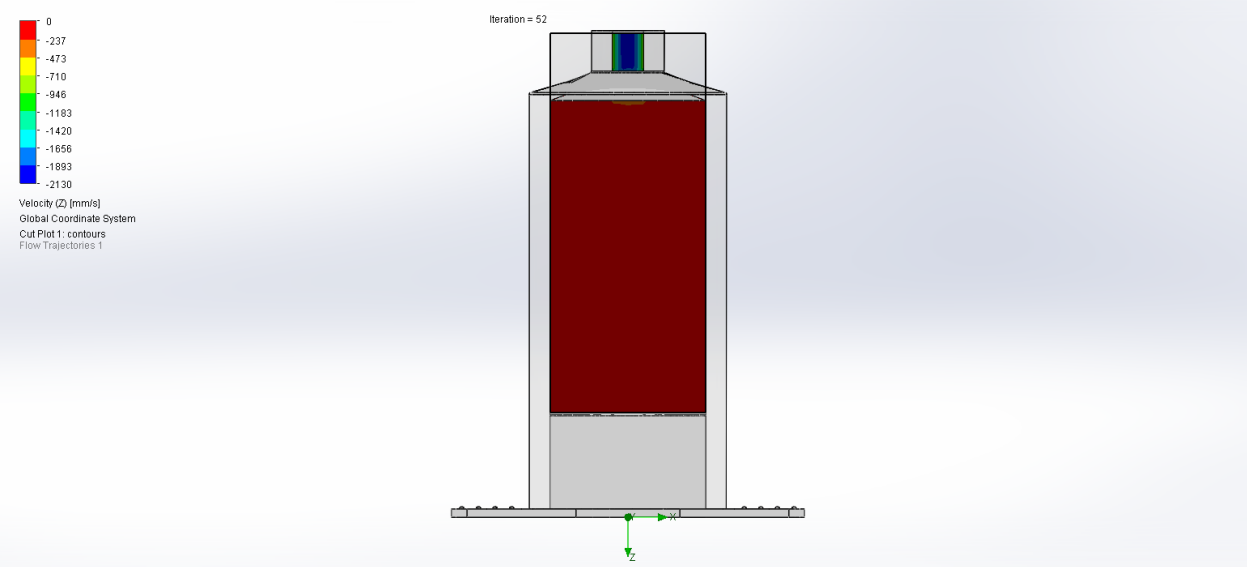

Figure 27: Velocity distribution along the z axis on the flow simulation

Again, two different behaviors can be appreciated corresponding to the main body of the syringe and the nozzle. While in the nozzle, the velocity changes along the area section, being greater in the center than on the surface. This results

can be, somehow, related to the viscosity variation. In the center of the nozzle, the values for viscosity were lower than in the surface showing that the resistance of the fluid to be moved is lower in this region, therefore, the fluid has a higher velocity. Respect to the distribution of the velocity along the body of the syringe, we can see that the velocity in all this region can be neglected and, therefore, there is no variation on the velocity. This can be explained because as it was deducted the velocity in the nozzle needs to be higher in since the difference in diameters is very high this velocity can be considered to be negligible but just respect to the velocity in the nozzle.

Also, the exit velocity is greater than the velocity obtained by the optimization problem. This value is approximately equal to 2 m/s. Therefore, we can conclude that the optimization problem was done under the worst circumstances.

6.4. Theoretical flow simulation

In this section, a theoretical analysis will be applied to obtain the rotatory speed of the stepper motor and the normal force the fluid is exposed to at the beginning of the flow motion. To do so we would apply the properties of the melted chocolate as well as the parameters obtained by the optimization problem.

Data:

$$K = 0.574\ Pas\ ;\ \ n = 0.57\ ;\ \ \rho = 1320\frac{kg}{m^3}\ ;\ \ v_1 = 0.0627\frac{m}{s}\ ;\ \ D_1 = 0.075\ m\ ;$$

$$L_1 = 0.151\ m\ ;\ \ D_2 = 0.015\ m\ ;\ \ L_2 = 0.020\ m$$

Ignoring the viscoelasticity effects that the fluid may have, the volume flow rate is constant along the syringe. Therefore, applying the conservation of mass we can obtain the velocity at the nozzle:

$$Q = cte \;\; Q = A_1 v_1 = A_2 v_2 \rightarrow \frac{\pi}{4} D_1^2 v_1 = \frac{\pi}{4} D_2^2 v_2 \rightarrow v_2 = \left(\frac{D_1}{D_2}\right)^2 v_1$$

Equation 98: Application of conservative Equation

$$v_2 = \left(\frac{0.075}{0.015}\right)^2 * 0.0627 = 1.5675 \frac{m}{s}$$

Equation 99: Result for the velocity of extrusion

To calculate the value of the force at the beginning of the extrusion process we need to calculate the pressure at this point. Applying Bernoulli Equation, previously simplified in the optimization formulation:

$$p_1 = \rho g \left(h_{f1} + h_{f2} + h_m + L_2 + L_1 + \frac{v_2^2 - v_1^2}{2g} \right)$$

Equation 100: Pressure expression after applying Bernoulli's Equation

Now we need to calculate the friction losses in the two different fragments of the syringe and the losses due to the contraction of the nozzle. Since the fluid is non-Newtonian there are some modifications on the expressions.

First, we need to calculate the value of the critic Reynolds number. This number will represent when the flow will start acting as turbulent. Therefore, if the value is lower the flow will be laminar [33].

$$Re_{critic} = \frac{6464n}{(1+3n)^2 \left(\frac{1}{2n}\right)^{\frac{2+n}{1+n}}} = \frac{6464 * 0.57}{(1+3*0.57)^2 \left(\frac{1}{2*0.57}\right)^{\frac{2+0.57}{1+0.57}}} = 2352.20$$

Equation 101: Critic Reynolds' Number for non-Newtonian fluids

Then we need to calculate the two number of Reynolds. The one corresponding for the wide part of the syringe and the one for the nozzle.

$$Re_G = \frac{D^n v^{2-n} \rho}{K 8^{n-1} \left(\frac{3n+1}{4n}\right)}$$

Equation 102: Reynolds' Number for non-Newtonian fluids

$$Re_{G1} = \frac{0.075^{0.57} * 0.0627^{2-0.57} * 1320}{0.574 * 8^{0.57-1} * \left(\frac{3 * 0.57 + 1}{4 * 0.57}\right)} = 20.5984$$

Equation 103: Reynolds' Number for non-Newtonian fluids applied to the base of the syringe

$$Re_{G2} = \frac{0.015^{0.57} * 1.5675^{2-0.57} * 1320}{0.574 * 8^{0.57-1} * \left(\frac{3 * 0.57 + 1}{4 * 0.57}\right)} = 821.2495$$

Equation 104: Reynolds' Number for non-Newtonian fluids applied to the nozzle of the syringe

These two values are lower than the critic Reynolds number, so the flow will be laminar along the syringe.

The primarly friction losses are expressed as:

$$h_f = \frac{4fLv}{D2g}$$

Equation 105: Primary losses expression

While the factor f has the following value:

$$f = \frac{16}{Re_G} \quad f_1 = \frac{16}{20.5984} = 0.7768 \quad f_2 = \frac{16}{821.2495} = 0.0195$$

Equation 106: Factor f expression

Applying these expressions and values we are able to obtain the primary friction losses:

$$h_{f1} = \frac{4 * 0.7768 * 0.151 * 0.0627}{0.075 * 2 * 9.81} = 0.02\ m$$

Equation 107: Primary losses at the base of the syringe

$$h_{f2} = \frac{4 * 0.0195 * 0.02 * 1.5675}{0.015 * 2 * 9.81} = 0.0083\ m$$

Equation 108: Primary losses at the nozzle of the syringe

To calculate the secondary losses due to the contraction of the syringe we need to apply the next expression:

$$h_m = \frac{kv_2^2}{2g}$$

Equation 109: Secondary losses expression

In order to calculate the factor k we need to apply the next relations for non-Newtonian fluids.

$$\alpha = \frac{2(n+1)(5n+3)}{3(3n+1)^2} = \frac{2(0.57+1)(5*0.57+3)}{3(3*0.57+1)^2} = 0.5682$$

Equation 110: Factor α expression

$$k' = \frac{0.55}{\alpha} = \frac{0.55}{0.5282} = 0.9679\,;\ \ \beta = k'500 = 0.9679 * 500 = 483.95$$

Equation 111: Factor k′ and β expressions

$$k = \frac{\beta}{Re_{G2}} = \frac{483.95}{821.2495} = 0.5893$$

Equation 112: Factor k expression

$$h_m = 0.5893 * \frac{1.5675^2}{2 * 9.81} = 0.6266\ m$$

Equation 113: Secondary losses

Once we obtained all the values for the losses we can obtain the value for pressure:

$$p_1 = \rho g \left(h_{f1} + h_{f2} + h_m + L_2 + L_1 + \frac{v_2^2 - v_1^2}{2g} \right)$$

Equation 114: Pressure expression after applying Bernoulli's Equation

$$p_1 = 1320 * 9.81 * \left(0.02 + 0.0083 + 0.6266 + 0.151 + 0.02 + \frac{1.5675^2 - 0.0627^2}{2 * 9.81}\right)$$

$$p_1 = 12313.8068\ Pa$$

Equation 115: Relative pressure at the beginnign of extrusion

$$P_1 = P + p_1 = 101300 + 12313.8068 = 113613.8068\ Pa$$

Equation 116: Absolute pressure at the beginnign of extrusion

Applying the definition of pressure, we obtain the force:

$$P = \frac{F}{A}$$

Equation 117: Relation between force and pressure

$$P_1 = \frac{F_1}{A_1} \rightarrow F_1 = P_1 A_1 = P_1 \frac{\pi}{4} D_1^2 = \frac{113613.8068 * \pi * 0.075^2}{4} = 501.9304\ N$$

Equation 118: Force to start with the extrusion

Now, we would try to obtain an approximate value for the rotative velocity of the stepper motor. Since the threaded rod is the one who moves structure 2 and consequently the plunge of the syringe is moved, depending on how was the threaded rod is spinning the initial velocity will change. The initial velocity desired to reached is set, therefore we can obtain the value of the rotative speed, applying the next expression:

$$rpm * e = v_1 \rightarrow rpm = \frac{v_1}{e} = \frac{0.0627}{0.0025} = 25.08\ rpm$$

Equation 119: Stepper motor revolutions

e is the value of the step of the thread of the rod.

Chapter 7:

Conclusions

As every innovative and new invention, it takes time to the model to be adapted to the consumers' necessities. Due to this, there is a long and difficult way for 3D Food printings to be introduced in every house kitchen in the world. This is not to say that they will never have an application on everyday life cooking. For example, one thousand years ago, no one would have imagined that a device such as a microwave will be able to warm up food and even cook it. Nowadays, we can find a microwave in almost every kitchen in the world. With this example, I want to stay that in the development process of this type of device, time is definitely as necessary as another main step on the development of the 2D food printers.

Regarding, 3D food printers there is a lot of development to do since right currently they do not only not offer the solution for a problem but they don't improve any process related with the time cooking or quality. However, a solution such as 3D food printing or similar need to be introduced because, as it was said, the food resources we are used to in countries in Europe or USA will be almost over in 50 years from now. Therefore, there is no other solution that ending up introducing those other food resources as part of our diet. Some of these other options are all types of insect and other plants like algae. These other options of food are very different from the kind of food we are used to, but they are also enriched with lots of proteins. In conclusion, these aliments need to be introduced to our diets somehow and since they have different taste, shape and texture of the currently used aliments, 3D food printer would be the perfect way to introduce them in the conventional recipes without even appreciating a difference.

Also, other of the applications of 3D printers is in the medical field. Since the food can be modified to have the desired texture. It would be perfect for those patients who are not able to swallow food. Or they need really specific food nutrients so the healing process is faster and more effective. Therefore, by introducing 3D food printers in the medical field a more scientific development can be achieved while providing the consumers' necessities. Also, these will produce useful feedback providing information about those features that need improvement.

Regarding the analysis done on the flow of the syringe, the maximum extrusion velocity was sought. It is important to obtain the faster velocity as possible because in that

way the faster the extrusion is done the faster the printer can move and the faster the printing process will be finished. But there are a lot of limits to be considered. Some of the most difficulties are to obtain that food ink with the perfect properties to obtain the desired velocity. But, of course, that food ink that will also proportionate the great portion of nutrients and taste possible. In order to achieve great food materials a lot of research has to be done related with the chemical composition of the hydrocolloids that can be added as well as the particle size and also the behavior of the food ink in its whole composition. Another problem is that since there is a great number of different products with very different properties and therefore very different behaviors of the nature of the fluid, it is very hard to obtain the optimum dimensions for a big range of aliments with very different behavior.

However, in the optimization problem done in this research, we introduced the worst properties that most food materials obtaining some values for the dimensions that were optimal for these conditions. With this, we could use the design in the better conditions to a big range of food aliments.

For a better understanding of the flow simulation of the fluid through the extrusion, we used SolidWorks obtaining the results for non-Newtonian fluids. The results obtained were much complex than the ones obtained for a Newtonian fluid. Also, a theoretical analysis was done for non-Newtonian which allowed to compare the results. There were differences in the values obtained, especially in the velocity of the extrusion. One of the reasons could be that in the theoretical analysis the fluid is supposed to be incompressible and as it was said most of the food materials as well as the chocolate that was the materials used in the project, are viscoelastic. However, this comparison was really useful. Regardless the expression of the viscoelasticity influence was not calculated, it could be seen in the difference of results. Concluding that the more viscoelastic a material is the more velocity can reach with not proportionating a great increase on pressure. This behavior could be expected since while the fluid is in motion the fluid is being comprised making the plunger to move faster.

ANNEX I:

Planes

1. Stepper Motor

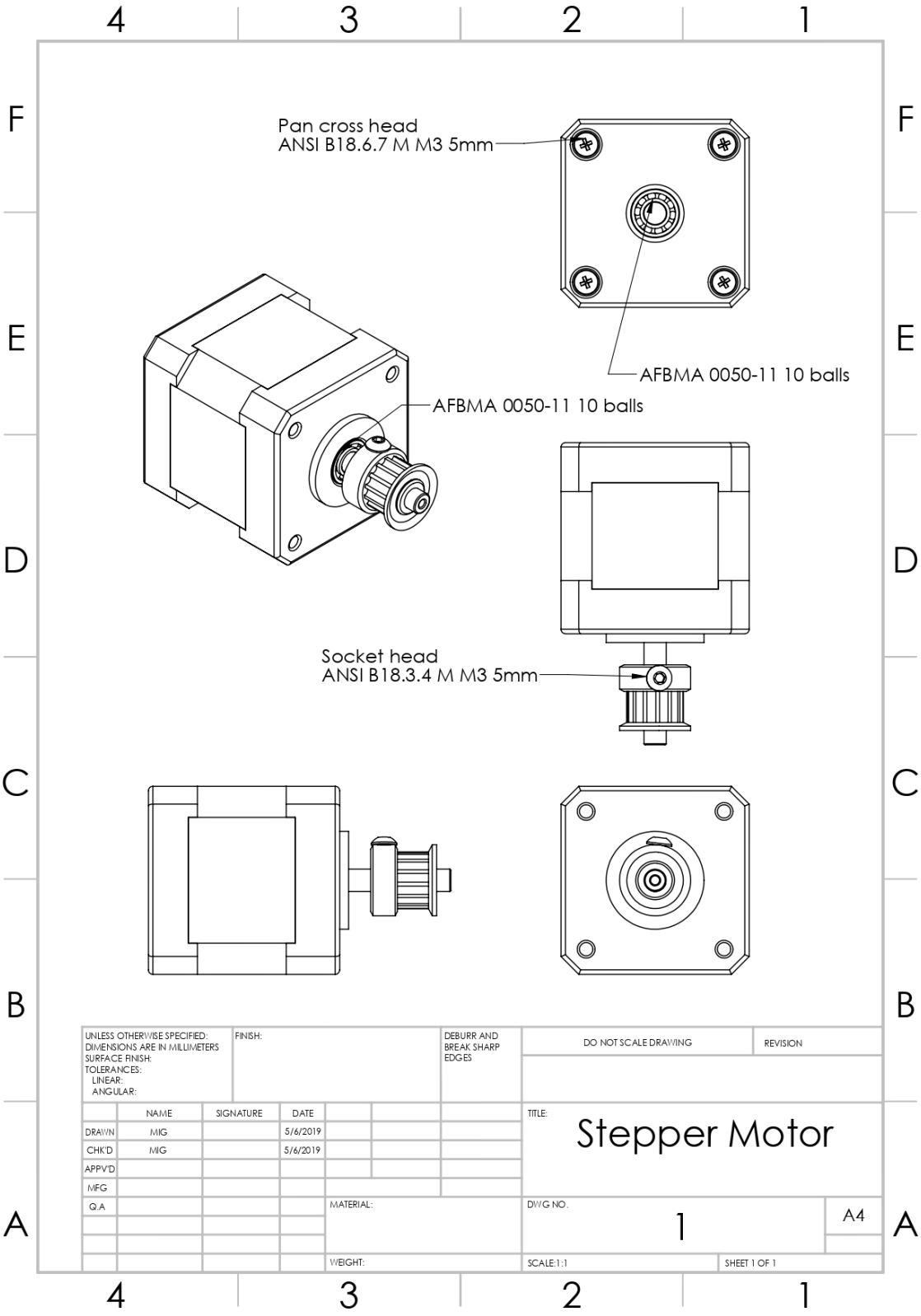

1.1. Base

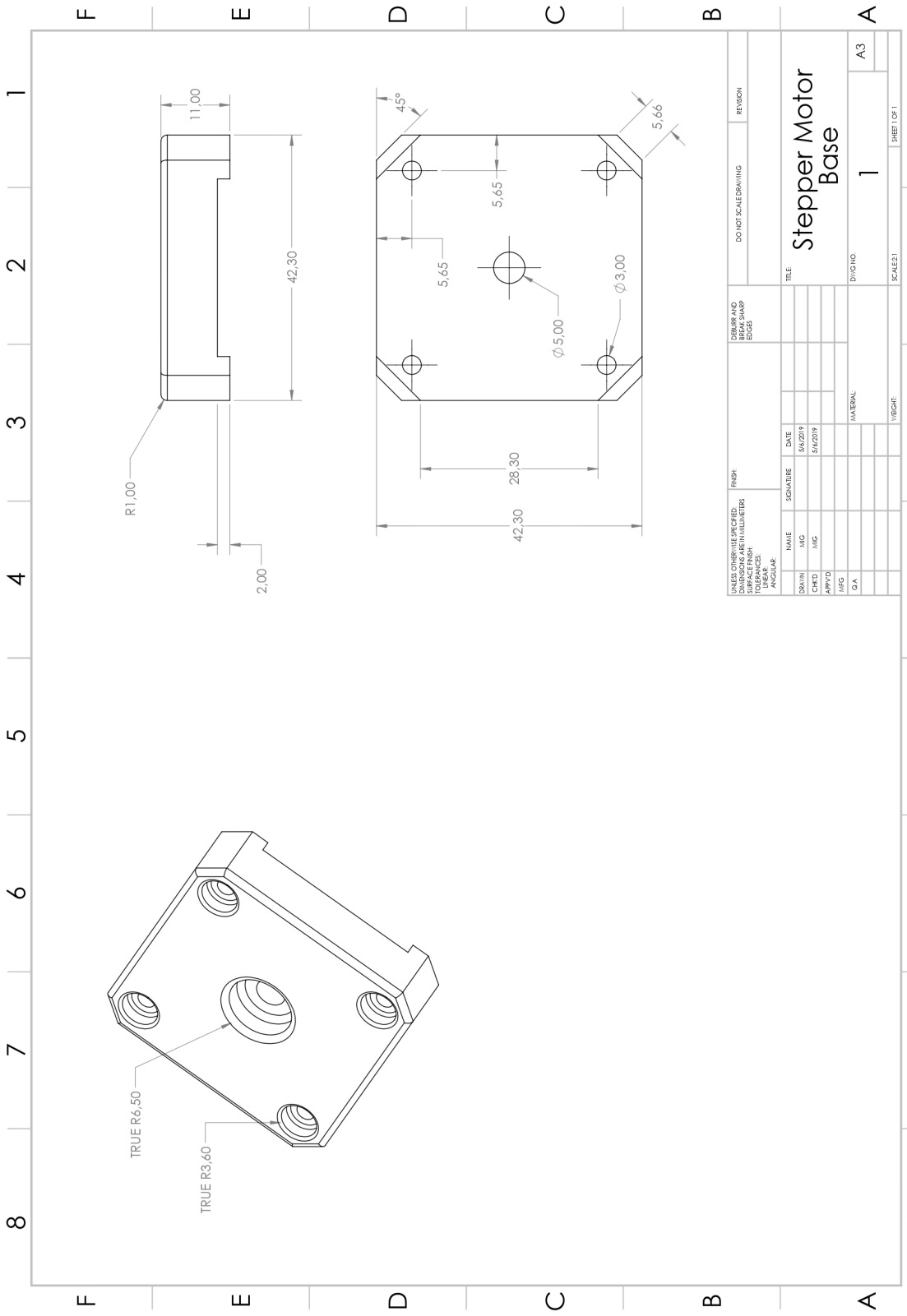
11,00
42,30
R1,00
2,00
45°
5,66
5,65
5,65
Ø5,00
Ø3,00
28,30
42,30
TRUE R6,50
TRUE R3,60
DO NOT SCALE DRAWING
REVISION
DEBURR AND BREAK SHARP EDGES
FINISH:
TOLERANCES:
LINEAR:
ANGULAR:
NAME
SIGNATURE
DATE
DRAWN
MG
5/6/2019
CHK'D
MG
5/6/2019
APPV'D
MFG
Q.A
MATERIAL:
WEIGHT:
TITLE:
Stepper Motor Base
DWG NO.
1
A3
SCALE:2:1
SHEET 1 OF 1

1.2. Backplate

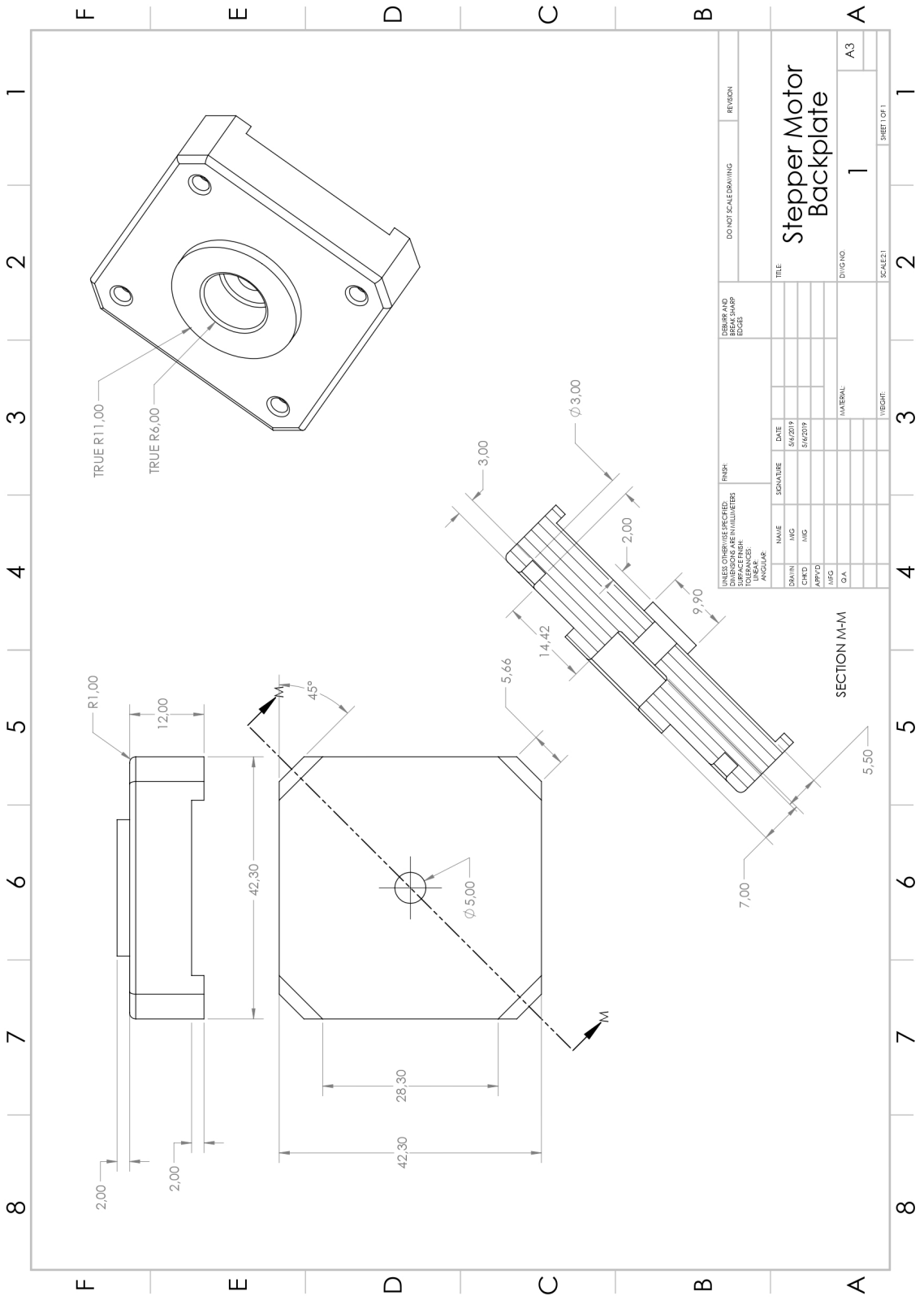

1.3. Body

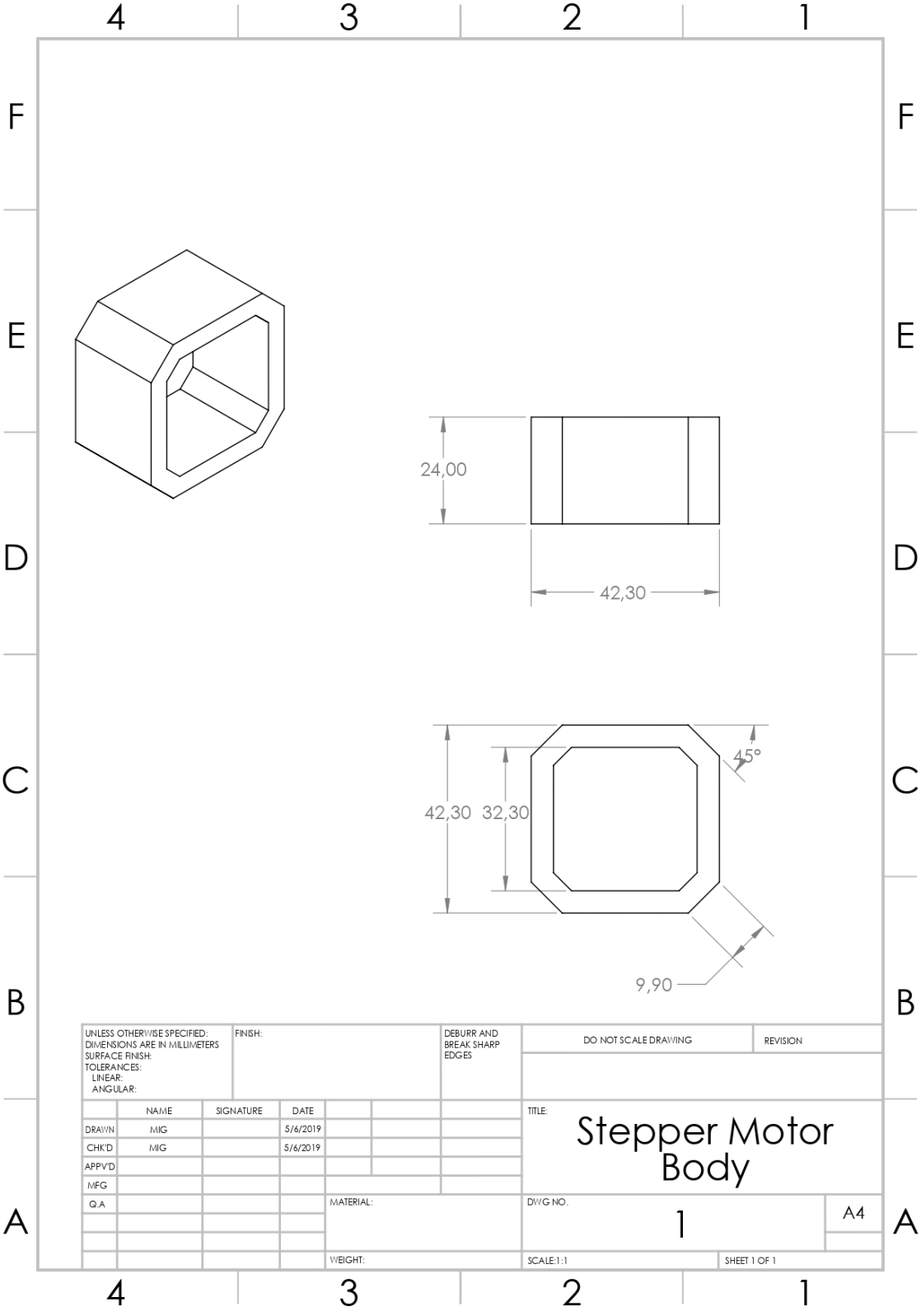
4
3
2
1
F
E
D
C
B
A
24,00
42,30
42,30
32,30
45°
9,90
UNLESS OTHERWISE SPECIFIED:
DIMENSIONS ARE IN MILLIMETERS
SURFACE FINISH:
TOLERANCES:
LINEAR:
ANGULAR:
FINISH:
DEBURR AND BREAK SHARP EDGES
DO NOT SCALE DRAWING
REVISION
NAME
SIGNATURE
DATE
DRAWN
MIG
5/6/2019
CHK'D
MIG
5/6/2019
APPV'D
MFG
Q.A
TITLE:
Stepper Motor Body
MATERIAL:
DWG NO.
1
A4
WEIGHT:
SCALE:1:1
SHEET 1 OF 1

1.4. Axial Rod

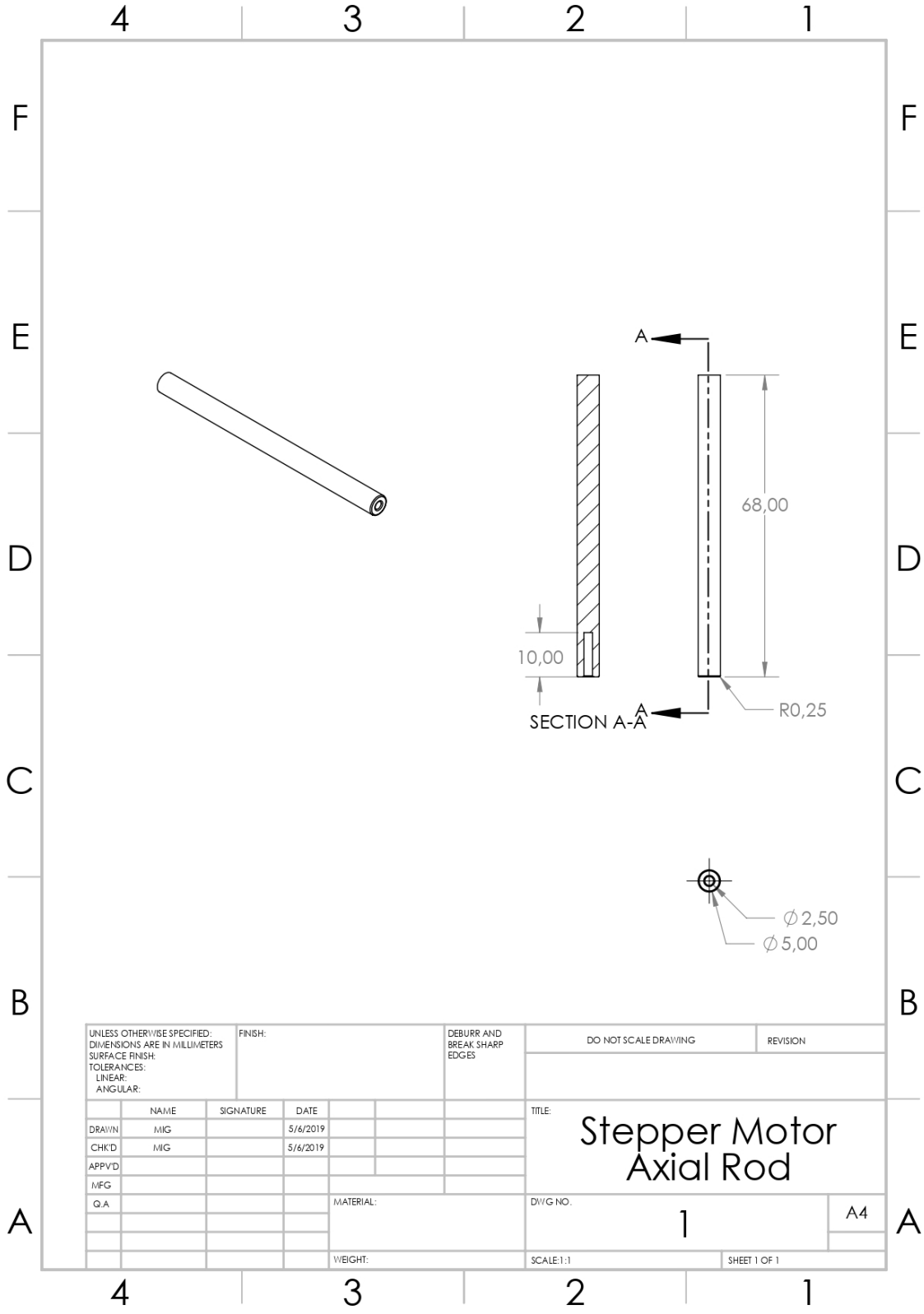
4
3
2
1
F
E
D
C
B
A
A
68,00
10,00
A
SECTION A-A
R0,25
∅2,50
∅5,00
UNLESS OTHERWISE SPECIFIED:
DIMENSIONS ARE IN MILLIMETERS
SURFACE FINISH:
TOLERANCES:
LINEAR:
ANGULAR:
FINISH:
DEBURR AND BREAK SHARP EDGES
DO NOT SCALE DRAWING
REVISION
NAME
SIGNATURE
DATE
DRAWN
MIG
5/6/2019
CHK'D
MIG
5/6/2019
APPV'D
MFG
Q.A
TITLE:
Stepper Motor Axial Rod
MATERIAL:
DWG NO.
1
A4
WEIGHT:
SCALE:1:1
SHEET 1 OF 1

1.5. Pulley

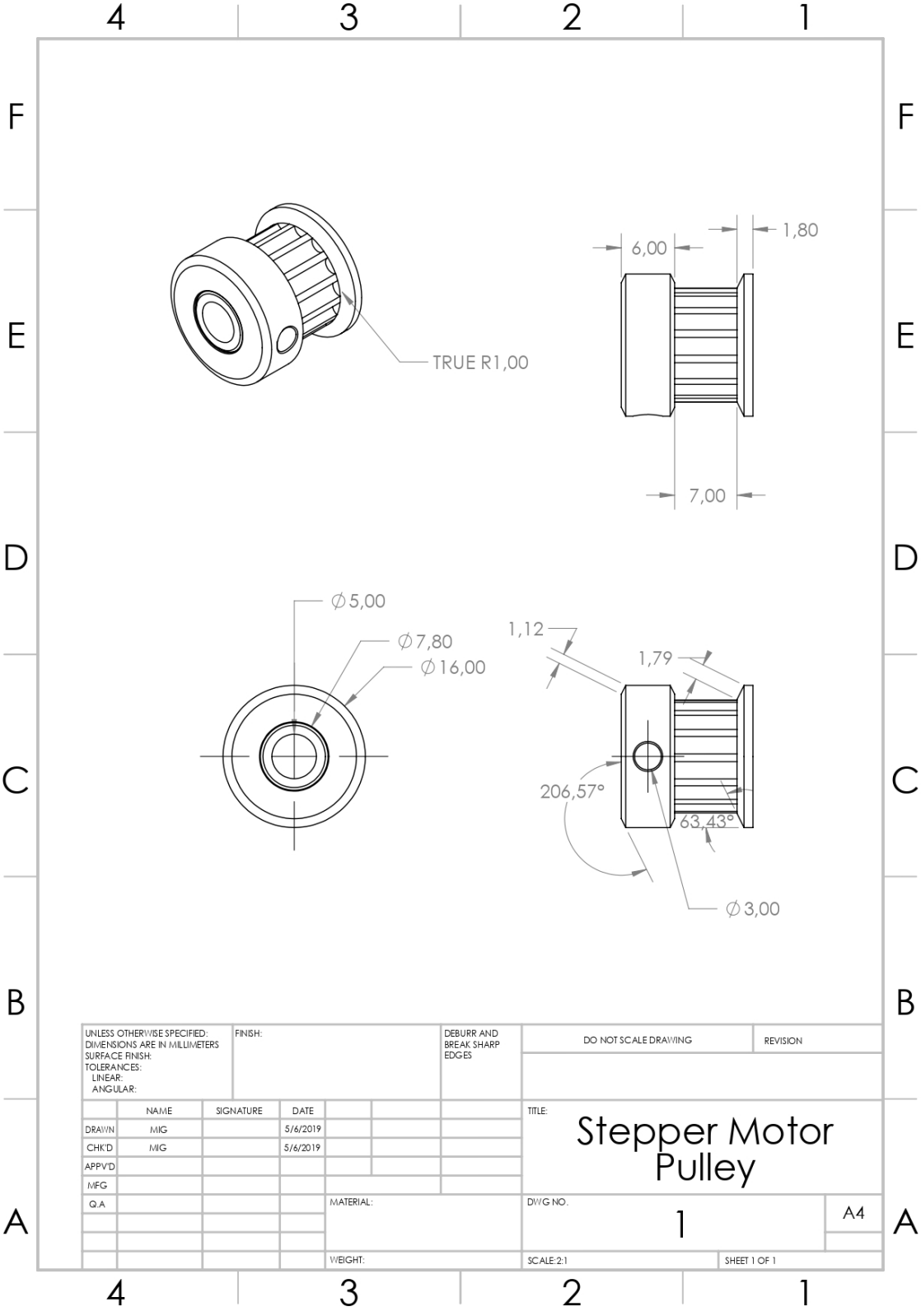
TRUE R1,00
6,00
1,80
7,00
∅5,00
∅7,80
∅16,00
1,12
1,79
206,57°
63,43°
∅3,00
UNLESS OTHERWISE SPECIFIED:
DIMENSIONS ARE IN MILLIMETERS
SURFACE FINISH:
TOLERANCES:
LINEAR:
ANGULAR:
FINISH:
DEBURR AND BREAK SHARP EDGES
DO NOT SCALE DRAWING
REVISION
NAME
SIGNATURE
DATE
DRAWN
MIG
5/6/2019
CHK'D
MIG
5/6/2019
APPV'D
MFG
Q.A
TITLE:
Stepper Motor Pulley
MATERIAL:
DWG NO.
1
A4
WEIGHT:
SCALE:2:1
SHEET 1 OF 1

2. Syringe

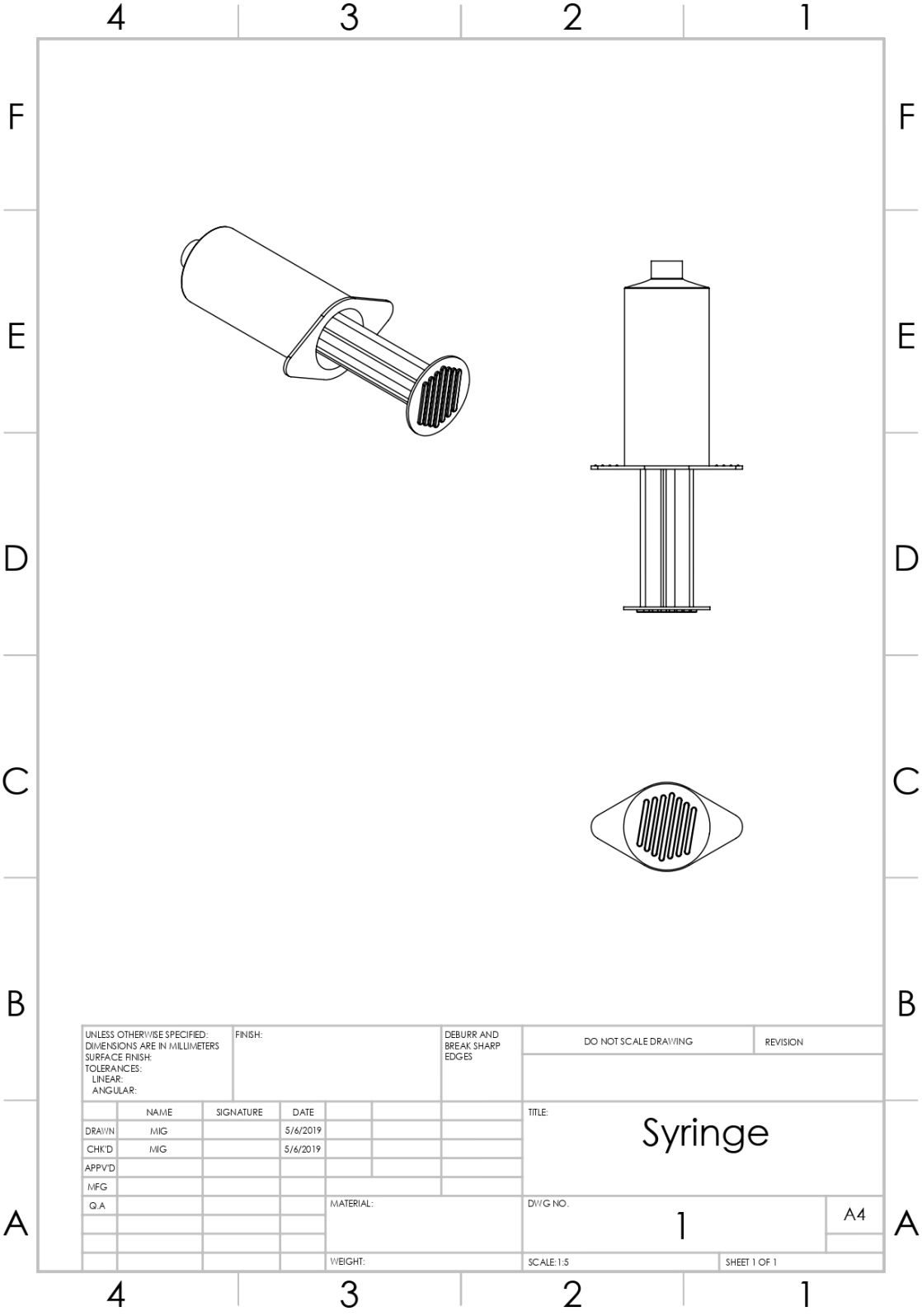
4
3
2
1
F
E
D
C
B
A
UNLESS OTHERWISE SPECIFIED:
DIMENSIONS ARE IN MILLIMETERS
SURFACE FINISH:
TOLERANCES:
LINEAR:
ANGULAR:
FINISH:
DEBURR AND BREAK SHARP EDGES
DO NOT SCALE DRAWING
REVISION
NAME
SIGNATURE
DATE
DRAWN
MIG
5/6/2019
CHK'D
MIG
5/6/2019
APPV'D
MFG
Q.A
TITLE:
Syringe
MATERIAL:
DWG NO.
1
A4
WEIGHT:
SCALE:1:5
SHEET 1 OF 1

2.1. Body

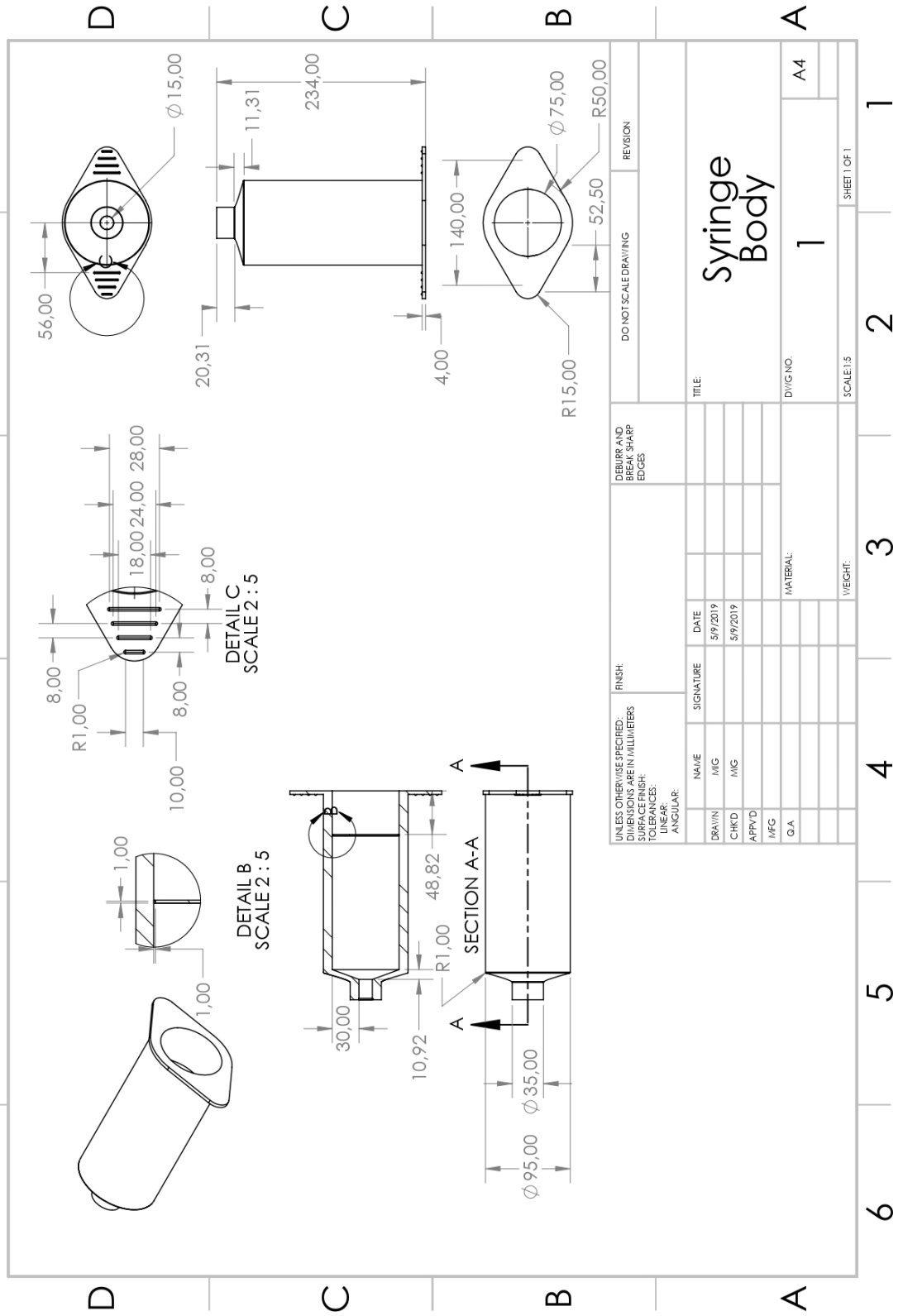
Syringe Body
DETAIL B SCALE 2 : 5
DETAIL C SCALE 2 : 5
SECTION A-A
DO NOT SCALE DRAWING
DEBURR AND BREAK SHARP EDGES
A4
SCALE:1:5
SHEET 1 OF 1

2.2. Plunger

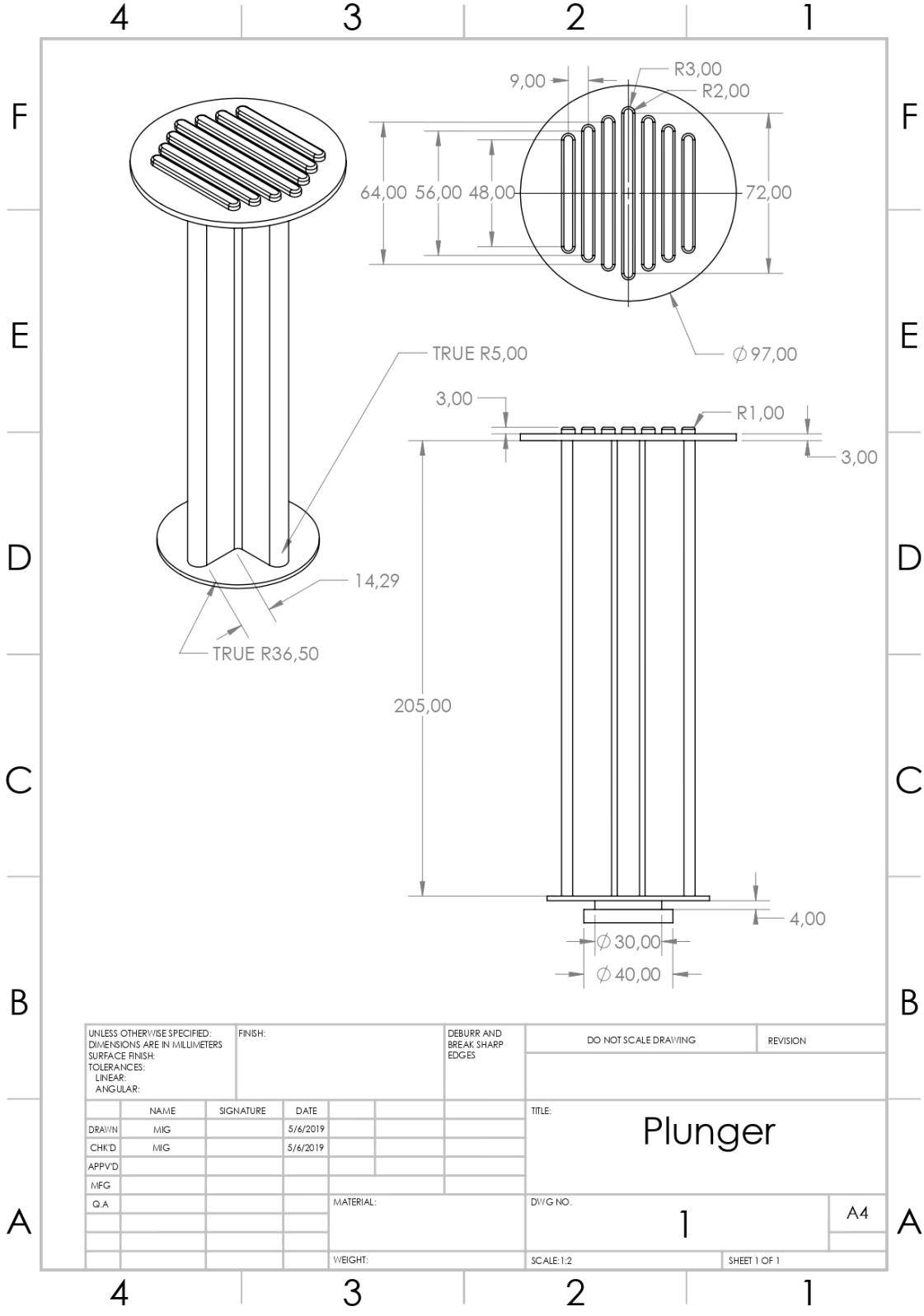
9,00
R3,00
R2,00
64,00
56,00
48,00
72,00
∅97,00
TRUE R5,00
3,00
R1,00
3,00
14,29
TRUE R36,50
205,00
4,00
∅30,00
∅40,00
UNLESS OTHERWISE SPECIFIED:
DIMENSIONS ARE IN MILLIMETERS
SURFACE FINISH:
TOLERANCES:
LINEAR:
ANGULAR:
FINISH:
DEBURR AND BREAK SHARP EDGES
DO NOT SCALE DRAWING
REVISION
NAME
SIGNATURE
DATE
DRAWN
MIG
5/6/2019
CHK'D
MIG
5/6/2019
APPV'D
MFG
Q.A
TITLE:
Plunger
MATERIAL:
DWG NO.
1
A4
WEIGHT:
SCALE:1:2
SHEET 1 OF 1

2.3. Rubber

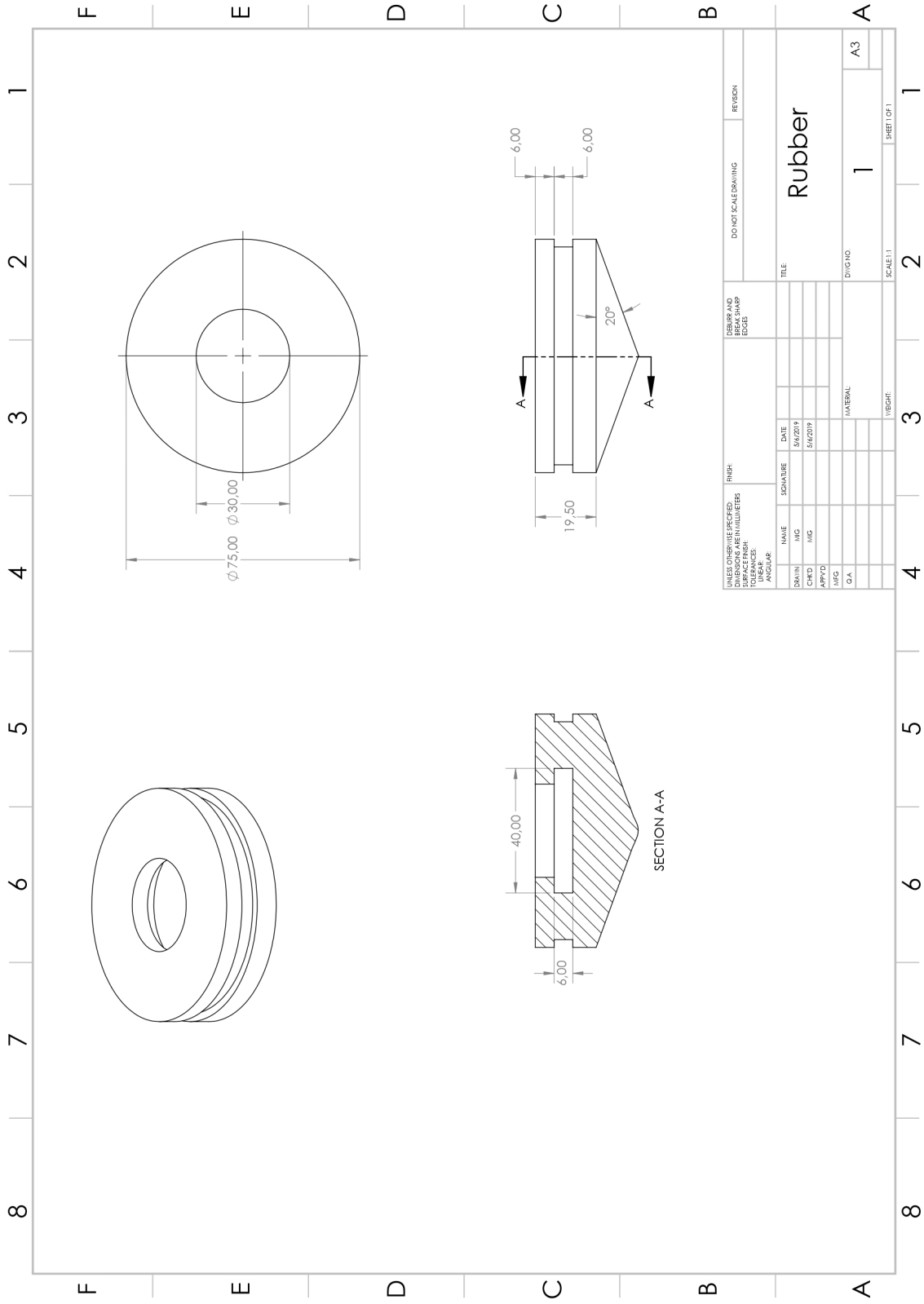
Rubber
DO NOT SCALE DRAWING
REVISION
TITLE:
DEBUR AND BREAK SHARP EDGES
FINISH:
UNLESS OTHERWISE SPECIFIED:
DIMENSIONS ARE IN MILLIMETERS
SURFACE FINISH:
TOLERANCES:
LINEAR
ANGULAR
NAME
SIGNATURE
DATE
DRAWN
MG
5/6/2019
CHK'D
MG
5/6/2019
APPV'D
MFG
Q.A
MATERIAL:
DWG NO
1
A3
WEIGHT:
SCALE: 1:1
SHEET 1 OF 1
6,00
6,00
20°
A
A
19,50
ϕ30,00
ϕ75,00
40,00
6,00
SECTION A-A

3. Structure 1

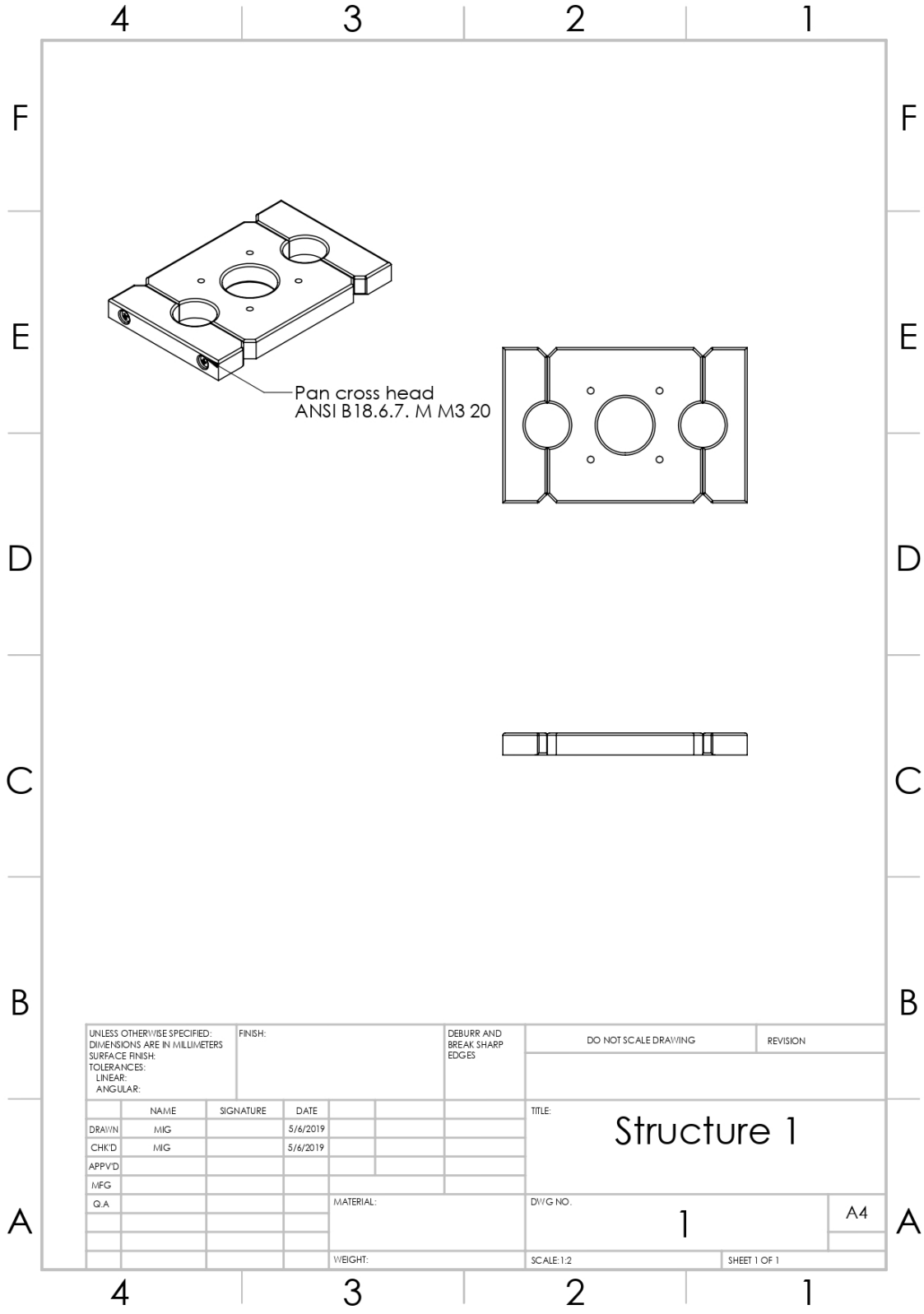

3.1. Part1

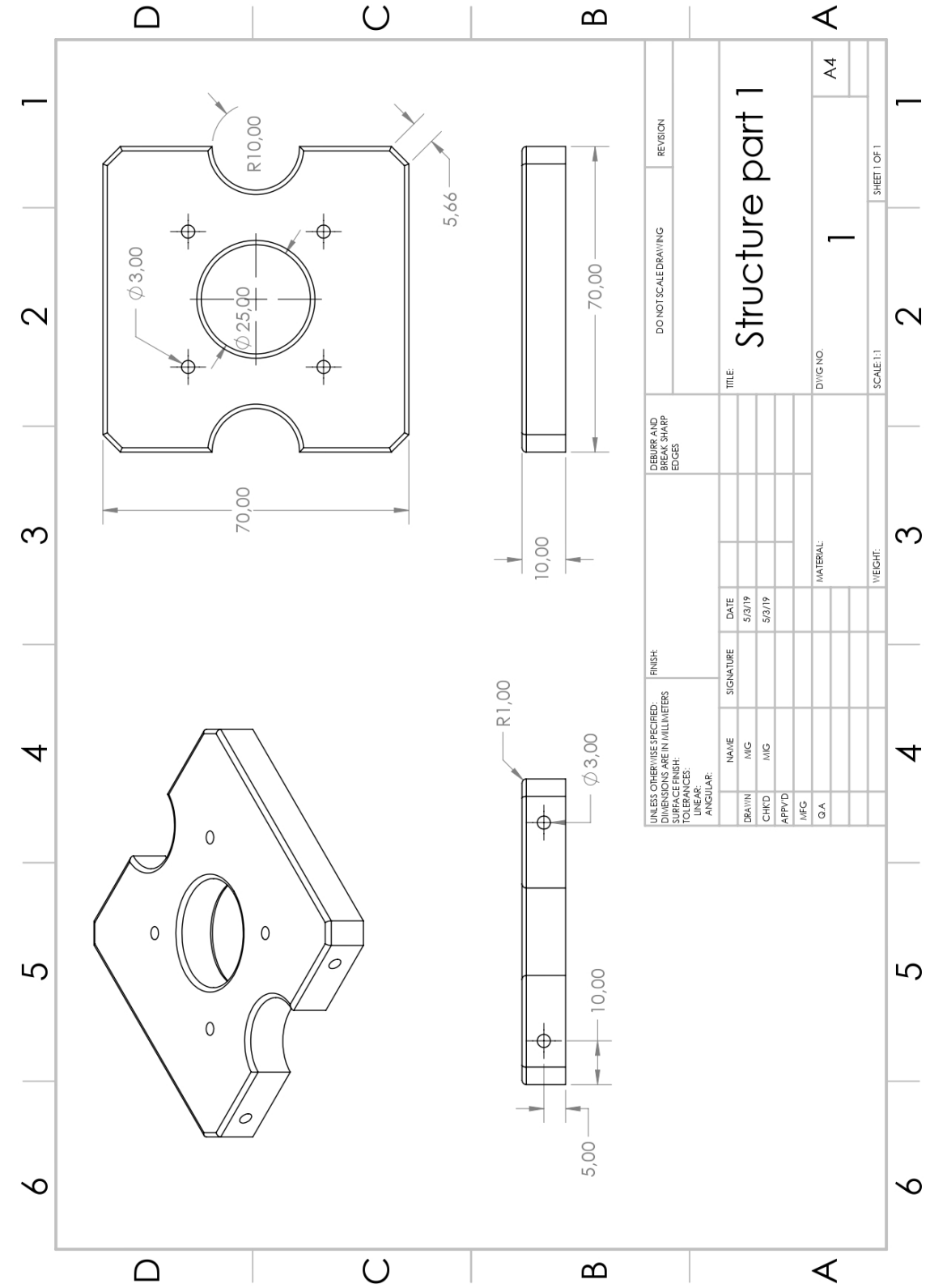
R10,00
5,66
Ø3,00
Ø25,00
70,00
70,00
10,00
R1,00
Ø3,00
10,00
5,00
UNLESS OTHERWISE SPECIFIED:
DIMENSIONS ARE IN MILLIMETERS
SURFACE FINISH:
TOLERANCES:
LINEAR:
ANGULAR:
FINISH:
DEBURR AND BREAK SHARP EDGES
DO NOT SCALE DRAWING
REVISION
NAME
SIGNATURE
DATE
DRAWN
MG
5/3/19
CHK'D
MG
5/3/19
APPV'D
MFG
Q.A
MATERIAL:
WEIGHT:
TITLE:
Structure part 1
DWG NO.
1
A4
SCALE: 1:1
SHEET 1 OF 1

3.2. Part2

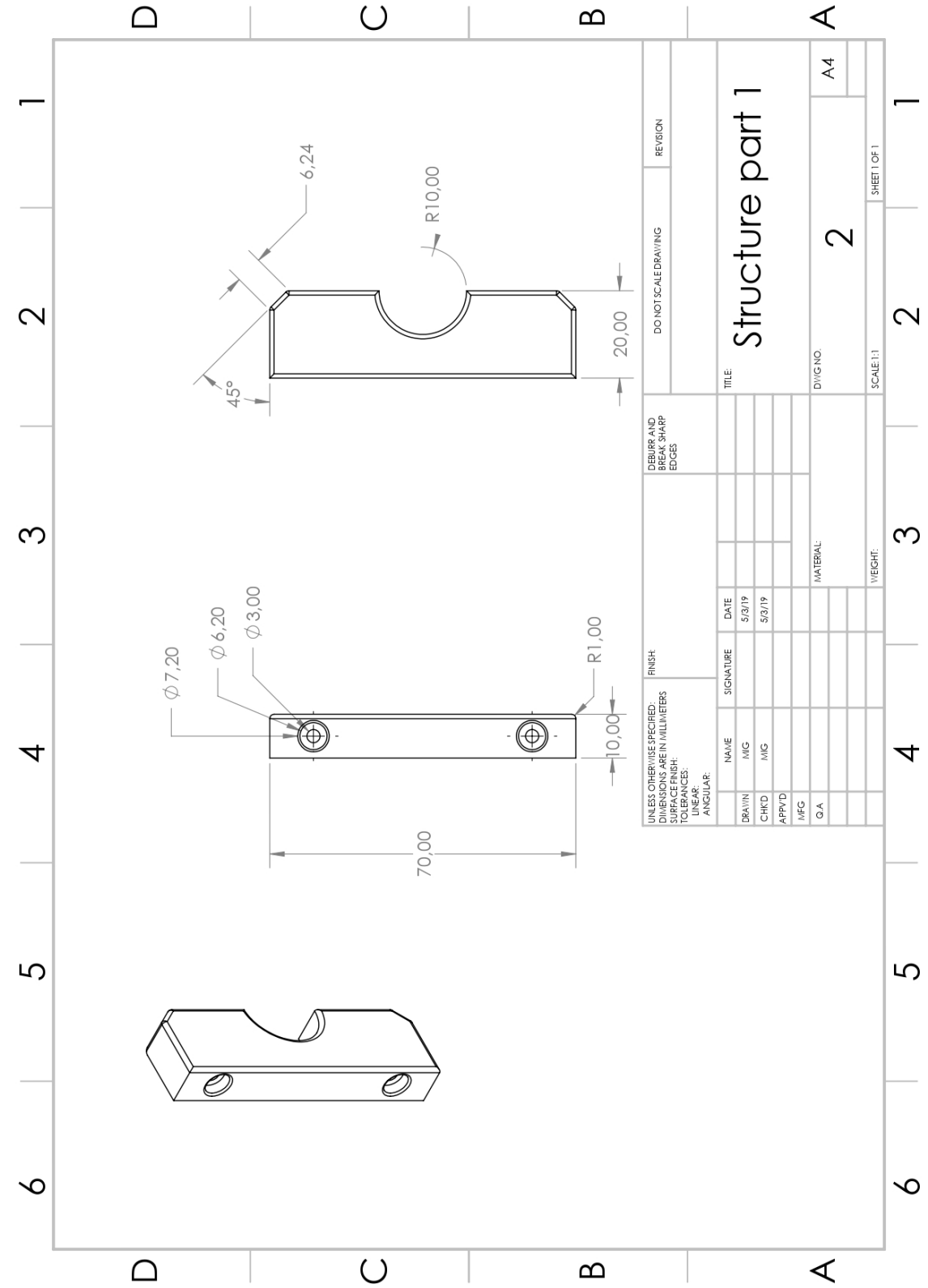
6,24
R10,00
45°
20,00
ϕ7,20
ϕ6,20
ϕ3,00
R1,00
10,00
70,00
DO NOT SCALE DRAWING
REVISION
Structure part 1
TITLE:
DWG NO.
2
A4
SCALE:1:1
SHEET 1 OF 1
WEIGHT:
MATERIAL:
DEBURR AND BREAK SHARP EDGES
FINISH:
UNLESS OTHERWISE SPECIFIED:
DIMENSIONS ARE IN MILLIMETERS
SURFACE FINISH:
TOLERANCES:
LINEAR:
ANGULAR:
NAME
SIGNATURE
DATE
DRAWN
MG
5/3/19
CHK'D
MG
5/3/19
APPV'D
MFG
Q.A

4. Structure 2

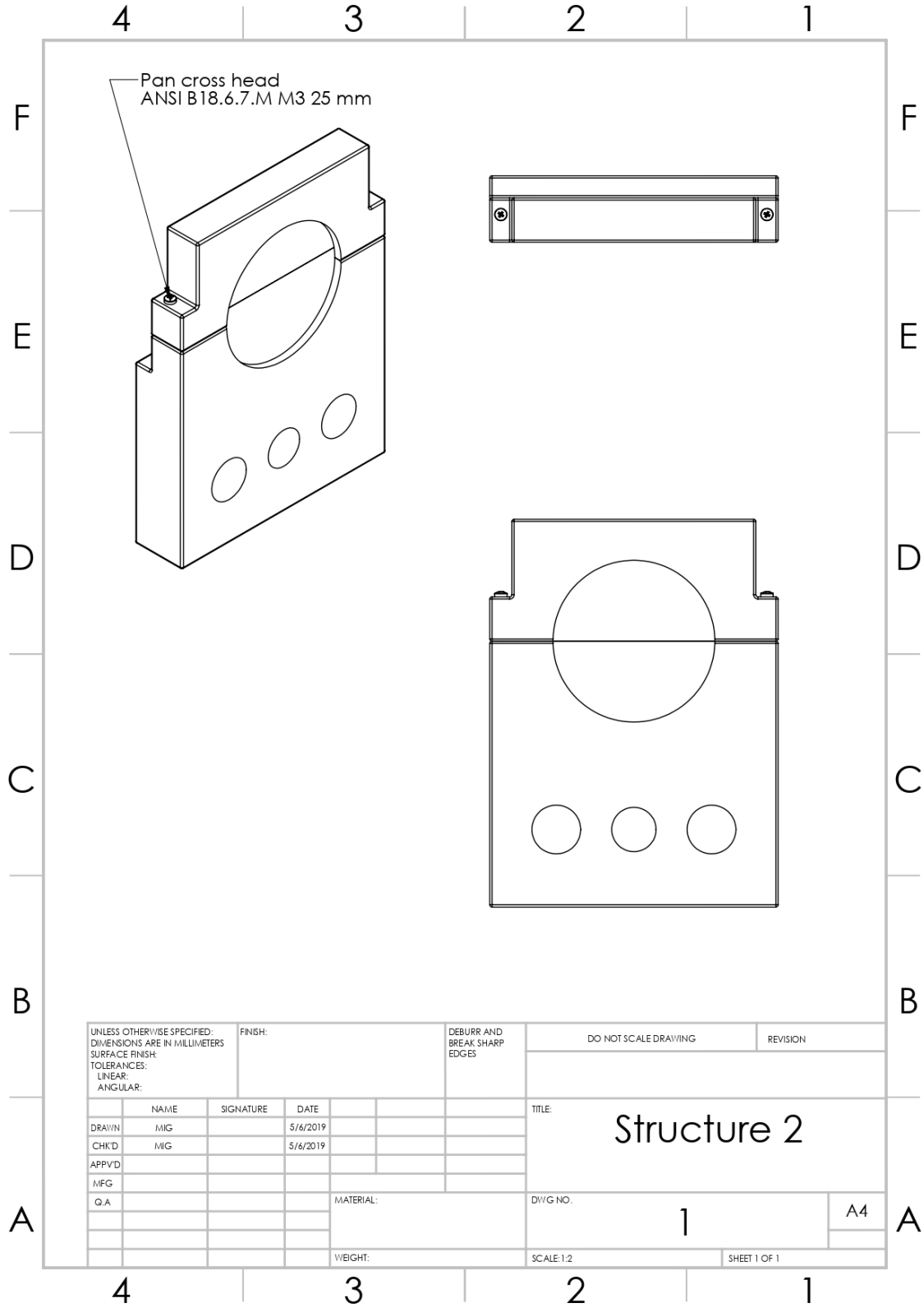

4.1. Part1

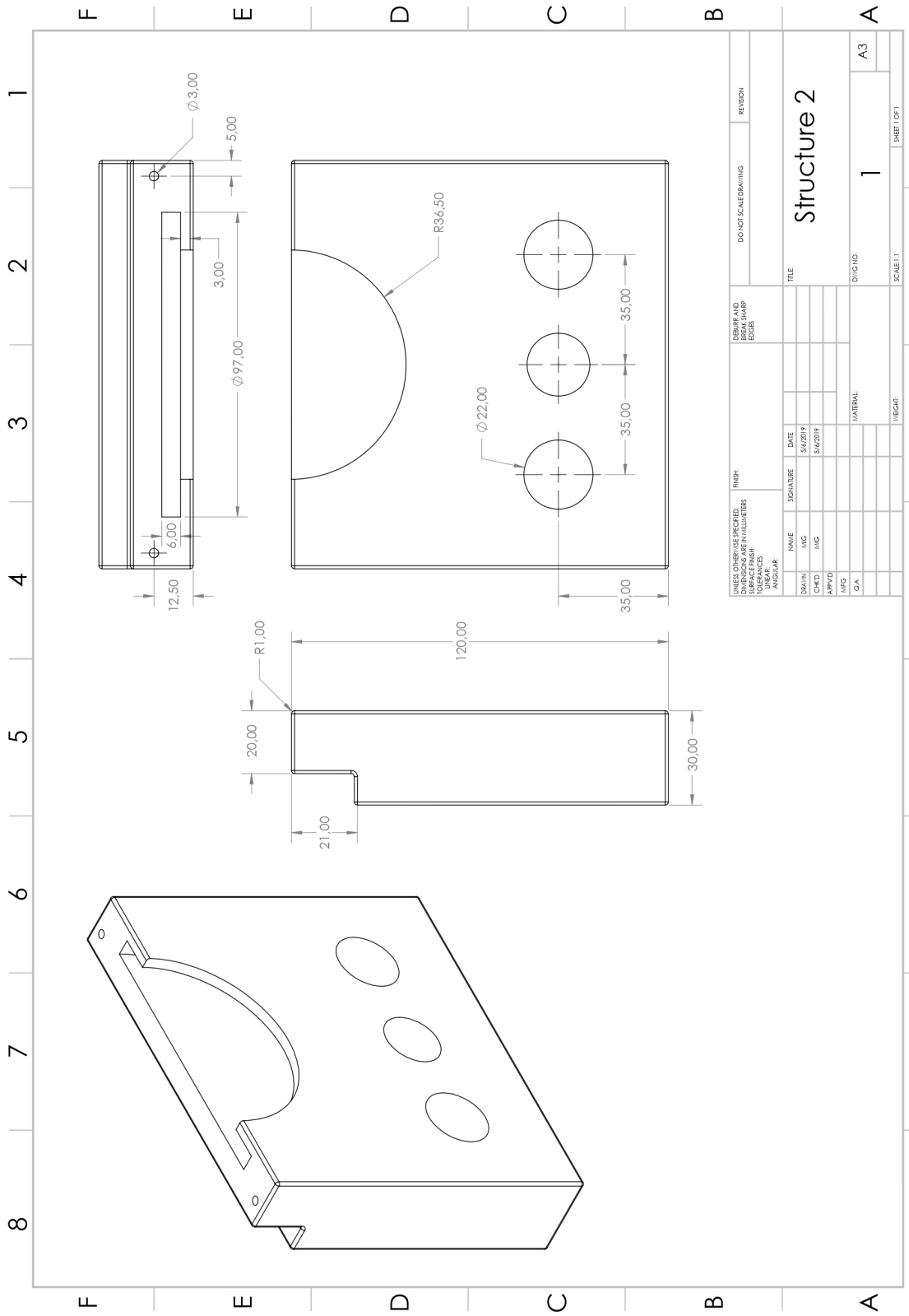
Structure 2
DO NOT SCALE DRAWING
REVISION
DEBURR AND BREAK SHARP EDGES
UNLESS OTHERWISE SPECIFIED:
DIMENSIONS ARE IN MILLIMETERS
SURFACE FINISH:
TOLERANCES:
LINEAR:
ANGULAR:
FINISH:
NAME
SIGNATURE
DATE
DRAWN
MG
5/6/2019
CHK'D
MG
5/6/2019
APPV'D
MFG
Q.A
MATERIAL:
WEIGHT:
TITLE:
DWG NO.
1
A3
SCALE: 1:1
SHEET 1 OF 1
Ø3,00
5,00
3,00
Ø97,00
6,00
12,50
R36,50
Ø22,00
35,00
35,00
35,00
R1,00
120,00
20,00
21,00
30,00

4.2. Part2

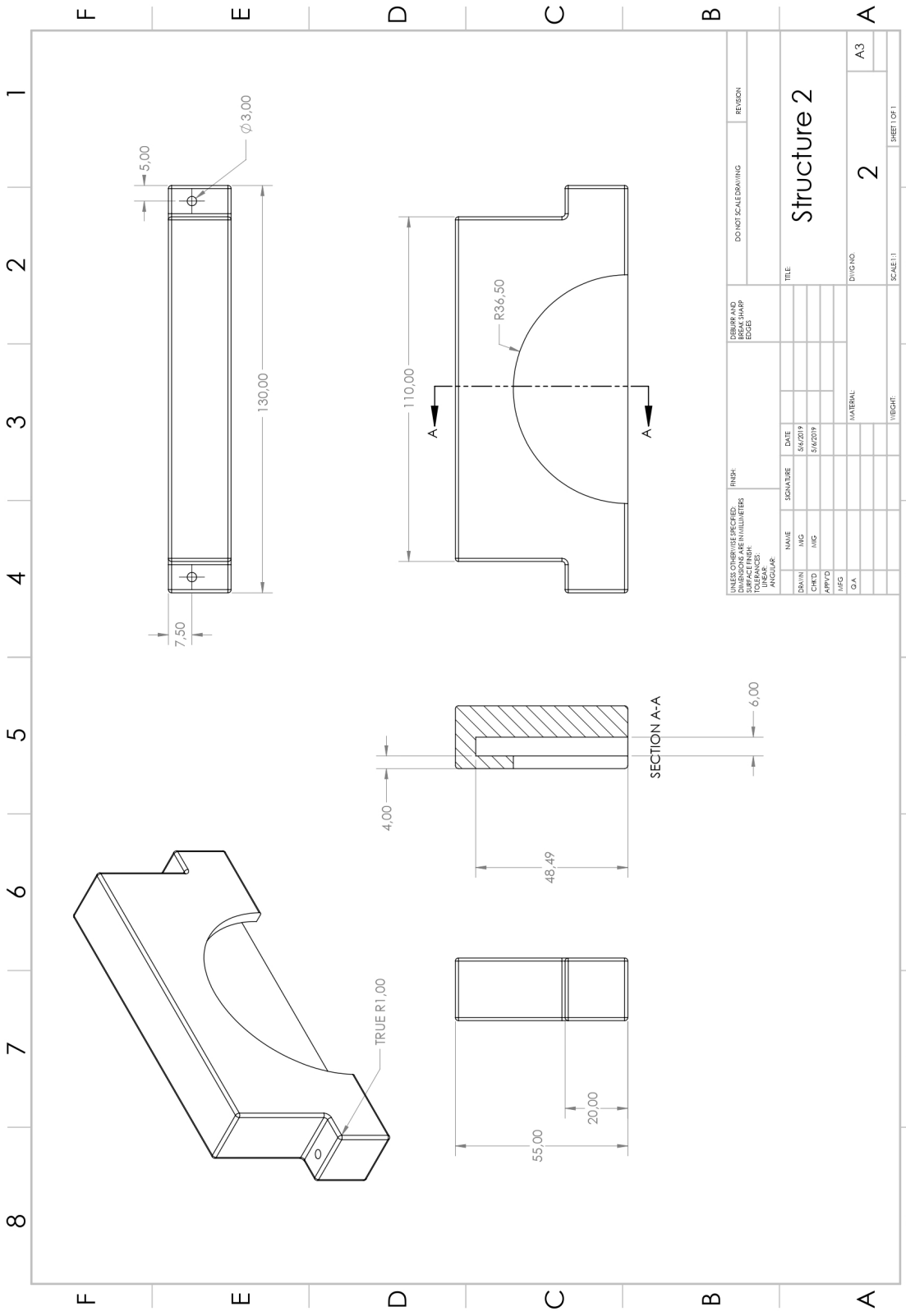
Structure 2
2
A3
SCALE: 1:1
SHEET 1 OF 1
DO NOT SCALE DRAWING
REVISION
DEBURR AND BREAK SHARP EDGES
UNLESS OTHERWISE SPECIFIED:
DIMENSIONS ARE IN MILLIMETERS
SURFACE FINISH:
TOLERANCES:
LINEAR:
ANGULAR:
FINISH:
NAME
SIGNATURE
DATE
DRAWN
MG
5/6/2019
CHK'D
MG
5/6/2019
APPV'D
MFG
Q.A
MATERIAL:
WEIGHT:
DWG NO.
TITLE:
Ø3,00
5,00
130,00
7,50
110,00
R36,50
A
A
SECTION A-A
6,00
4,00
48,49
55,00
20,00
TRUE R1,00

5. Structure 3

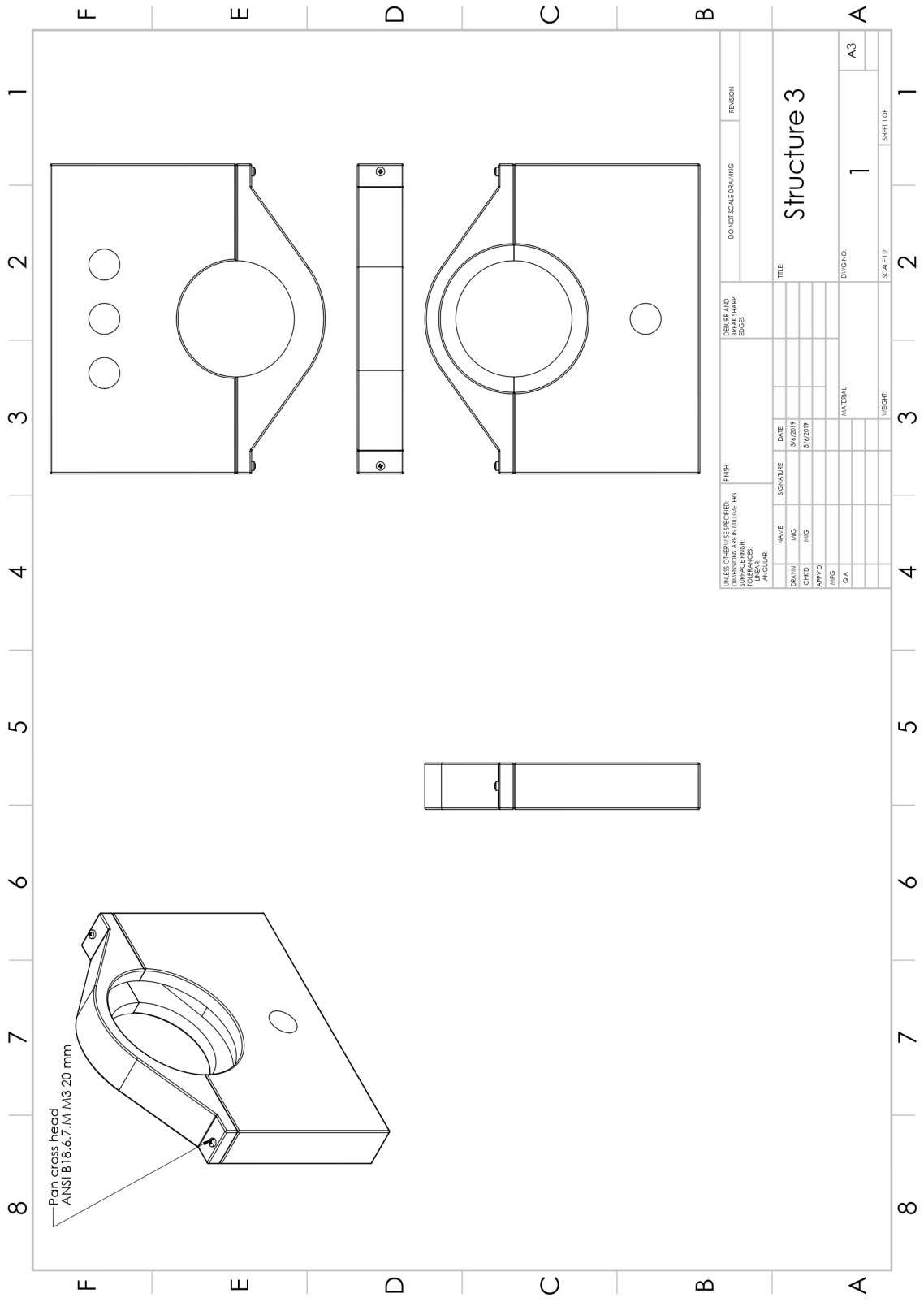

5.1. Part1

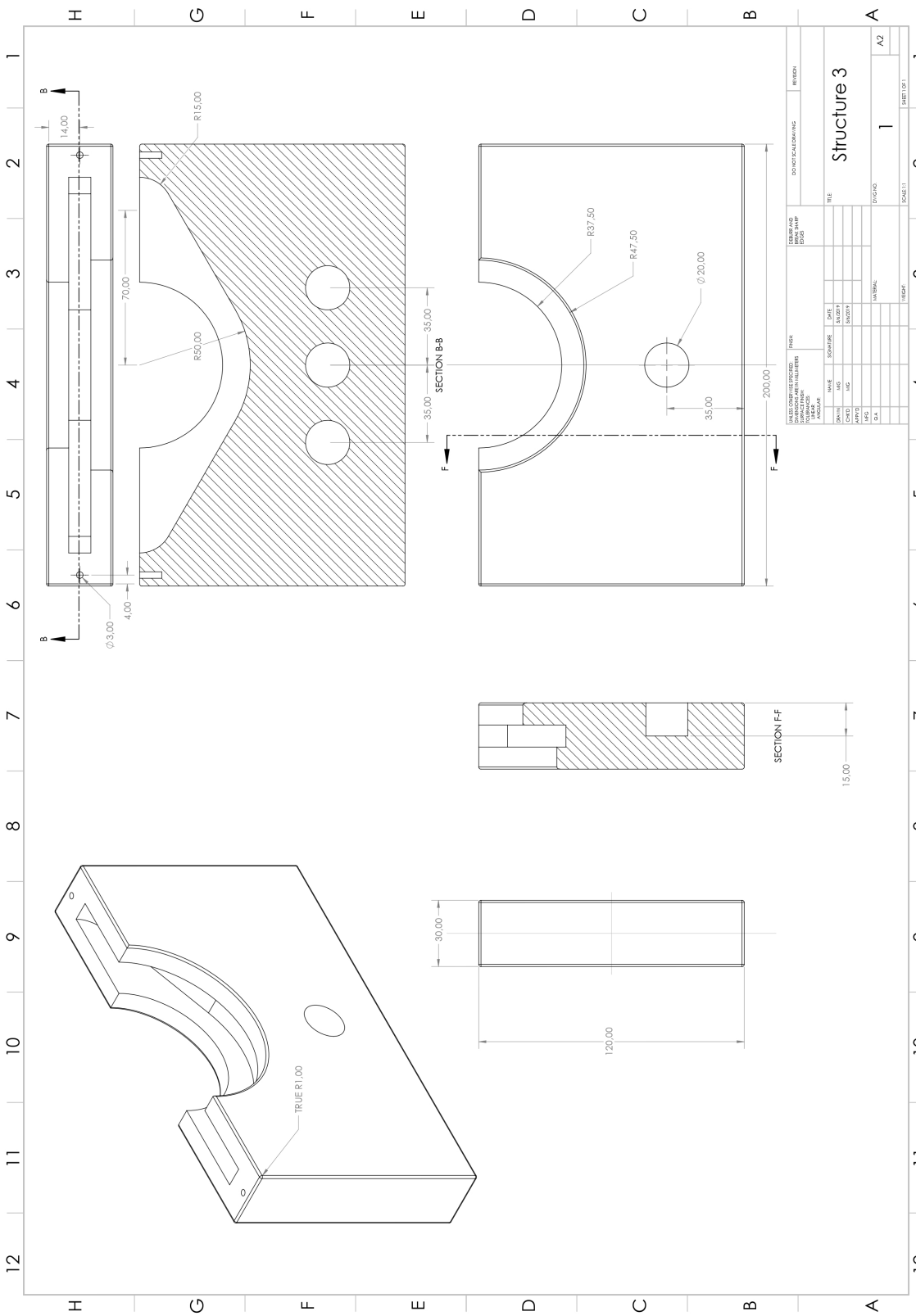
Structure 3
SECTION B-B
SECTION F-F
R15,00
R50,00
R37,50
R47,50
Ø20,00
Ø3,00
14,00
70,00
4,00
35,00
200,00
30,00
120,00
15,00
TRUE R1,00

5.3. Part2

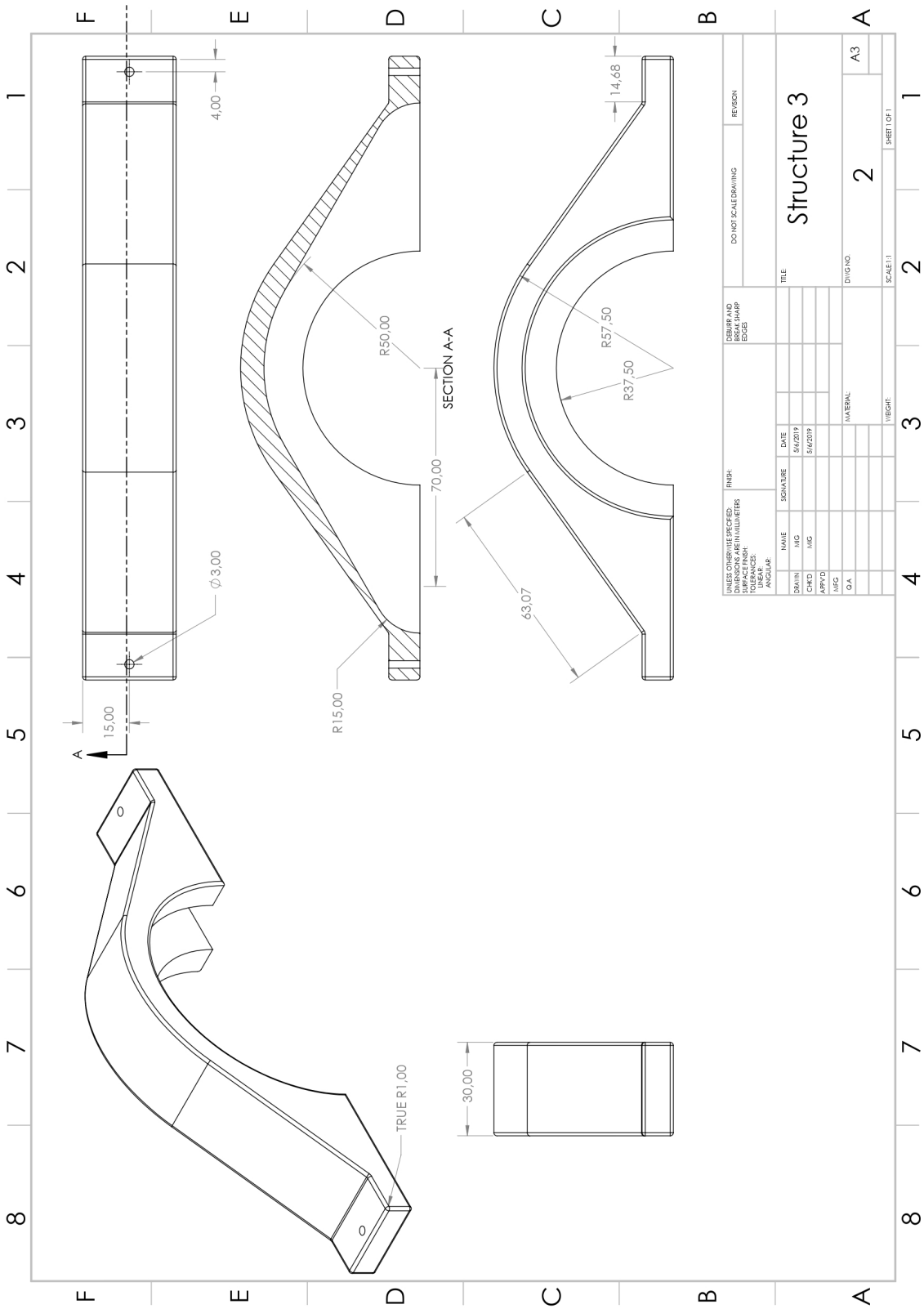
Structure 3
2
A3
SCALE 1:1
SHEET 1 OF 1
DO NOT SCALE DRAWING
REVISION
TITLE:
DWG NO
MATERIAL:
WEIGHT:
DEBURR AND BREAK SHARP EDGES
FINISH:
UNLESS OTHERWISE SPECIFIED:
DIMENSIONS ARE IN MILLIMETERS
SURFACE FINISH:
TOLERANCES:
LINEAR:
ANGULAR:
NAME
SIGNATURE
DATE
DRAWN
MG
5/6/2019
CHK'D
MG
5/6/2019
APPVD
MFG
QA
4,00
Ø3,00
15,00
A
R50,00
70,00
SECTION A-A
R15,00
14,68
R57,50
R37,50
63,07
30,00
TRUE R1,00

6. Rods

6.1. Smooth Rod

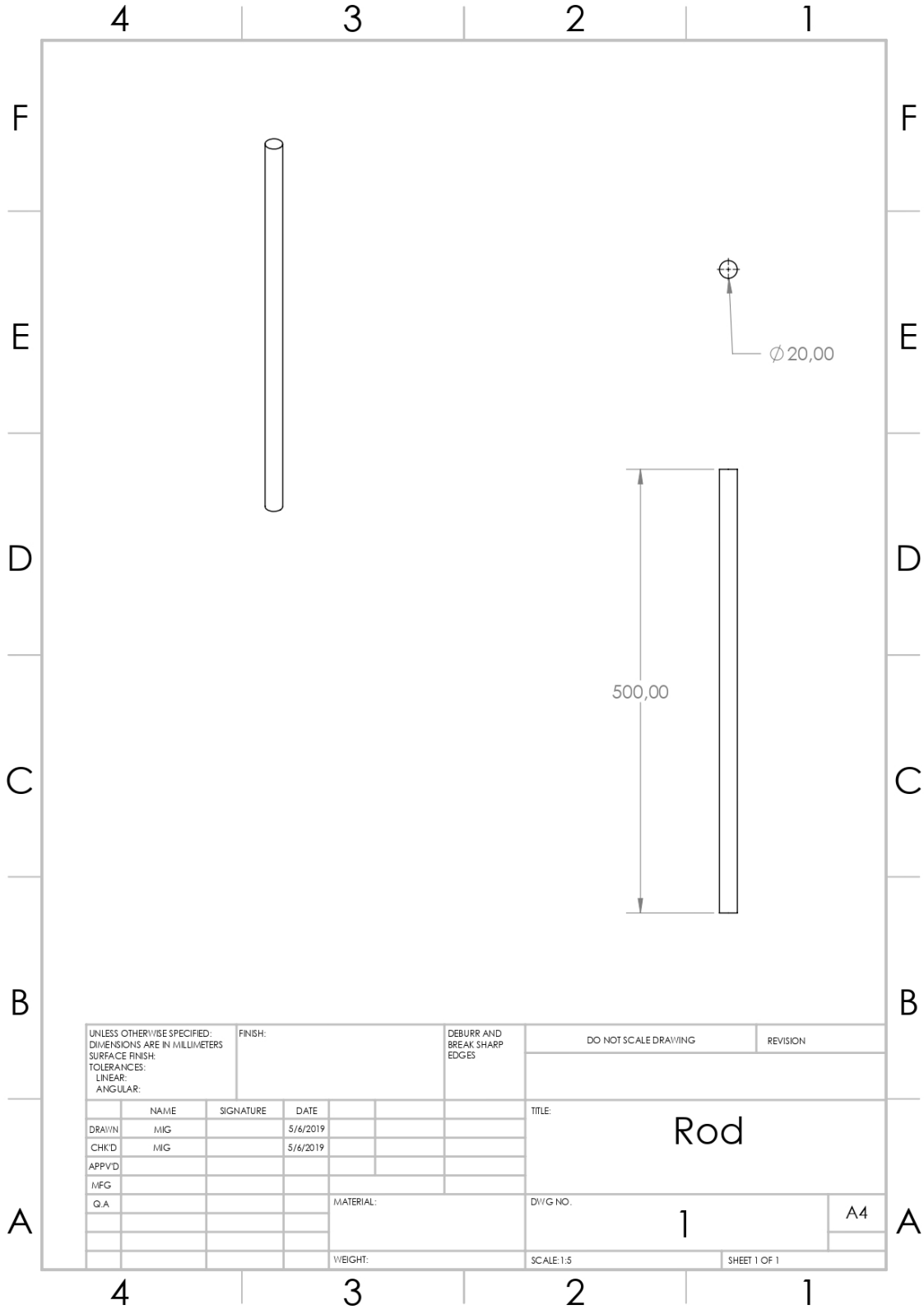

6.2. Threaded Rod

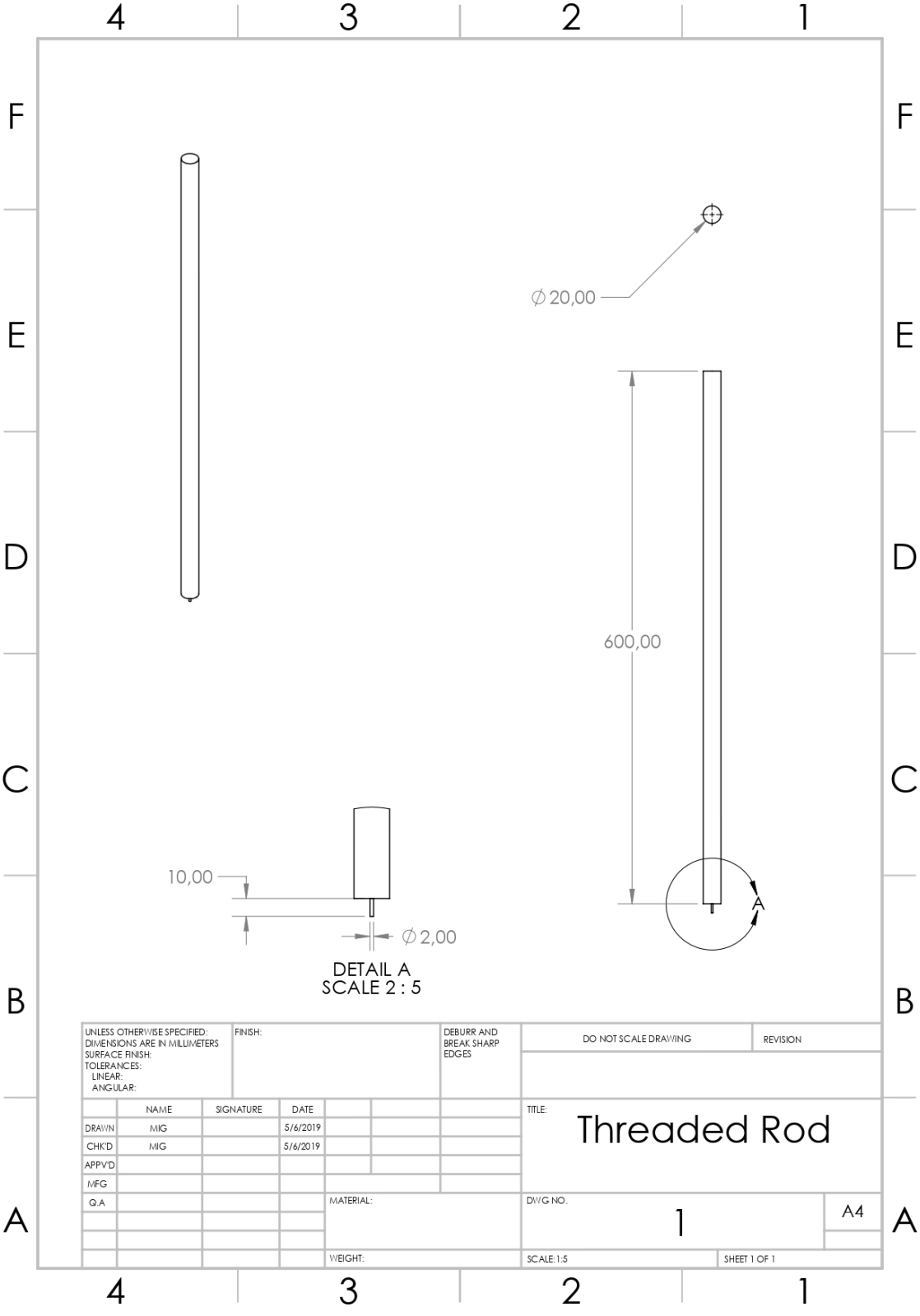

7. Pump Structure

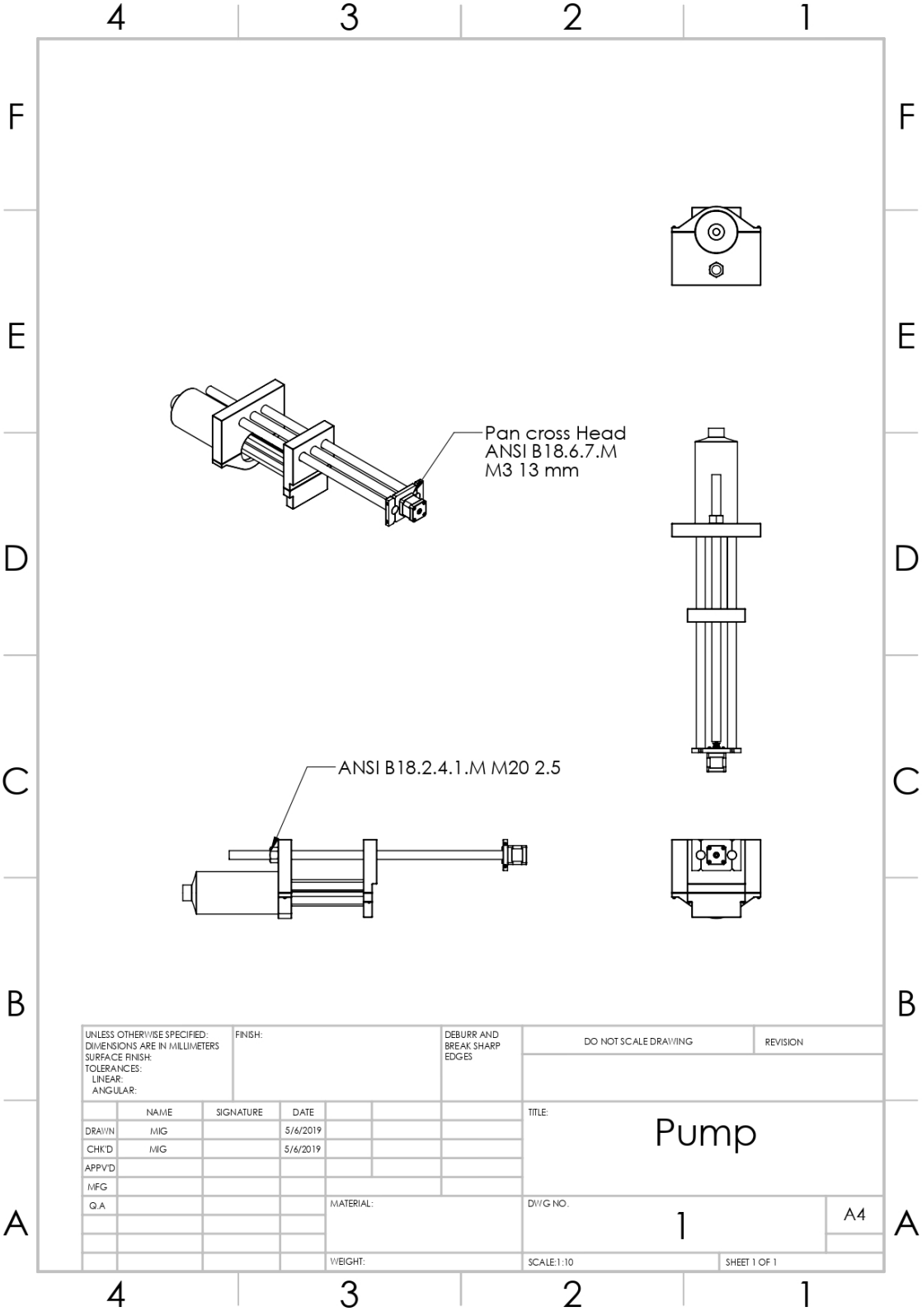

References

[1] Walker, A. ‘’3D Printing for Dummies: How Do 3D Printers Work?’’ June 2013

[2] López Gardeano, J.A. ‘’3D Printing Food: The Sustainable Future’’ 2015

[3] Bensoussan, H. ‘’The History of 3D Printing: 3D Printing Technologies from the 80s to Today’’ December 2016

[4] Roberson, D. ‘’The Five Keys 3D Printing Applications’’ June 2018

[5] Alois, E. ‘’Your Guide to Digital Cooking with 3D Printers’’ September 2016

[6] Carlota, V. ‘’A Guide to 2D Printed Food-Revolution in the Kitchen?’’ February 2019

[7] Tan, C. Toh,W.Y. Wong, G. Li,L ‘’Extrusion-based 3D Food Printing – Materials and Machines’’ June 2018

[8] ‘’3D Food Printing: What Options the New Technology Offers’’ April 2017

[9] Liu,C. Ho,C. Wang,J. ‘’The Development of 3D Food Printer for Printing Fibrous Meat Materials’’ 2017

[10] Vogt, S. ‘’3D Food Printing: What Options the New Technology Offers’’ April 2017

[11] Huang, C.Y ‘’Extrusion-based 3D Printing and Characterization of Edible Materials’’ 2018

[12] Zeleny, P. Ruzicka, V. ‘’The Design of the 3D Printer for Use in Gastronomy’’ February 2017

[13] Millen, C. I. ‘’Food printing System’’ 2012

[14] Watile, V. Wadive, S. Urkude, P. Karokar, S. Kumar, M. ‘’Development of 3D Food Printer for Food Industry’’ March 2018

[15] Sozer, N. ‘’3D Food Printing: A Disruptive Food Manufacturing Technology’’ June 2017

[16] Robyt, J. F. ‘’Starch: Structure, Properties, Chemistry, and Enzymology’’

[17] Sang-Ho, Y. ‘’Structures, Properties, and Biogenesis of starch and Cynobacterial Glycon’’ 2001

[18] BeMiller, J. N. ‘’An introduction to Pectins: Structure and Properties’’

[19] Comaposada, J. Gou, P. Marcos, B. Arnau, J. ‘’Physical Properties of Sodium Alginate Solutions and Edible Wet Calcium Alginate Coatings’’ November 2015

[20] Yong Lee, K. Mooney D. J. ‘’Alginate: Properties and Biomedical Applications’’ January 2012

[21] Porto, S. ‘’ Carrageenan: Overview’’

[22] Ward, A. G. ‘’The Physical Properties of Gelatin Solutions and Gels’’ 1954

[23] ‘’Fluidos Viscosos’’

[24] ‘’Viscosity of Newtonian and non-Newtonian Fluids’’

[25] ‘’Viscoelasticidad’’

[26] ‘’Viscoelasticidad’’

[27] ICAI ‘’Dinámica II’’

[28] Sandoval, J. ‘’Guia de Mecanica de Fluidos. Perdidas de Energia’’

[29] ICAI ‘’Tema 7 Fractura 17 18’’

[30] ICAI ‘’Ejercicios Tema 7 IM’’

[31] ‘’Theories of Failure’’

[32] ‘’Propylene’’

[33] Esquerrre Arribasplata, W ‘’ Trasvase del Chocolate en Fase Fluida Viscosa No Newtoniana Calculo del Equipo de Bombeo de una Planta de Chocolate’’ 2005

[34] ‘’ Se Derrite en tu viscosimetro, no en tu mano’’

[35] ‘’The Thermal Conductivity of Chocolate’’

[36] ‘’ Specific Heat of Food and Foodstuff’’

[37] Watile, V. Wadive, S. Urkude, P. Karokar, S. Kumar, M. ‘’Development of 3D Food Printer for Food Industry’’ March 2018